The Texas Medical Center Library

DigitalCommons@TMC

Dissertations and Theses (Open Access)

MD Anderson UTHealth Houston Graduate School

5-2014

Modulated Functions Of The Fanconi Anemia Core Complex

Yaling Huang

Follow this and additional works at: https://digitalcommons.library.tmc.edu/utgsbs_dissertations

Part of the Cancer Biology Commons, Medical Genetics Commons, and the Molecular Genetics Commons

Recommended Citation

Huang, Yaling, "Modulated Functions Of The Fanconi Anemia Core Complex" (2014). *Dissertations and Theses (Open Access)*. 429.
https://digitalcommons.library.tmc.edu/utgsbs_dissertations/429

This Dissertation (PhD) is brought to you for free and open access by the MD Anderson UTHealth Houston Graduate School at DigitalCommons@TMC. It has been accepted for inclusion in Dissertations and Theses (Open Access) by an authorized administrator of DigitalCommons@TMC. For more information, please contact digcommons@library.tmc.edu.

MODULATED FUNCTIONS OF THE FANCONI ANEMIA CORE COMPLEX

by

Yaling Huang, M.D.

APPROVED:

Lei Li, Ph.D.
Supervisory Professor

Randy J. Legerski, Ph.D.

Pierre D. McCrea, Ph.D.

Junjie Chen, Ph.D.

Bin Wang, Ph.D.

APPROVED:

Dean, The University of Texas
Graduate School of Biomedical Sciences at Houston

MODULATED FUNCTIONS OF THE FANCONI ANEMIA CORE COMPLEX

A

DISSERTATION

Presented to the Faculty of
The University of Texas
Health Science Center at Houston
and
The University of Texas
M. D. Anderson Cancer Center
Graduate School of Biomedical Sciences

in Partial Fulfillment
of the Requirements
for the Degree of

DOCTOR OF PHILOSOPHY

by

Yaling Huang, M.D.

Houston, Texas

May, 2014

DEDICATION

This dissertation is dedicated to my husband, Yong Lu,

my son, Zhongxi Lu, my daughter, Zhongling Lu,

and my parents, Wenbiao Huang and Mengjuan Xie,.

ACKNOWLEDGEMENTS

It is my great pleasure to thank those who gave me support and made this dissertation possible.

First and foremost, I am extremely thankful to my mentor Dr. Lei Li for his guidance and continuous support during my PhD studies. His patience, encouragement, immense knowledge, and advice have guided me though over the years. His optimistic attitude towards research inspired me to get through all the failures. I am honored to be his student and greatly appreciate the opportunity to participate in his research team.

I like to express my sincere gratitude to all my committee members, Dr. Junjie Chen, Dr. Randy Legerski, Dr. Bin Wang, Dr. Pierre McCrea, Dr. Mong-Hong Lee, Dr. Andreas Bergmann, Dr. Michelle Barton, Dr. Jian Kuang, Dr. Elsa Flores and Dr. Lalitha Nagarajan. Their insightful suggestions and comments kept my project on the right track.

Many warm thanks to all my colleagues in Dr. Li's laboratory and previous rotation labs, Dr. Yucai Wang, Dr. Xi Shen, Dr. Yingjun Jiang, Huong Do, Dr. Natalie Fonville, Dr. Haoyi Chen, Dr. Xin Wang, Dr. Chang Xu, Dr. Yanyan Tian, Dr. Joo-Myung Ahn and for their discussions and experimental assistances.

I sincerely thank Dr. Junjie Chen (MDACC) for his constructive advice and critical perspective on research. Thanks to Dr. Minoru Takata (Kyoto Univ., Japan) for their collaboration and Dr. Weidong Wang (NIA, NIH) for their valuable reagents. I also thank Megan Lowery and Jia Liu for help with survival assays and gel filtration assay, respectively.

I gratefully acknowledge the support from GSBS and the Department of Experimental Radiation Oncology at MDACC as well as the funding by NIH.

Last but certainly not least, I am truly and deeply indebted to my family. I give my earnest gratitude to my parents, Wenbiao Huang and Mengjuan Xie, for their unconditional love and inspiration. I sincerely thank my parents-in-law, Rongguang Lu and Shaozhen Fan, for their understanding and contribution. My son, Zhongxi Lu and my daughter, Zhongling Lu, deserve my warmest thanks. They are the main source of my happiness and strength. My deepest gratitude goes to my husband, Yong Lu, not only for his patience and care, but also for his humor, which helped me go through the frustrating days. None of my achievements would have been possible without his love and support. He has my everlasting love.

MODULATED FUNCTIONS OF THE FANCONI ANEMIA CORE COMPLEX

Yaling Huang, M.D.

Supervisory Professor: Lei Li, Ph.D.

Cells derived from Fanconi anemia (FA) patients are characterized by hypersensitivity to DNA interstrand crosslinks (ICLs), suggesting that FA genes play a role in ICL repair. Fanconi anemia core complex (including A, B, C, E, F, G, L, FAAP20, and FAAP100) activates the Fanconi pathway by providing the essential E3 ligase activity for FANCD2 mono-ubiquitination. Previous studies suggested the existence of three protein-protein interaction groups. However, the functions of most FA core complex protein are still limited to their presence in the complex. How the spatially-defined FANCD2 ubiquitination is accomplished by the core complex remains unknown.

To elucidate the roles of FA core complex proteins in ICL response, especially their contribution to FANCD2 ubiquitination, we established isogenic knockout mutants deficient in FA core genes and determined the loss-of-function effects on the activation of FA pathway and on cellular survival against ICLs. Our results suggest three potential functional modules in the FA core complex: FANCB-FANCL-FAAP100 (B-L-100), FANCA-FANCG-FAAP20 (A-G-20), and FANC-FANCE-FANCF (C-E-F). We showed that the B-L-100 sub complex is the catalytic module absolutely required for the E3 ligase function of FA core complex. The A-G-20 module anchors the catalytic module to the chromatin. The C-E-F module acts as a loading factor of the core complex through FANCM. Our work revealed that the FA core complex is assembled with functional modules and carries out the spatially-defined FANCD2 monoubiquitination reaction to ensure that nucleases for DNA damage processing are

enriched at the site of lesion. The deviate functions of different FA core complementation groups imply differential disease biology related to prognosis and treatment.

TABLE OF CONTENTS

Approval Page i

Title Page ii

Dedication iii

Acknowledgements iv

Abstract vi

Table of Contents viii

List of Illustrations xi

List of Tables xiii

Chapter I. Background and Significance 1

  Fanconi anemia 1

  Fanconi anemia genes 2

  Fanconi anemia pathway in DNA interstrand crosslink repair 5

  Fanconi anemia core complex and its E3 ligase activity 13

  Fanconi anemia sub complex 16

Chapter II. Generation of Somatic Knockout Cell Lines 18

  Introduction 18

  Materials and Methods 20

  Results 25

    Targeting strategy of *FANCG* 25

    Generation of heterozygous *FANCG*$^{+/-}$ clones 28

    Generation of *FANCG*$^{n/-}$ somatic knockout cell lines 31

Generation of *FANCG*$^{-/-}$ somatic knockout cell line......34

Confirmation of *FANCB*$^{-}$ cell line and Generation of *FAAP20*$^{-/-}$ and *FANCL*$^{-/-}$ knockout cell line......37

Complementation of FA knock out cell lines......40

Generation of *FANCG*$^{-/-}$ *FANCB*$^{-}$, *FAAP20*$^{-/-}$ *FANCB*$^{-}$, and *FANCG*$^{-/-}$ *FANCM*$^{-/-}$ somatic double knockout cell lines......43

Discussion......46

Chapter III. FANCL, FANCB, and FAAP100 form the catalytic module of the FA core complex......48

Introduction......48

Materials and Methods......51

Results......54

Confirmation of sub complexes in the FA core complex......54

FA core complex is not an integral complex......58

Identification of the catalytic module in the FA core complex, FANCB-L-100 sub complex......61

FANCB-L-100 sub complex is more essential for the cellular resistance to MMC than FANCA-G-20 sub complex......67

FANCB-L-100 sub complex is epistatic to FANCA-G-20 sub complex in cellular resistance to ICLs......70

Discussion......73

Chapter IV. Chromatin Anchoring and Loading of the Core Complex......75

Introduction......77

Materials and Methods....78
Results....81
FANCG is important for FANCL chromatin loading....81
FANCG is important for FANCL recruitment to ICL sites....84
Generation of FANCF stable knockdown cell lines....87
A-G-20 and C-E-F modules are required for the full function of FA core complex....90
FANCG and FANCM are required for the full function of FA core complex in recruiting FANCL into ICL sites....93
FANCM functions epistatically with the chromatin loading module....96
Discussion....99
Chapter V. Conclusion and Future Directions....102
Conclusion....102
Working Model....103
Future Directions....107
Chromatin/DNA anchoring machinery of A-G-20 sub complex....107
Epistatic analysis of FA genes....115
Role of FA genes in DNA-protein crosslink (DPC) repair....133
References....138
Vita....151

LIST OF ILLUSTRATIONS

Fig. 1.1 Interstrand crosslink repair pathways in vertebrates. 9

Fig. 1.2 Fanconi anemia pathway. 11

Fig. 1.3 FANC core complex E3 ligase compared with two classes of E3 ligases – one of a kind or fitting in? 14

Fig. 2.1 Schematics of homologous recombination-mediated targeting of *FANCG* in HCT116 cell line. 26

Fig. 2.2 Generation of *FANCG*$^{+/n}$ and *FANCG*$^{+/-}$ clones 29

Fig. 2.3 Generation of the *FANCG*$^{n/-}$ clone.. 32

Fig. 2.4 Generation of the *FANCG*$^{-/-}$ clone 35

Fig. 2.5 Generation of *FANCB*$^{-}$, *FAAP20*$^{-/-}$, and *FANCL*$^{-/-}$ cell line 38

Fig. 2.6 Complementation of *FANCG*$^{-/-}$, *FANCB*$^{-}$, and *FANCL*$^{-/-}$ single knockout cell lines..41

Fig. 2.7 Generation of *FANCG*$^{-/-}$*FANCB*$^{-}$, *FAAP20*$^{-/-}$*FANCB*$^{-}$, and *FANCG*$^{-/-}$*FANCM*$^{-/-}$ double knockout cell lines. 44

Fig. 3.1 Formation of sub modules within the FA core complex. 56

Fig. 3.2 FANC core complex is not an integral complex. 59

Fig. 3.3 FANCL, FANCB, and FAAP100 form the catalytic module of the FA core complex.. 63

Fig. 3.4 FANCD2 levels in HCT116 and DT40 knockout mutants. 65

Fig. 3.5 B-L-100 sub complex is more essential for the cellular resistance to MMC than A-G-20 sub complex 68

Fig. 3.6 B-L-100 sub complex is epistatic to A-G-20 sub complex in cellular resistance to ICLs....71

Fig. 4.1 FANCG is important for FANCL chromatin loading. 82

Fig. 4.2 FANCG is important for FANCL recruitment to ICL sites. 85

Fig. 4.3 Generation of FANCF shRNA knockdown cell lines. 88

Fig. 4.4 A-G-20 and C-E-F modules are required for the full function of FA core complex. 91

Fig. 4.5 FANCG and FANCM are required for the full function of FA core complex in recruiting FANCL into ICL sites. 94

Fig. 4.6 FANCM functions epistatically with the chromatin loading module. 97

Fig. 5.1 Working model for FA core genes in activating FA pathway 105

Fig. 5.2 Sequence alignment of the PWWP domain-containing proteins and FANCA.......108

Fig. 5.3 Sequence alignment of the “PWWP-like” domain of FANCA homologs across species....111

Fig. 5.4 Construction of human cellular knockout mutants....116

Fig. 5.5 Clonogenicity of the FA mutants. 119

Fig. 5.6 Cell cycle profile of the FA mutants with or without mitomycin C treatment. 122

Fig. 5.7 Cellular resistance of the FA mutants to mitomycin C. 125

Fig. 5.8 Cytogenetic characterization of the FA mutants with or without mitomycin C treatment....128

Fig. 5.9 Recombination-independent repair efficiency of the FA mutants 131

LIST OF TABLES

Table 1.1 Fanconi anemia genes 4

Table 1.2 Fanconi anemia-associated genes 5

CHAPTER I

Background and Significance

Fanconi anemia

Fanconi anemia (FA) is named after the Swiss pediatrician Guido Fanconi, who first described this human disease in 1927 (Lobitz and Velleuer, 2006). FA is a rare genetic disease typically characterized with bone marrow failure, a broad spectrum of developmental abnormalities, and a propensity to cancer. FA occurs in all ethnic groups with an average incidence of 1/130,000 births in US, although it is more prevalent in Israel with a birth incidence of 1/35,000 (Rosenberg et al., 2011). The heterozygous carrier frequency is 1/181 in US, while the carrier frequency is up to 1/93 in Israel and 1/100 in Ashkenazi Jews, Afrikaners, Spanish Gypsies, black sub-Saharan Africans (Rosenberg et al., 2011). The median age at death of FA patients was 30 as recorded in 2000 (D'Andrea).

The major symptoms of FA are pancytopenia, diverse congenital abnormalities, and a marked susceptibility to develop cancer. It is most commonly characterized in clinical practice by pancytopenia, leading to hypoxia in organs, higher risk of infection, and continuous bleeding, as result of patient bone marrow failure. Thus bone marrow and umbilical cord blood transplantation are relatively effective treatment for FA patients.

Congenital defects occur in about 67% FA patients, including but not limited to skeletal malformations (manifested by short stature, microcephaly, dangling thumbs, and rocker bottom feet, etc.), urogenital abnormalities, and skin pigmentation, etc. (Auerbach et al., 1989). FA patients have high risk of cancer development, 48-fold and 800-fold higher risk of developing solid tumor and acute myeloid leukemia, respectively (Rosenberg et al., 2003). They are also prone to many other cancer types such as leukemia, head-and-neck squamous cell carcinoma, esophageal carcinoma, gynecological carcinoma, and tumors in liver, brain, skin, and kidney. Among them acute myeloid leukemia has the highest frequency (Kutler et al., 2003). Certain genetically defined groups of FA patients are more prone to breast cancer and ovarian cancer (Akbari et al., 2010; Howlett et al., 2002).

FA is a DNA repair-deficiency disorder which is closely associated with chromosomal instability and hypersensitivity to DNA damage reagents. Other examples of DNA repair-deficiency disorders include Nijmengen syndrome, Bloom syndrome, and Xeroderma pigmentosum. One of the key features of FA is that cells derived from patients are hypersensitive to DNA crosslinking agents, such as mitomycin C (MMC), cisplatin, formaldehyde, etc. This specific feature is used to clinically diagnose the FA disease. And DNA interstrand crosslinking repair in FA cells has been investigated to understand the biological mechanism of this disease.

Fanconi anemia gene

FA is a highly complex genetic disorder, consisting of at least 16 complementation groups (A, B, C, D1, D2, E, F, G, I, J, L, M, N, O, P, Q). Each FA complementation group is caused by mutation(s) of a distinct disease gene encoding a corresponding FA protein. Previously, complementation assay based on cell fusion techniques were used to distinguish different FA genes. With the emergence of functional cloning and sequencing technique, several new FA genes were discovered (Bogliolo et al., 2013). Among the 16 FA genes, most were autosomal recessive, except for *FANCB*, which is X-linked. The summary of the prevalence, chromosomal location, and conservation is listed in Table 1.1.

Another group of genes are found to be physically and/or functionally associated with FA genes. Therefore, most of their protein products were named as FA-associated proteins, including FAAP24, FAAP20, FAAP100, FAAP16 (also named MHF1), and FAAP10 (MHF2), and, FAN1 (FANCD2-associated nuclease). Until now, no mutation has been found in these FA-associated genes even though they contribute to DNA interstrand crosslink repair. The summary of these genes is listed as Table 1.2.

Table 1.1 Fanconi anemia genes.

FA gene	Chromosome location	Prevalence in FA patients	conservation	important for FANCD2 ubiquitnation	Function in FA pathway	Protein features
FANCA	16q24.3	63%	vertebrate	+	Core complex	Phosphorylated following DNA damage
FANCB	Xp22.2	~2%	vertebrate	+	Core complex	Contains nuclear localization sequence
FANCC	9q22.3	12%	vertebrate	+	Core complex	
FANCD1 (BRCA2)	13q12.3	~2%	vertebrate, worm	-	Homologous recombination	Contains BRC repeats and an OB‑fold DNA binding domain; regulates RAD51
FANCD2	3p26	~3%	vertebrate, worm, insect, slime mould	+	ID complex	Monoubiquitylated and phosphorylated following DNA damage; exonuclease activity
FANCE	6p22-p21	~2%	vertebrate	+	Core complex	Phosphorylated by Chk1 following DNA damage
FANCF	11p15	~2%	vertebrate	+	Core complex	
FANCG (XRCC9)	9p13	9%	vertebrate	+	Core complex	Contains TPR repeats; phosphorylated following DNA damage
FANCI	15q26.1	~1%	vertebrate, worm, insect, slime mould	+	ID complex	Monoubiquitylated and phosphorylated following DNA damage
FANCJ (BRIP1, BACH1)	17q22.2	~2%	vertebrate, invertebrate, yeast	-	Homologous recombination	5’ to 3’ DNA helicase; binds BRCA1; phosphorylated following DNA damage; G-quadruplex resolution
FANCL (PHF9)	2p16.1	~0.1%	vertebrate, insect, slime mould	+	Core complex	PHD/ring-finger ubiquitin-ligase activity; contains WD40 repeats
FANCM (Hef)	14q21.2	~0.2%	vertebrate, invertebrate, yeast, archaea	+	Core complex	Contains helicase and endonuclease domains; phosphorylated following DNA damage
FANCN (PALB2)	16p12.2	~0.6%	vertebrate	-	Homologous recombination	An essential partner for BRCA2 stability and nuclear localization
FANCO (RAD51C)	17q22	~0.4%	vertebrate, invertebrate, yeast	-	Homologous recombination	RAD51 paralogue, single-stranded DNA-dependent ATPase activity
FANCP (SLX4)	16p13.3	~0.5%	vertebrate, worm, insect, yeast, bacteria	-	Nucleolytic cleavage / Homologous recombination	Scaffold protein in structure-specific endonuclease complex; Holliday junction resolvase
FANCQ (XPF, ERCC4)	16p13.12	~0.1%	vertebrate, insect, plant yeast, bacteria, archaea	-	Nucleolytic cleavage	contains the nuclease domain, HhH2 domain, and helicase-like domain

Adapted (with permission) from NATURE PUBLISHING GROUP on behalf of Nature Reviews Genetics, (Wang, 2007), copyright (2007).

Prevalence in FA patients are calculated as total number of individuals with variants of the specific FA gene/ total genetically identified FA patients

Table 1.2 Fanconi anemia-associated genes.

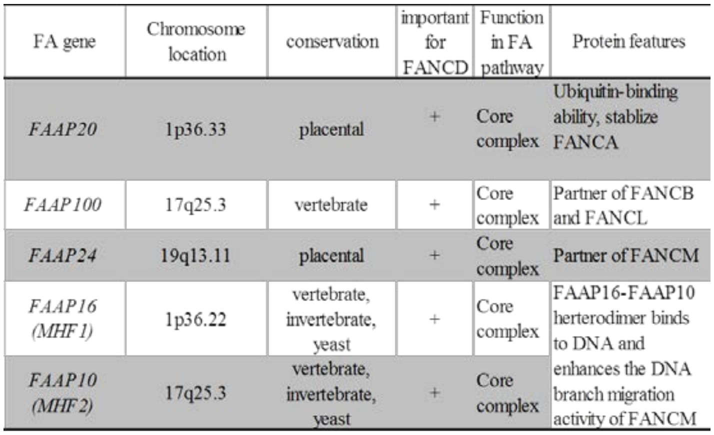

FA gene	Chromosome location	conservation	important for FANCD	Function in FA pathway	Protein features
FAAP20	1p36.33	placental	+	Core complex	Ubiquitin-binding ability, stablize FANCA
FAAP100	17q25.3	vertebrate	+	Core complex	Partner of FANCB and FANCL
FAAP24	19q13.11	placental	+	Core complex	Partner of FANCM
FAAP16 (MHF1)	1p36.22	vertebrate, invertebrate, yeast	+	Core complex	FAAP16-FAAP10 herterodimer binds to DNA and enhances the DNA branch migration activity of FANCM
FAAP10 (MHF2)	17q25.3	vertebrate, invertebrate, yeast	+	Core complex	

Fanconi anemia pathway in DNA interstrand crosslink repair

A DNA interstrand crosslink (ICL) is formed when DNA crosslinking agent covalently links two nucleotide residues from the opposite strands. ICLs block essential cellular DNA metabolism especially DNA replication and transcription by preventing DNA strand separation. It is extremely toxic to cells if left unrepaired, the fatal dosage is one for unicellular organism, and 20-40 for mammalian cells (Lawley and Phillips, 1996; Magana-Schwencke et al., 1982). The genotoxicity and mutations from ICLs lead to genomic instability and cancer development. The cancer risk manifestation of FA and the ICL repair deficient disease fully demonstrated this notion. On the other hand, the strong cytotoxicity of ICLs in dividing cells prompt the clinical application of ICL agents in cancer therapy, both in solid and blood-borne tumors since 1940.

The crosslinking agents exist both intrinsically and extrinsically. The natural crosslinking agents include mitomycin C, psoralens, nitrous acids, etc. Mitomycin C (MMC), also named [6-Amino-8a-methoxy-5-methyl-4,7-dioxo-1,1a,2,4,7,8,8a,8b-octahydroazireno[2',3':3,4]pyrrolo[1,2-a]indol-8-yl]methyl carbamate, is originated from fungi. MMC functions as an antibiotic by causing DNA crosslinking to kill bacteria. As an anti-cancer agent, MMC has been administrated to treat breast, esophageal, and bladder cancer. There are also synthetic sources of crosslinking agents such as cisplatin, nitrogen mustard, etc. Cisplatin, also named (SP-4-2)-diamminedichloridoplatinum, is the first member of the platinum-containing anti-cancer agents. Until now it is still one of the most widely-used chemotherapeutical agents for cancer treatment. Another DNA crosslinking agents used in my study is formaldehyde. Aldehyde is a metabolite of alcohol consuming and a major byproduct of cellular demethylation process. Recent studies have shown that formaldehyde is an internal risk for genomic instability and embryogenesis (Rosado et al.).

Understanding of cellular mechanism in response to ICLs is important not only because failure in proper ICL repair results in genomic instability and cancer development, but also because ICL-inducing agent with its profound cytotoxicity is a widely-used chemotherapeutic drug for cancer treatment. To date, two repair mechanisms have shown to be involved in ICL repair in eukaryotes, a recombination-dependent and arecombination-independent pathway. The recombination-dependent ICL repair, also called the replication-dependent ICL repair, mainly occurs in S or G2 phases of cell cycle when the undamaged sister chromatid is present. The recombination-independent ICL repair, also known as the replication-independent ICL repair, mainly occurs in G1 phase of the cell cycle and is usually mutagenic.

Recombination-dependent ICL repair is initiated by the stalling of the replication fork, and processed by nucleotide excision repair (NER), translesion synthesis, and homologous recombination (HR). Current model is derived from studies in the Xenopus laevis egg extracts (Raschle et al., 2008) as shown in Fig. 1.1A. In this model, either dual replication forks converge at the DNA ICL site (20%) or single replication fork get stalled at the ICL site and FANCM-MHF1/MHF2 complex mediates the replication traverse (>50%) (Huang et al., 2013). Then structure-specific nucleases such as XPF-ERCC1 make dual incisions flanking the lesion site on one DNA strand, which is also called an ICL unhooking step. Next, a translesion DNA polymerase fills the resulting gap. This strand is later ligated to the downstream Okazaki fragment, which is synthesized before the replication fork stalling. This restored DNA duplex is then further repaired by NER factors by removing the crosslinked oligonucleotides. This fully repaired duplex subsequently serves as template to rejoin the double strand break on the other duplex by homologous recombination.

In the recombination-dependent ICL repair mechanism, the FA pathway is indispensable from the initial recognition of stalled replication forks to the final recombination process (Wang and Gautier, 2010). As shown in Fig. 1.2, the FA classical core complex (consisting of A, G, FAAP20, C, E, F, B, L, and FAAP100) is recruited to the ICL sites by FANCM and its associated proteins (FAAP24, MHF1/2). The core complex activates the FANCI/D2 complex by ubiquitination. The monoubiquitinated FANCI/D2 then recruits crucial ICL repair factors, including excision factors such as SLX4 and FAN1, through their ubiquitin-binding domains (Liu et al.; Yamamoto et al., 2011). Also, the homologous recombination factors of FA pathway is central for the ensuing homologous recombination in order to complete the repair of the DSB-bearing sister chromatid (Garcia-Higuera et al., 2001).

Recombination-independent repair or mutagenic ICL repair is initiated when ICL is recognized by native DNA damage recognition factors such as XPC and consists of NER incision and translesion synthesis (Sarkar et al., 2006; Zheng et al., 2003), as shown in Fig. 1.1B. NER incision factors are utilized to unhook the covalently-joined strand, in which XPF-ERCC1 and XPG provide the 5’ and 3’ incision, respectively. The resulting gap of unhooking is then filled by lesion bypass DNA polymerase ζ (Shen et al., 2006). A second incision then occurs on the other strand to accomplish the repair of the DNA ICL. The FA core and FANCI/D2 complexes are also involved in this process (Shen et al., 2009), but downstream FA proteins, such as FANCJ, are not. Also a recent study demonstrated that FAAP20 protein may recruit the FA core complex to the ICL site in the replication-independent pathway (Yan et al.).

Fig. 1.1 Interstrand crosslink repair pathways in vertebrates.

(***A***) Recombination-dependent ICL repair pathway includes initiation, unhooking, (SNMA1 digestion), translesion synthesis, nucleotide excision, gap filling, and homologous recombination.

Note, it is adapted from Raschle, M., et al. in 2008 (Raschle et al., 2008). However, in their study, as shown in green-arrowed strands, SNM1A digestion step is not necessary. Instead, the new strand is extended to one base beyond the lesion, nucleases exerts unhooking, Rev1 inserts a cytosine across the lesion, and Pol ζ processes the lesion bypass synthesis.

(***B***) Recombination-independent ICL repair pathway includes initiation, unhooking, translesion bypass synthesis, nucleotide excision, and gap filling.

Note, it is adapted from Zheng H. et al. in 2003 (Zheng et al., 2003).

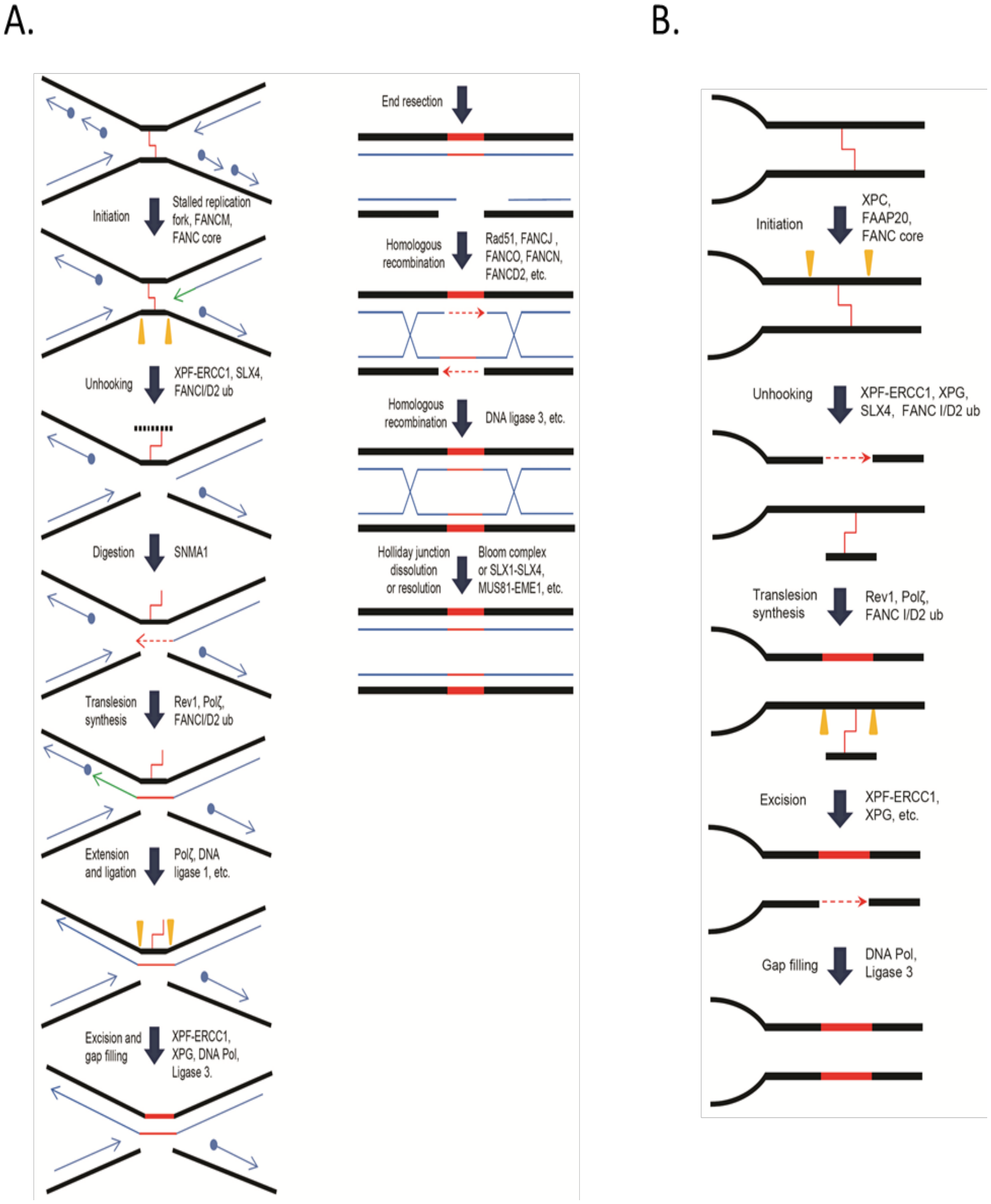
A.
B.
Initiation
Stalled replication fork, FANCM, FANC core
Unhooking
XPF-ERCC1, SLX4, FANCI/D2 ub
Digestion
SNMA1
Translesion synthesis
Rev1, Polζ, FANCI/D2 ub
Extension and ligation
Polζ, DNA ligase 1, etc.
Excision and gap filling
XPF-ERCC1, XPG, DNA Pol, Ligase 3.
End resection
Homologous recombination
Rad51, FANCJ , FANCO, FANCN, FANCD2, etc.
Homologous recombination
DNA ligase 3, etc.
Holliday junction dissolution or resolution
Bloom complex or SLX1-SLX4, MUS81-EME1, etc.
Initiation
XPC, FAAP20, FANC core
Unhooking
XPF-ERCC1, XPG, SLX4, FANC I/D2 ub
Translesion synthesis
Rev1, Polζ, FANC I/D2 ub
Excision
XPF-ERCC1, XPG, etc.
Gap filling
DNA Pol, Ligase 3

Adapted (with permission) from Pioneer Bioscience Publishing Company on behalf of Translational Cancer Research, (Huang and Li, 2013), copyright (2013)

Fig. 1.2 Fanconi anemia pathway.

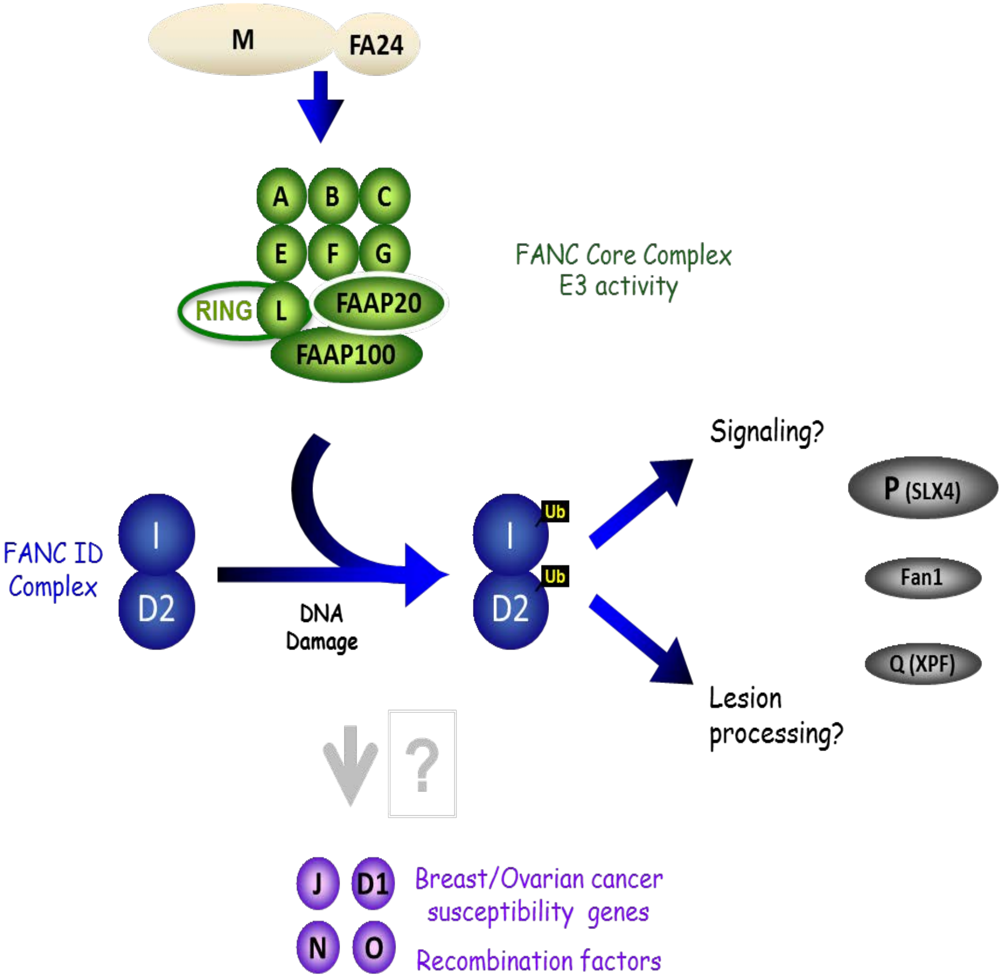
M
FA24
A
B
C
E
F
G
RING
L
FAAP20
FAAP100
FANC Core Complex
E3 activity
FANC ID
Complex
I
D2
DNA
Damage
Ub
Ub
I
D2
Signaling?
P (SLX4)
Fan1
Q (XPF)
Lesion
processing?
?
J
D1
N
O
Breast/Ovarian cancer
susceptibility genes
Recombination factors

Fanconi anemia core complex and its E3 ligase activity

As mentioned above, the classical Fanconi anemia core complex consists of A, G, C, E, F, B, L, and two FA associated protein FAAP100 and FAAP20. So far, the functional understanding of the core complex is limited to the E3 ligase activity for FANCI/D2 ubiquitination which is central for FA pathway activation. The general paradigm is that all the core components work together as an integral complex to exert the E3 ligase function; deficiency of either component will collapse the whole complex, leading to the loss of FANCD2 ubiquitination. Aside from FANCL that possesses the RING domain and bears the E3 ligase activity (Alpi et al., 2008; Meetei et al., 2003), most other components do not have recognizable domains or clearly-designated functions as to how they contribute to the FANCD2/I ubiquitination upon ICL agent-induced DNA damage.

In order to study the E3 ligase activity of the core complex, we have compared the composition of the core complex with other types of E3 ligases. There are two general categories of E3 ligases as shown in Fig. 1.3. One is the Cullin-based multi-components E3 with adaptor and substrate-binding modules. The other is the monomeric E3s including the HECT domain and U-box domain proteins (Metzger et al., 2012; Zimmerman et al., 2010). By sheer number of components, the FA core complex fits in the former category, but it is conflicted by the experimental observation that FANCL itself was sufficient to ubiquitinate the FANCD2 (Alpi et al., 2008; Longerich et al., 2009). Also there is a unique aspect for the FA core complex, which is apparently recruited to and anchored at the site of DNA damage to prevent the detrimental impact of enriching lesion-processing nucleases to undamaged DNA. Therefore we hypothesize that certain core complex components must function to support the spatially defined FANCD2 monoubiquitination reactions upon DNA damage.

Fig. 1.3 FA core complex E3 ligase compared with two classes of E3 ligases – one of a kind or fitting in?

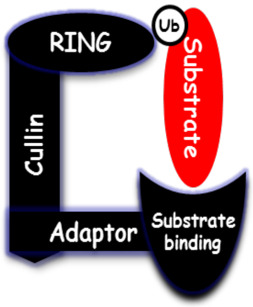
RING
Ub
Substrate
Cullin
Adaptor
Substrate binding

Cullin-based E3 ligases

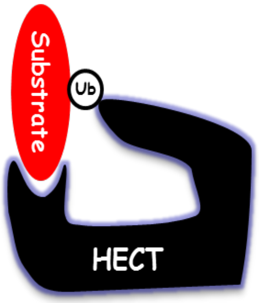
Substrate
Ub
HECT

HECT domain-based E3 ligases

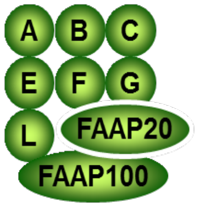
A
B
C
E
F
G
L
FAAP20
FAAP100

FANC core E3 ligases

Fanconi anemia sub complex

Previous protein-protein interaction studies suggested that FA core proteins form sub complexes. These sub complexes may be important in loading the core complex to the damaged sites and in response to other kinds of DNA damage such as oxidative stress (Futaki et al., 2002). Before our study, these sub complexes and their specialized functions in ICL-induced DNA damage response are not clear.

As to the sub complex involving FANCG, previous studies have shown that FANCG interacts with FANCA and FAAP20, forming an FANCA-FANCG sub complex (Ali et al.; Yan et al.). FAAP20 is suggested to anchor FANCL to the damaged site through binding to ubiquitinated histone (Yan et al.). FANCA has been shown to bind to DNA which likely contributes to the recruitment of the core components to the DNA damage site for ICL repair (Yuan et al., 2012). Additionally, FANCG plays a structural role as a scaffolding protein with the TPR motifs (Blom et al., 2004; Hussain et al., 2006).

FANCB, FANCL, and FAAP100 form the B-L-100 sub complex as (Ling et al., 2007; Medhurst et al., 2006). Interestingly, *in vitro* studies have indicated that FANCL itself was sufficient to ubiquitinate the FANCD2, in the absence of the whole core complex (Longerich et al., 2009; Sato et al., 2012). Thus, it suggests that the function of other core components might be either optimizing the E3 ligation action to enhance the efficiency, or facilitating its localization to the damage sites.

FANCC, FANCE, and FANCF form the third sub complex inside the FA core complex. Similar to the A-G-20 and B-L-100 sub complexes, FANCC, FANCE, and FANCF also interact and stabilize each other. Previous studies have shown that FANCF acts as an adapter protein for the core complex (Leveille et al., 2004). Recent studies also showed that

FANCF binds to FANCM through the N-terminal 158aa motif of FANCF and the MM2 motif of FANCM. This interaction might contribute to the loading of the core complex to the DNA damage sites (Deans and West, 2009).

Taken together, there are three sub complexes existing in the core complex, which may exert unique functions contributing to the FANCI/D2 ubiquitination and ICL repair. Based on the presence of the sub complexes, we performed epistatic analysis among the core component genes and hypothesized that there are different functional modules in the core complex enabling the spatially defined monoubiquitination reaction of FANCI/D2 complex.

CHAPTER II

Generation of FA Core Gene Somatic Knockout Cell Lines

Introduction

Based on the current model, FA core complex consisting of six FA proteins (A, B, C, E, F, G, and L) and two FA associate proteins (FAAP20 and FAAP100), activates the FA pathway upon DNA damage by ubiquitinating the FANCI/D2 complex. This ubiquitination event is a hallmark of the FA pathway activation. Monoubiquitinated FANCI/D2 complex has presumed functions of recruiting DNA lesion-processing endonucleases (Kratz et al.; Liu et al.; MacKay et al.; Smogorzewska et al.) (Knipscheer et al., 2009) and transcriptional activation factor of tumor suppressor gene(s) (Park et al., 2013). For example, mono-ubiquitinated FANCI/D2 enables the recruitment of FAN1 (named as FANCD2-associated nuclease). FAN1 is the virus-type replication-repair nuclease domain shown to have 5'-3' exonuclease activity and structure-specific 5'-flap endonuclease activity. These activities enable FAN1 to unhook crosslinks in ICL repair (Kratz et al.; Liu et al.; MacKay et al.; Smogorzewska et al.).

Although the FA core complex provides the key E3 ligase for FANCI/D2 ubiquitination, understanding of most FA core components is limited to their presence in the core complex. Studies have shown that FANCL containing the RING domain bears the E3 ligase activity (Alpi et al., 2008; Meetei et al., 2003). Aside from that, most other components of the core complex do not have recognizable motifs or clearly defined functions regarding their contributions to the DNA damage induced FANCD2/I monoubiquitination.

Therefore, it is important to study the epistatic relationship among the FA core complex and define functions of each FA core component as to how they contribute to the FANC I/D2 monoubiquitination and cellular response to DNA damage.

Previous studies suggested that FA proteins form three distinct sub complexes A-G-20, B-L-100, C-E-F (Ali et al.; Yan et al.) (Ling et al., 2007; Medhurst et al., 2006) (Leveille et al., 2004). These sub complexes and their functions in ICL-induced DNA damage response have not been revealed. FANCF binds to FANCM which might contribute to the loading of the core complex to the DNA damage sites (Deans and West, 2009).

FANCM, a highly conserved helicase, has a DEAH helicase domain with ATP-dependent DNA translocase activity (Hoadley et al.; Meetei et al., 2005). FANCM forms a complex with FAAP24 and the histone-fold protein MHF1/MHF2 (Ciccia et al., 2007; Yan et al.). This complex is important for recruiting the FA core complex to the ICL site (Kim et al., 2008) and stabilizing and remodeling the stalled DNA replication forks (Gari et al., 2008a; Gari et al., 2008b; Yan et al.). Also, the FANCM/FAAP24 complex is suggested to play a role in ATR-mediated cell cycle checkpoint activation (Collis et al., 2008; Huang et al.; Schwab et al.) and to load the Bloom complex to the ICL sites to suppress sister chromatid exchange (Deans and West, 2009). FANCM is also involved in recombination-independent ICL repair by promoting PCNA ubiquitination thus facilitating the recruitment of NER factor ERCC1 to the ICL sites (Wang et al., 2013).

Since the classical FA pathway is primarily conserved within vertebrates, genetic platforms such as drosophila and yeast could not be employed. Although FA knockout mouse models have been established, few of them showed the developmental abnormalities as FA patient, or bone marrow failure nor developed acute myeloid leukemia (Koomen et al., 2002;

Yang et al., 2001). In this study, I generated a series of isogenic cells with single and double knockout of several key core complex genes in the human cell line HCT116, which allows the epistatic analysis in human cells and elucidation of the functions of the FA core components in an isogenic background. This chapter describes the generation of the knockout cell lines while the following chapters will describe the epistatic analysis and functional studies.

Materials and Methods

Cell culture

Human colorectal carcinoma cell line (HCT116) and human embryonic kidney cell line 293T (HEK293T) were obtained from the American Type Culture Collection (ATCC). HCT116 cells and the somatic knockout derivatives were all cultured in Dulbecco's Modification of Eagles Medium (DMEM) plus 10% fetal calf serum (FBS) with humidified 5% CO2 at 37°C.

Targeting construct

FANCG targeting vector was constructed with the USER cloning system (New England BioLabs). In detail, two homology arms (about 1.5 kb) were PCR amplified from parental HCT116 genomic DNA with the following primers (the underlined sequence were the specific primers, while the prefix sequences each with a uracil were for cloning purpose).

FANCG Left arm forward: GGGAAAGUAGCAGTGCAAGTACAGAGCGGCAC

FANCG Left arm reverse: GGAGACAUTGTTGGTCTTACAGACTGCTCCCCCA

FANCG Right arm forward: GGTCCCAUACGAGGAGGTTGTAGGCTTGGAGC

FANCG Right arm reverse: GGCATAGUGGCCCCCAGACTGGACAGACAGAA

The amplified homologous arms were resected by USER to give end overhangs and cloned into the digested modified pAAV-USER vector (triple Flag tag removed from the previous AAV-USER-3×FLAG-KI vector) with a floxed neomycin resistance gene (*neo*) cassette (Zhang et al., 2008) (Fig 2.1).

rAAV-mediated gene targeting

The recombinant adeno-associated virus (rAAV) was packaged by co-transfecting the targeting vector, pAAV-RC and pHelper plasmid into HEK293T cells. The viral stocks were obtained 3 days after transfection by a freeze-thaw lysis method. Briefly, cells were pelleted and lysed with 3 cycles of freeze in dry ice-ethanol bath for 10 min and thaw in 37 °C water bath for 10 min. After centrifugation the viral supernatant was used to infect the HCT116 cells, which were then plated at low density 2 days later for single colony formation under G418 selection (1mg/ml).

PCR screening

About 14 days later, G418-resistant single colonies were picked into 96-well plate. Pools were made, genomic DNA of pools were prepared and screened for the gene targeting event with PCR with the following primers. Single colonies in the positive pool were screened with the Lyse-and-Go PCR reagents (Thermo Scientific). PCR primer pairs to detect positive targeting events were designed as one in the neo cassette, the other outside of the homologous arm to ensure the correct homology-mediated replacement (Fig 2.2).

FANCG TAF: GCCCGGCCCCAGCGTATGAC

FANCG TAR: GCGCATCGCCTTCTATCGCCTTCTTG

neoS2: GCGGCATCAGAGCAGCCGATTGTCT

3F1: GCGCATCGCCTTCTATCGCCTTCTTG

The positive clones were infected with Ade-Cre virus to remove the *neo* cassettes. After 1 day of incubation, cells were seeded in low density (about 100-200 cells/10cm plate), and then about 24 colonies were picked 14 days later. The colonies were screened by PCR for the complete removal of the *neo* cassette with the primers as follows:

FANCG TAF: GCCCGGCCCCAGCGTATGAC

FANCG KOR: CACCTGGACCAACACAGGCCG

To target the second allele of *FANCG*, the heterozygous clones were infected with the targeting rAAV virus again. During the screening for positive targeting event, primers as following specific to amplify wild type *FANCG* was used to exclude re-targeting event.

FANCG lossF: AGGATATCCAGCGGAGCCTAGAGAGAG

FANCG lossR: GATGATCTATTCCAGCGTGCCTCCTCA

Confirmed null clones were then infected with Ade-Cre virus to excise *neo* cassette. And PCR were carried out with the primers (named as *FANCG* KOF+KOR, *FANCG* lossF+lossR) to confirm the total loss of the target gene (Fig 2.3).

Complementation of FA knock out cell lines

For complementation purpose, *FANCB*$^{-}$ cells were transfected with Flag-FANCB cDNA in a pIRES-NEO3 vector. *FANCG*$^{-/-}$ cells were transfected with pIRES-PURO3-FANCG. The vector pIRES-PURO3 is modified by adding 3*Flag upstream of the MCS. *FANCL*$^{-/-}$ cells were transfected with pDEST-SFB-FANCL.

Generation of double knockout cell lines

FANCB was targeted in the *FANCG*$^{-/-}$ and *FAAP20*$^{-/-}$ cells to make the FANCG-/- *FANCB*$^{-}$ and *FAAP20*$^{-/-}$ *FANCB*$^{-}$ cells. *FANCB* targeting vector was constructed by a former lab member Yingjun Jiang with the same cloning system with the primers as the following.

FANCB Left arm forward: GGGAAAGUatatggtgagaggtaggagtctgg

FANCB Left arm reverse: GGAGACAUtacttgtcttgcaactcactctcc

FANCB Right arm forward: GGTCCCAUtctgagtacaacctgatggtgttt

FANCB Right arm reverse: GGCATAGUtgtttttcccctaccatttcttta

FANCB LF: aaaatccttgcccagcccaatgtca

FANCB RR: gggattcaaacccagggtacgtgtg

neoS2: GCGGCATCAGAGCAGCCGATTGTCT

3F1: GCGCATCGCCTTCTATCGCCTTCTTG

FANCB lossF: gctaaggcagagagtgggaaaccac

FANCB lossR: agtcaccacactgctgtaagcagga

To make *FANCG*$^{-/-}$*FANCM*$^{-/-}$ cells, the FANCM targeting on the *FANCG*$^{-/-}$ was carried out as before (Wang et al., 2013).

Western blot

Cells were lysed by NETN buffer (150 mM NaCl, 20 mM Tris-HCl, pH 8.0, 1 mM EDTA, 0.5% Nonidet P-40, with complete Mini Protease Inhibitor Cocktail (Roche 04693159001)) on ice for 30min. After centrifuging at 4°C, 14,000 rpm for 5min, the supernatants were collected as whole cell extracts. Protein concentration was measured by Bradford's methods. The whole cell extracts with equal amount of total protein were boiled with SDS 2×loading buffer, boiled at 100°C heat block for 10min, short spun, brief vortexed, and loaded to SDS-PAGE gel for electrophoresis. Semi-dry transfer was applied with nitrocellulose membrane. The blots were blocked and incubated with primary antibody over night at 4°C. After washing, HRP-conjugated secondary antibody was applied at room temperature for 1 hr. And then wash the membrane before exposure to enhanced chemiluminescence reagent (Amershanm Biosciences) and film development.

Immunoprecipitation

Whole cell lysates were obtained with NETN buffer. Protein concentration was measured by Bradford's methods. Lysates with equal amount of total protein were incubated with protein G beads for 2 hour at 4°C. The pre-cleared sample were obtained by collecting the supernatant after centrifugation and incubated with specific immunoprecipitation antibody over night at 4°C. Then protein G beads were added and rotated for at least 1 hr. at 4°C, after which the beads washed and were boiled with SDS sample buffer to collect the immunoprecipitates.

Immunofluorescence Staining

Cells were seeded on cover slips in 6-well plate with low density and then treated with MMC. After 24 hours of treatment, cells were washed with PBS, fixed with 3% formaldehyde, and permeabilized with 0.5% Triton buffer (20 mM HEPES pH7.4, 50 mM NaCl, 3 mM MgCl2, 300 mM sucrose, 0.5% Triton-X-100). Samples were then incubated with 5% BSA buffer for blocking, then the specific primary and secondary antibodies each for 1 hour at room temperature. Finally the cover slips were mounted onto glass slides with VECTASHIELD® Mounting Media with DAPI (Vector Laboratories H-1200) and observed with Nikon Eclipse 90i fluorescence microscopy.

Antibodies

Anti-human FANCB, FANCM, FANCL, and FAAP20 was described previously (Meetei et al., 2005; Wang et al., 2013). The commercial antibodies used in this study are shown as follows, anti-human FANCD2 (Novus NB100-182); anti-human FANCG (Novus

NB100-2566); anti-β-tubulin (Sigma-Aldrich T4026); peroxidase-conjugated rabbit anti-mouse (Jackson ImmunoResearch 315-035-048); peroxidase-conjugated goat anti-rabbit (Jackson ImmunoResearch 111-035-144); Fluorescein (FITC)-conjugated donkey anti-rabbit (Jackson ImmunoResearch 711-095-152).

Results

Targeting strategy of *FANCG*

Homologous recombination mediated gene targeting was used to knockout *FANCG* in HCT116 cells. The target vector carried by rAAV contained a neo cassette for selection, flanked by two ~1.5kb homologous arms (Fig 2.1). Through homologous replacement, exon 3 and 4 should be substituted by the neo cassette, leading to early frame shift mutation of *FANCG* gene and thus premature termination and disruption of *FANCG* expression. After excision of neo cassette by introduction of Ade-Cre virus, the heterozygous *FANCG* clone could be targeted again for the second allele and thus to make the *FANCG* null cell line.

Fig. 2.1 Schematics of homologous recombination-mediated targeting of *FANCG* in HCT116 cell line.

UTR: untranslated region; HA: homologous arm; TK: thymidine kinase gene promoter; Neo: neomycin resistance gene expression cassette; L-ITR: left inverted tandem repeats; R-ITR: right inverted tandem repeats. The number labeled on top of each exon is the exon name.

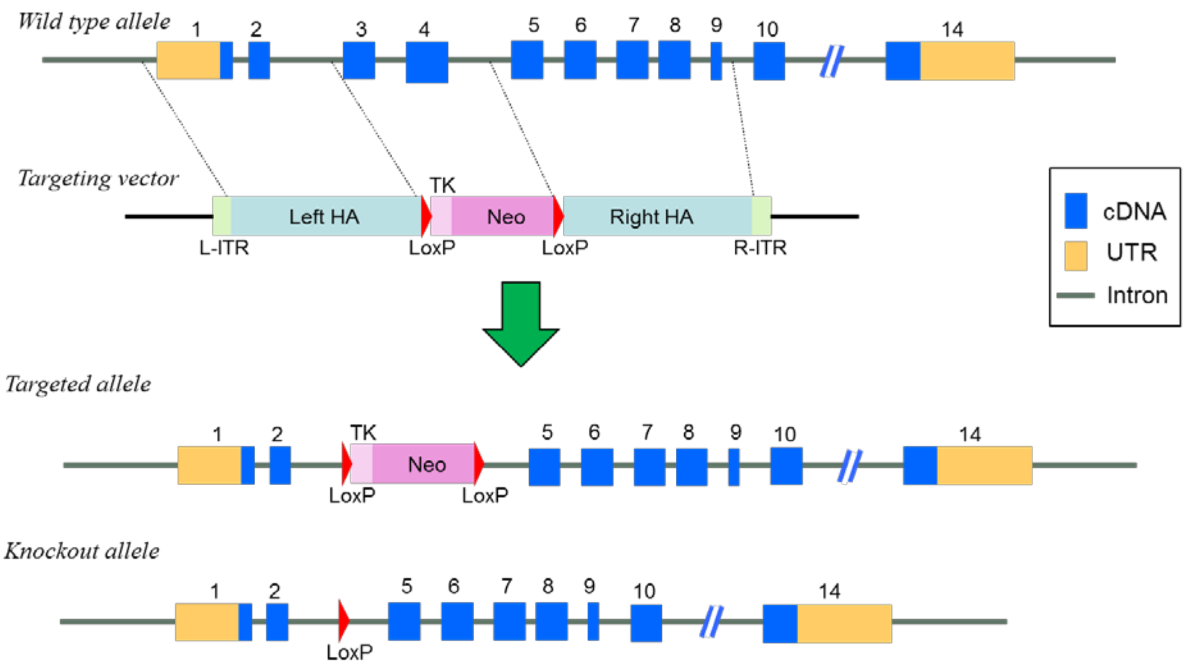
Wild type allele
1
2
3
4
5
6
7
8
9
10
14
Targeting vector
TK
Left HA
Neo
Right HA
L-ITR
LoxP
LoxP
R-ITR
cDNA
UTR
Intron
Targeted allele
1
2
TK
Neo
5
6
7
8
9
10
14
LoxP
LoxP
Knockout allele
1
2
5
6
7
8
9
10
14
LoxP

Generation of heterozygous *FANCG*$^{+/-}$ cell lines

The FANCG targeting vector-containing rAAV stocks were used to infect HCT116 cells, colonies after G418 selection were screened for positively-targeted clones by PCR with primers as indicated (Fig 2.2A). For *FANCG* first allele targeting, I have picked ~300 colonies, and screened out 2 *FANCG* $^{+/n}$ clones, as shown (Fig 2.2B).

One of the positive clones was expanded, exposed to Ad-Cre virus, plated at low density to obtain *FANCG*$^{+/-}$ clones. The viral stock had high titer, resulting in high frequency of positive excision events. As shown (Fig. 2.2C, D), 22 out of 24 colonies picked were positive. These *FANCG*$^{+/-}$ clones with neo cassette removed and genotyping confirmed (Fig. 2.2C, D), were ready for second allele targeting.

Fig. 2.2 Generation of *FANCG*$^{+/n}$ and *FANCG*$^{+/-}$ clones.

(A) PCR primers designed to screen for *FANCG*$^{+/n}$ clone. HA: homologous arm; TK: thymidine kinase promoter; Neo: neomycin resistance gene cassette.

(B) PCR confirming the correct targeting of *FANCG* using *FANCG* TAF/neoS2 primer pair and 3F1/*FANCG* TAR primer pair. *FANCG*$^{+/n}$ clone #2 was used for the Cre excision.

(C) PCR primers designed to screen for *FANCG*$^{+/-}$ clone. HA: homologous arm; TK: thymidine kinase promoter; Neo: neomycin resistance gene cassette.

(D) PCR screening for *FANCG*$^{+/-}$ clone after Cre excision using *FANCG* TAF/KOR primer pair. As seen, out of 24 clones, only the neo cassettes of #10 and #11 were not excised. Δ, knockout allele. wt, wild type allele.

MW, molecular weight size maker.

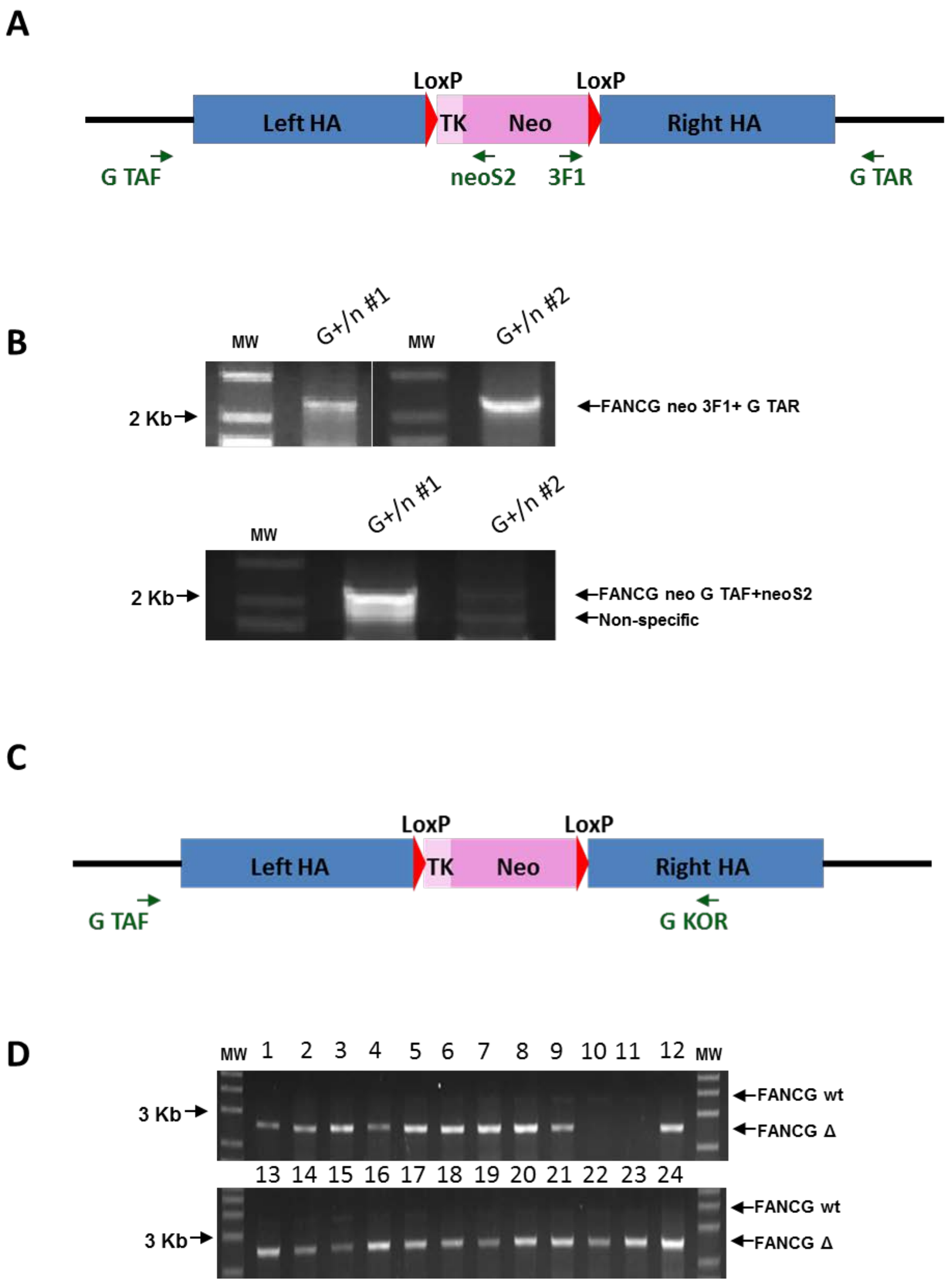
A
LoxP
LoxP
Left HA
TK
Neo
Right HA
G TAF
neoS2
3F1
G TAR
B
MW
G+/n #1
MW
G+/n #2
2 Kb
FANCG neo 3F1+ G TAR
MW
G+/n #1
G+/n #2
2 Kb
FANCG neo G TAF+neoS2
Non-specific
C
LoxP
LoxP
Left HA
TK
Neo
Right HA
G TAF
G KOR
D
MW 1 2 3 4 5 6 7 8 9 10 11 12 MW
3 Kb
FANCG wt
FANCG Δ
13 14 15 16 17 18 19 20 21 22 23 24
3 Kb
FANCG wt
FANCG Δ

Generation of *FANCG*$^{n/-}$ somatic knockout cell lines

One of the *FANCG*$^{+/-}$ clone was seeded for second allele targeting. After infected with the *FANCG* targeting vector containing rAAV virus, cells were again selected by G418. The resistant clones were picked and screened for positive targeting. Since both alleles can be targeted with equal frequency, re-targeting event should be excluded by PCR to confirm the complete disruption of both alleles (Fig 2.3A, B). In total, ~1000 colonies were screened, 4 clones are positively targeted, from which only one was confirmed to be *FANCG*$^{n/-}$ clone by genotyping with wild type allele specific primers (Fig 2.3C, D).

Fig. 2.3 Generation of the *FANCG*$^{n/-}$ clone.

(A) Primers designed for screening *FANCG*$^{-/n}$ clone identification. TK: thymidine kinase promoter; HA: homologous arm; Neo: neomycin resistance gene.

(B) PCR genotyping of the *FANCG*$^{-/n}$ clones (#4), the retargeted *FANCG*$^{+/n}$ clones (#6) , and the non-targeted *FANCG*$^{+/-}$(# 1, 2, 3, 5, 7, 8). Δ, knockout allele. wt, wild type allele.

(C) Primers designed to confirm the *FANCG*$^{-/n}$ clone. This primer pair was specific to the targeting sequence which should be replaced by neo cassette in targeted allele.

(B) PCR genotyping of the *FANCG*^{wt} clone, *FANCG*$^{+/n}$ clone, *FANCG*$^{+/-}$ clone, *FANCG*$^{n/-}$, and non-template control (-, in which distilled water was amplified). Δ, knockout allele. wt, wild type allele.

MW, molecular weight size marker.

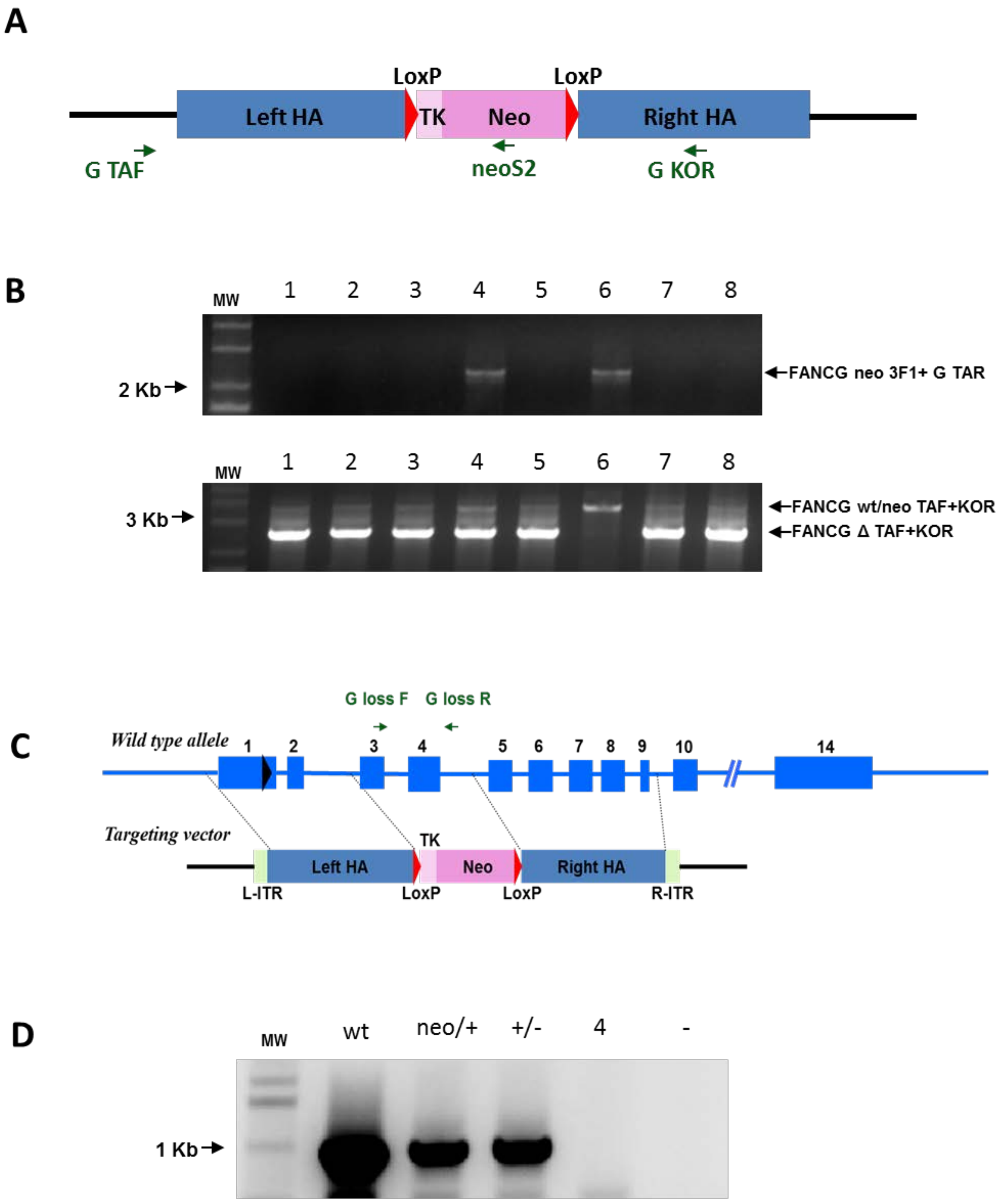
A
LoxP
LoxP
Left HA
TK
Neo
Right HA
G TAF
neoS2
G KOR
B
MW
1
2
3
4
5
6
7
8
2 Kb
FANCG neo 3F1+ G TAR
MW
1
2
3
4
5
6
7
8
3 Kb
FANCG wt/neo TAF+KOR
FANCG Δ TAF+KOR
G loss F
G loss R
C
Wild type allele
1
2
3
4
5
6
7
8
9
10
14
Targeting vector
TK
Left HA
Neo
Right HA
L-ITR
LoxP
LoxP
R-ITR
D
MW
wt
neo/+
+/-
4
-
1 Kb

Generation of *FANCG*$^{-/-}$ somatic knockout cell lines

The *FANCG*$^{n/-}$ clone was infected with Ade-Cre virus and seeded in low density to obtain clones with the neo cassette removed (Fig 2.4A, B). Western blot was used to confirm the complete loss of *FANCG* expression in the *FANCG*$^{-/-}$ cells (Fig 2.4C).

Fig. 2.4 Generation of the *FANCG*$^{-/-}$ clone.

(A) PCR screening for *FANCG*$^{-/-}$ clone with primer *FANCG* TAF+KOR. #4, #5, #12, and #19 could be *FANCG*$^{n/-}$, while the rest are all *FANCG*$^{-/-}$. Δ, knockout allele. wt, wild type allele.

(B) PCR genotyping of the *FANCG*^{wt} clone, *FANCG*$^{+/-}$ clone, two *FANCG*$^{-/-}$ clones, and non-template control (-, in which distilled water was amplified). Primers for PCR were indicated under the corresponding image. Δ, knockout allele. wt, wild type allele.

(C) Western blots confirming the complete loss of *FANCG* expression in *FANCG*$^{-/-}$ cells.

MW, molecular weight size marker.

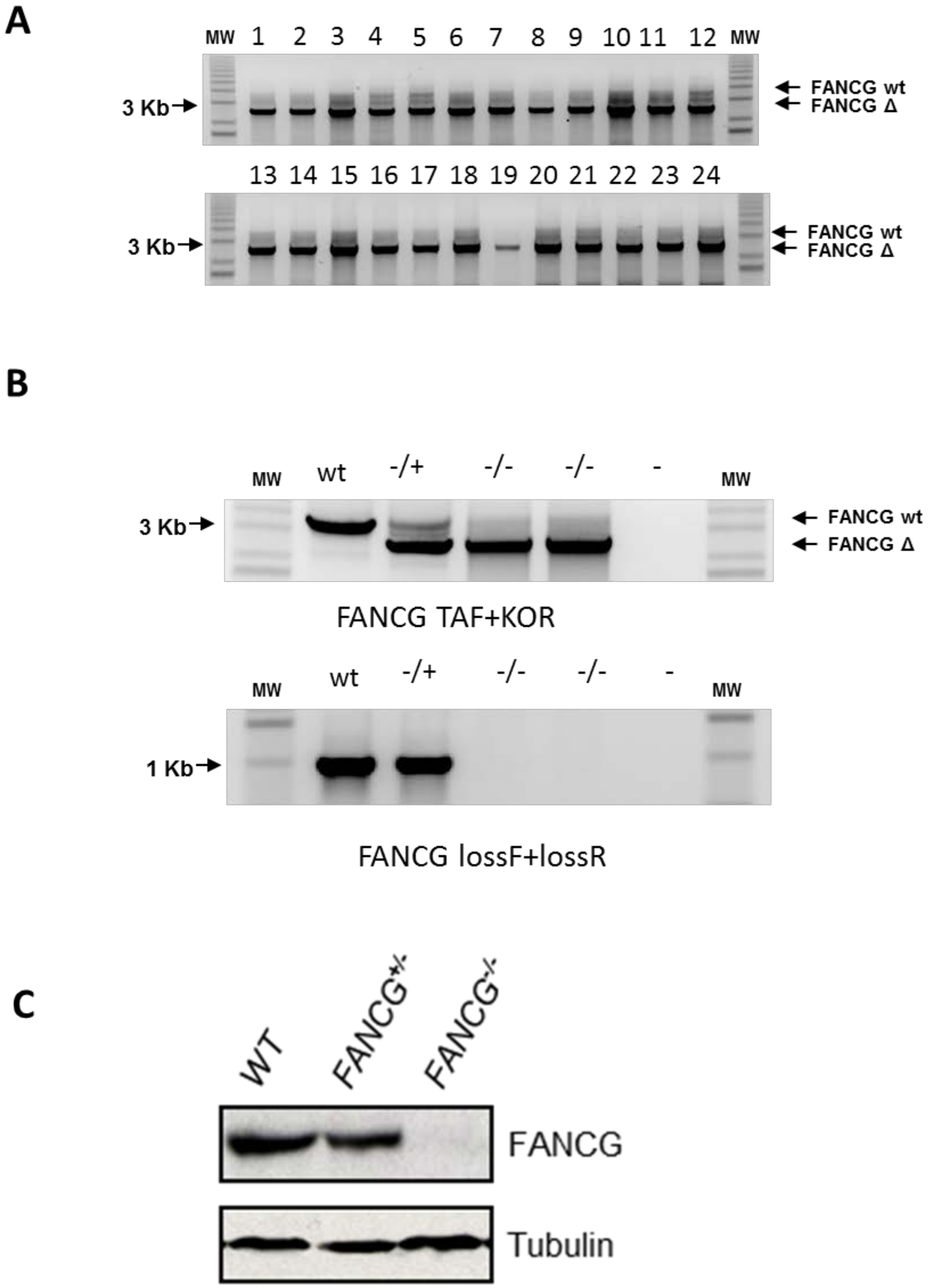
A
MW 1 2 3 4 5 6 7 8 9 10 11 12 MW
3 Kb
FANCG wt
FANCG Δ
13 14 15 16 17 18 19 20 21 22 23 24
3 Kb
FANCG wt
FANCG Δ
B
MW wt -/+ -/- -/- - MW
3 Kb
FANCG wt
FANCG Δ
FANCG TAF+KOR
MW wt -/+ -/- -/- - MW
1 Kb
FANCG lossF+lossR
C
WT
FANCG+/-
FANCG-/-
FANCG
Tubulin

Confirmation of *FANCB*$^{-}$ cell line and Generation of *FAAP20*$^{-/-}$ and *FANCL*$^{-/-}$ knockout cell line

FANCB targeting was designed and done by Dr. Yingjun Jiang (a former postdoctoral researcher in Dr. Lei Li's lab). Since *FANCB* gene is an X-linked gene and HCT116 cell line is derived from a male patient, Dr. Yingjun Jiang removed the only allele to generate the *FANCB* null mutant. As shown (Fig 2.5A), exon 3, the first coding exon was deleted through homologous recombination-mediated targeting strategy. To verify the loss of FANCB, I did IP-western as shown (Fig 2.5B).

FAAP20 and *FANCL* targeting was designed and done by Dr. Justin Leung (a former postdoctoral fellow in Dr. Junjie Chen's lab) (Leung et al.). I obtained the *FAAP20*$^{n/-}$ and *FANCL*$^{n/-}$ from him and added Ade-Cre virus to remove the neo cassette. As shown (Fig 2.5C, D), I verified the genotype of *FAAP20*$^{-/-}$ and *FANCL*$^{-/-}$ clone by PCR and the corresponding protein loss by western blot.

Fig. 2.5 Generation of *FANCB*$^{-}$, *FAAP20*$^{-/-}$, and *FANCL*$^{-/-}$ cell lines.

(A) Schematics of *FANCB* targeting strategy. UTR: untranslated region; HA: homologous arm; TK: thymidine kinase gene promoter; Neo: neomycin resistance gene expression cassette; L-ITR: left inverted tandem repeats; R-ITR: right inverted tandem repeats. The number labeled on top of each exon is the exon name.

(B) IP-Western result showing complete loss of FANCB protein expression in the *FANCB*$^{-}$ cell line.

(C) PCR result confirming the *FAAP20*$^{-/-}$ and *FANCL*$^{-/-}$ cell lines. Δ, knockout allele. wt, wild type allele.

(D) Western result showing complete loss of FAAP20 and FANCL protein expression in the *FAAP20*$^{-/-}$ and *FANCL*$^{-/-}$ cell lines, respectively.

MW, molecular weight size marker.

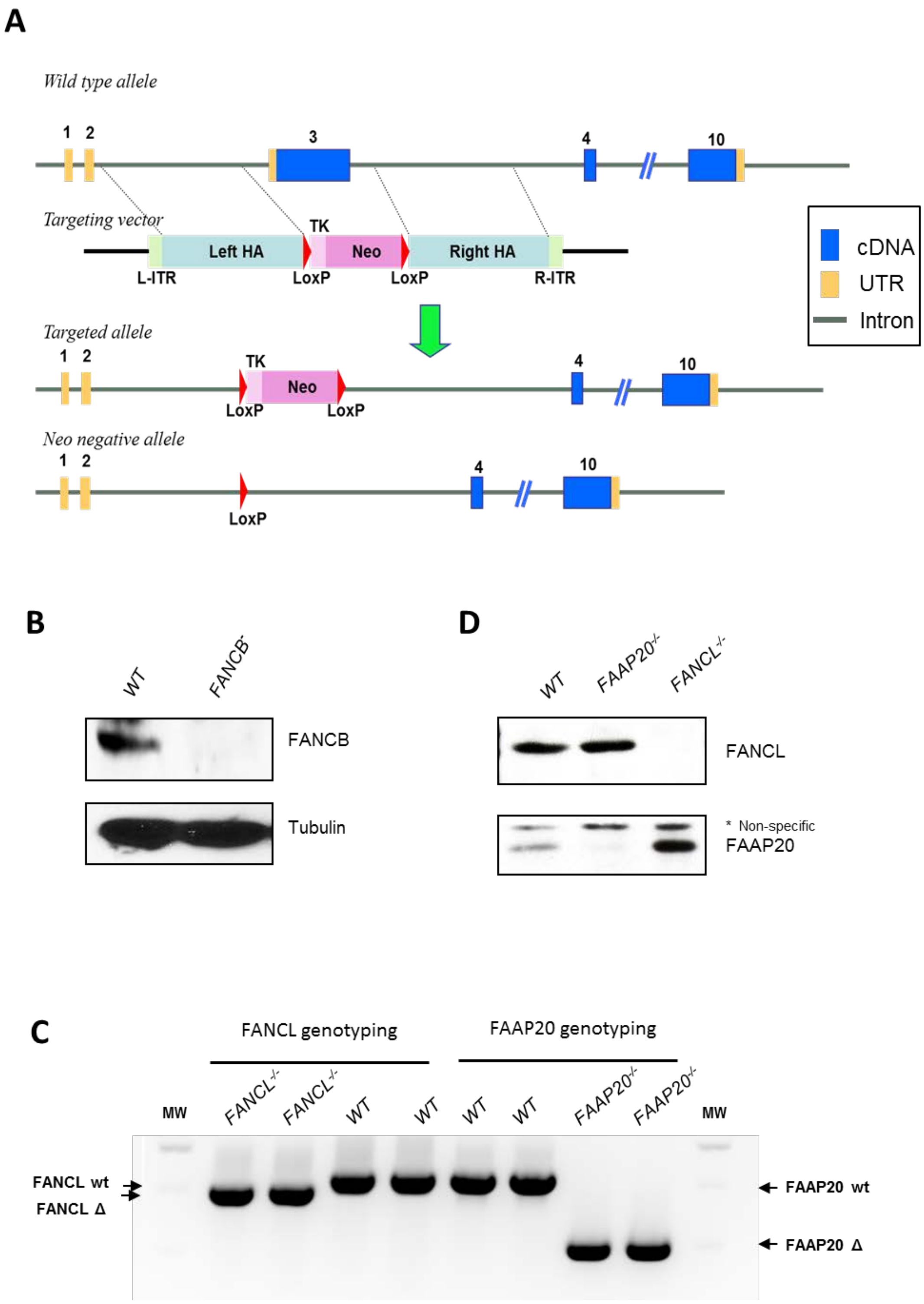
A
Wild type allele
1
2
3
4
10
Targeting vector
TK
Left HA
Neo
Right HA
L-ITR
LoxP
LoxP
R-ITR
cDNA
UTR
Intron
Targeted allele
1
2
TK
Neo
LoxP
LoxP
4
10
Neo negative allele
1
2
LoxP
4
10
B
WT
FANCB-
FANCB
Tubulin
D
WT
FAAP20-/-
FANCL-/-
FANCL
* Non-specific
FAAP20
C
FANCL genotyping
FAAP20 genotyping
MW
FANCL-/-
FANCL-/-
WT
WT
WT
WT
FAAP20-/-
FAAP20-/-
MW
FANCL wt
FANCL Δ
FAAP20 wt
FAAP20 Δ

Complementation of FA knock out cell lines

In order to exclude the clonal effect of each FA knockout cell lines, complementation of the single knock out cell lines, *FANCG*$^{-/-}$, *FANCB*$^{-}$, and *FANCL*$^{-/-}$ was carried out. Full length *FANCG*, *FANCB*, and *FANCL* were introduced back to the corresponding mutant cell lines. Immunofluorescence staining was conducted to confirm that FANCD2 foci formation, a marker for the FA activation, could be restored when the deficient cell were complemented with the specific gene (Fig 2.6A-C).

Fig. 2.6 Complementation of *FANCG*$^{-/-}$, *FANCB*$^{-}$, and *FANCL*$^{-/-}$ single knockout cell lines.

(A) Immunofluorescence staining for MMC-induced FANCD2 foci formation confirming the complementation of *FANCG*$^{-/-}$ cell line. *GFL*, full-length *FANCG*.

(B) Immunofluorescence staining for MMC-induced FANCD2 foci formation confirming the complementation of *FANCB*$^{-}$ cell line. *BFL*, full-length *FANCB*.

(C) Immunofluorescence staining for MMC-induced FANCD2 foci formation confirming the complementation of *FANCL*$^{-/-}$ cell line. *LFL*, full-length *FANCL*.

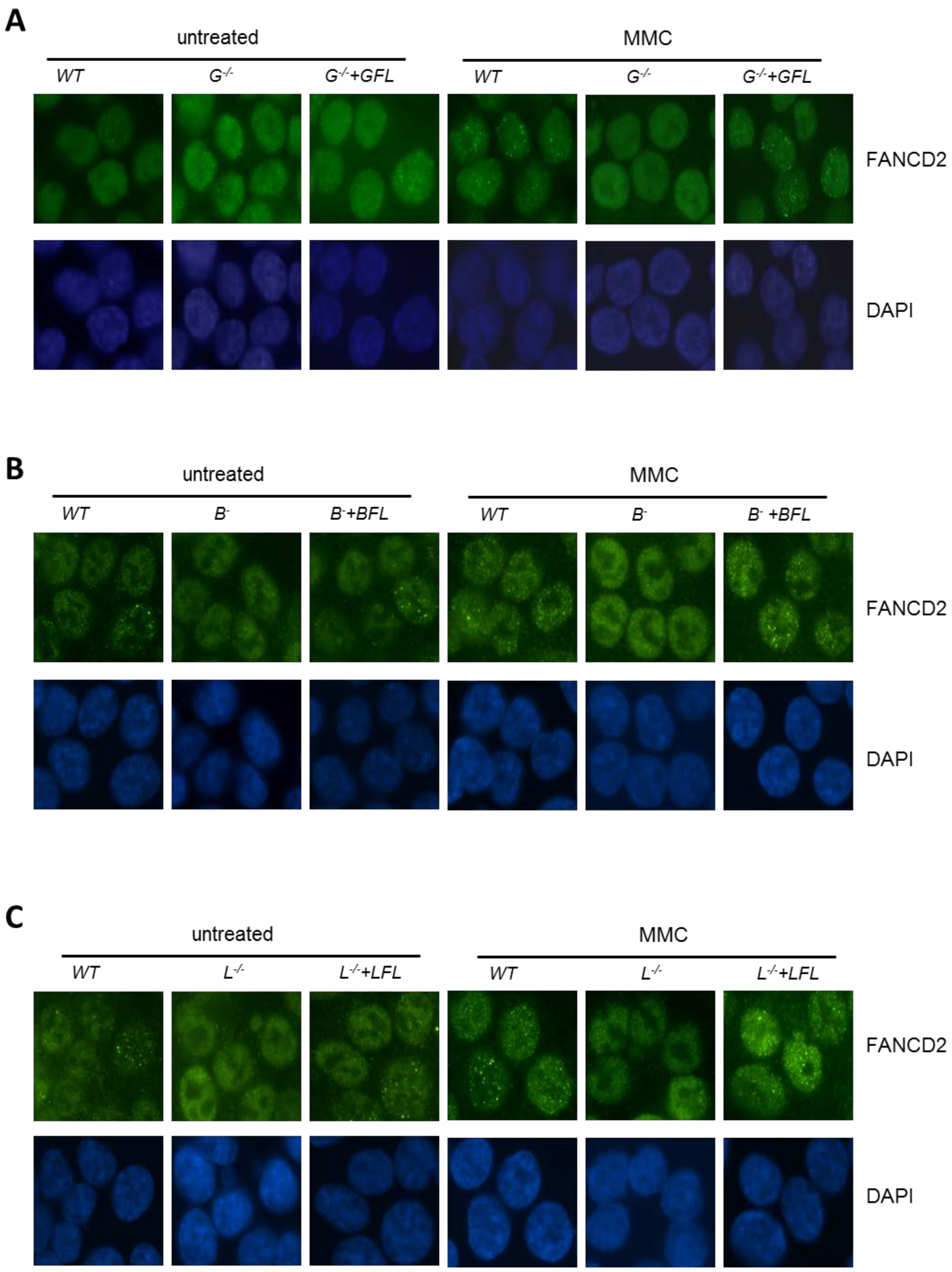
A
untreated
MMC
WT
$G^{-/-}$
$G^{-/-}$+GFL
WT
$G^{-/-}$
$G^{-/-}$+GFL
FANCD2
DAPI
B
untreated
MMC
WT
B^{-}
B^{-}+BFL
WT
B^{-}
B^{-} +BFL
FANCD2
DAPI
C
untreated
MMC
WT
$L^{-/-}$
$L^{-/-}$+LFL
WT
$L^{-/-}$
$L^{-/-}$+LFL
FANCD2
DAPI

Generation of *FANCG*$^{-/-}$ *FANCB*$^{-}$, *FAAP20*$^{-/-}$ *FANCB*$^{-}$, and *FANCG*$^{-/-}$ *FANCM*$^{-/-}$ somatic double knockout cell lines

FANCB was targeted in the *FANCG*$^{-/-}$ and *FAAP20*$^{-/-}$ mutant cells to obtain the *FANCG*$^{-/-}$*FANCB*$^{-}$ and *FAAP20*$^{-/-}$*FANCB*$^{-}$ double mutants, respectively. *FANCB* targeting vector was constructed by a former lab member Yingjun Jiang with the same cloning system with the primers as shown before. The *FANCB* targeting efficiencies in *FANCG*$^{-/-}$ cells and *FAAP20*$^{-/-}$ cells were 2/500 clones and 7/1200 clones respectively. The genotyping of representative cell lines were confirmed as shown (Fig 2.7A, B)

To make *FANCG*$^{-/-}$*FANCM*$^{-/-}$ cells, the *FANCM* targeting on the *FANCG*$^{-/-}$ was carried out as previously described (Wang et al., 2013). In the first allele targeting, one out of ~400 screened clones was positive as *FANCG*$^{-/-}$*FANCM*$^{n/+}$. Following the standard procedure, Ade-Cre virus was added to remove the neo cassette. For the second allele target, one out of ~240 clones screened turned out to be *FANCG*$^{-/-}$*FANCM*$^{n/-}$. Again, neo cassette was excised by Cre to generate the *FANCG*$^{-/-}$*FANCM*$^{-/-}$ cell line (Fig 2.7C). Western blot was also used to verify the complete disruption of FANCM protein expression (Fig 2.7D).

Fig. 2.7 Generation of *FANCG*$^{-/-}$*FANCB*$^{-}$, *FAAP20*$^{-/-}$*FANCB*$^{-}$, and *FANCG*$^{-/-}$*FANCM*$^{-/-}$ double knockout cell lines.

(A) PCR genotyping of *FANCG* and *FANCB* in wt, *FANCG*$^{-/-}$, *FANCB*$^{-}$, and *FANCG*$^{-/-}$*FANCB*$^{-}$ clones. Δ, knockout allele. wt, wild type allele.

(B) PCR genotyping of *FAAP20* and *FANCB* in wt, *FAAP20*$^{-/-}$, *FANCB*$^{-}$, and *FAAP20*$^{-/-}$*FANCB*$^{-}$ clones. Δ, knockout allele. wt, wild type allele.

(C) PCR genotyping of *FANCG* and *FANCM* in wt, *FANCG*$^{-/-}$, *FANCM*$^{-/-}$, and *FANCG*$^{-/-}$*FANCM*$^{-/-}$ clones. Δ, knockout allele. wt, wild type allele.

(D) Western blot confirming complete protein loss of *FANCG* and *FANCM* in the *FANCG*$^{-/-}$*FANCM*$^{-/-}$ cell line.

MW, molecular weight size maker

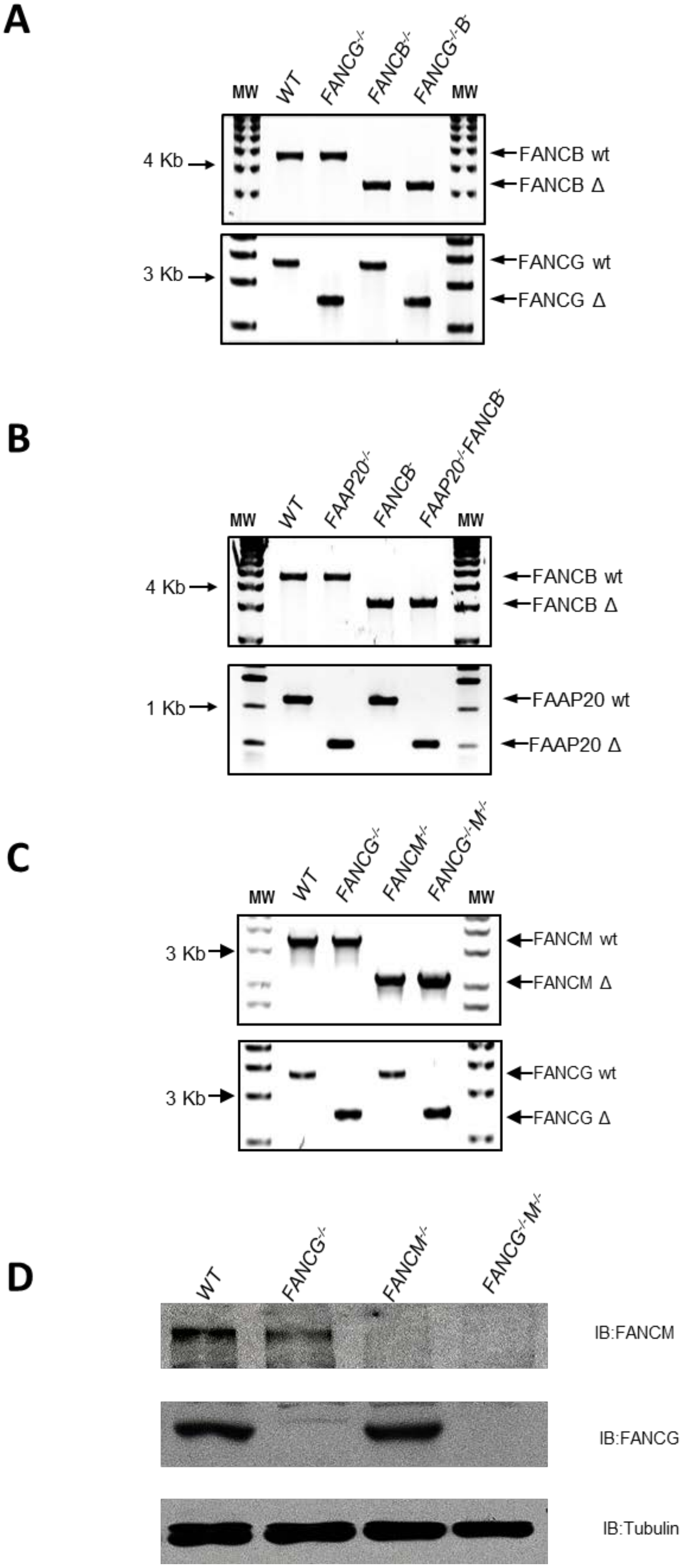
A
MW
WT
FANCG-/-
FANCB-/-
FANCG-/-B-
MW
4 Kb
FANCB wt
FANCB Δ
3 Kb
FANCG wt
FANCG Δ
B
MW
WT
FAAP20-/-
FANCB-
FAAP20-/-FANCB-
MW
4 Kb
FANCB wt
FANCB Δ
1 Kb
FAAP20 wt
FAAP20 Δ
C
MW
WT
FANCG-/-
FANCM-/-
FANCG-/-M-/-
MW
3 Kb
FANCM wt
FANCM Δ
3 Kb
FANCG wt
FANCG Δ
D
WT
FANCG-/-
FANCM-/-
FANCG-/-M-/-
IB:FANCM
IB:FANCG
IB:Tubulin

Discussion

The FA core complex plays an essential role as the E3 ligase activity for FANCI/D2 ubiquitination, which is the central event of the FA pathway activation in response to DNA damage. As the classical FA pathway is primarily conserved within vertebrates, genetic models such as yeast and drosophila could not be used. While mouse models with FA deficiency failed in generating phenotype compared to FA patients, the hypomorphic nature of mutations in FA patient cells prevents reliable functional readout of FA core components. Thus, I generated *FANCG* null human cell line in HCT116 background, which allows the functional study of *FANCG* in the FA pathway and cellular response to DNA damage.

To conduct the epistatic study among FA genes, I took advantage of *FANCM* and *FANCB* previously established to construct *FANCG*$^{-/-}$*FANCB*$^{-}$, *FAAP20*$^{-/-}$*FANCB*$^{-}$, and *FANCG*$^{-/-}$*FANCM*$^{-/-}$ cell lines. With these mutants, epistatic relationship among the FA core genes can be accessed by conducting functional studies on these cell lines comparing with wild type and the single mutants.

As mentioned before, FANCG forms a sub complex with FANCA and FAAP20. FANCA has been suggested to have DNA binding activity (Yuan et al., 2012). FAAP20 was also proposed to anchor ubiquitinated histone to recruit the FA core complex (Yan et al.). The role of the A-G-20 sub complex in the loading of FA core complex is of particular interest to us. FANCG is considered as a scaffolding protein with seven TPR motifs (Blom et al., 2004; Hussain et al., 2006). A likely function is to maintain the integrity of the sub complex. By studying the epistasis of *FANCG* with other core component using the isogenic cell lines, we are able to determine whether *FANCG* has functions independent of the FA core complex and how it interacts genetically with other core complex components.

The advantage of our model lies on the isogenicity of the cell lines created (Rago et al., 2007). Compared with the patient cell line, our system provide a complete isogenic null background In contrast to siRNA/shRNA-based, off-target effect is minimum, since the long homologous arms make the targeted recombination highly specific. Although the HCT116 cell line is immortalized and transformed from a colon cancer cell line, it is a stable diploid cell line with relatively normal background (Roschke et al., 2002). Despite the defined mutation in mismatch-repair gene MLH1, it has proficient machineries for all other DNA damage repair (Papadopoulos et al., 1994; Umar et al., 1994). These features make it suitable platform for DNA damage response, checkpoint and chromosomal stability studies.

In conclusion, I have generated *FANCG*$^{-/-}$, *FANCG*$^{-/-}$*FANCB*$^{-}$, *FAAP20*$^{-/-}$*FANCB*$^{-}$, and *FANCG*$^{-/-}$*FANCM*$^{-/-}$ cell lines and employed the previously established *FANCM*, *FAAP20*, *FANCL*, and *FANCB* null mutants. Those models not only allow the precise functional studies of the FA core genes but also make it possible for epistatic analysis among FA core genes in a human cellular system.

CHAPTER III

FANCL, FANCB, and FAAP100 Form the Catalytic Module of the FA Core Complex

Introduction

Upon DNA damage, signaling kinases such as ATM or ATR phosphorylate several FA proteins that contribute to the activation of the FA pathway. The FA core complex provide the E3 ligase activating the FA pathway through monoubiquitination of the FANCI/D2 complex on FANCD2 lysine 561 (Garcia-Higuera et al., 2001) and FANCI lysine 523 (Smogorzewska et al., 2007), respectively. FANCI/D2 complex monoubiquitination is the key event of the FA pathway activation. The functions of this modified FANCI/D2 have been suggested to have nuclease activity (Pace et al., 2010), nucleosome chaperone and assembly activity (Sato et al., 2012), and transcriptional activity (Park et al., 2013). More directly related to DNA ICL repair, FANCI/D2 complex itself can recognize stalled forks or processed lesion (Joo et al.). And the monoubiquitinated FANCI/D2 are suggested to recruit downstream effectors, including endonucleases (Knipscheer et al., 2009; Kratz et al.; Liu et al.; MacKay et al.; Smogorzewska et al.). For the S-phase DNA interstrand cross link repair, ubiquitinated FANCI/D2 is required for the nucleolytic incisions near the lesion and translesion DNA synthesis bypassing the lesion (Knipscheer et al., 2009).

One example of the endonuclease recruited to chromatin by the monoubiquitinated FANCI/D2 is FAN1, which has 5’-3’ exonuclease and 5’-flap structure-specific endonuclease activities (Liu et al.). With the FANCD2-dependent recruitment to the DNA damaged site, FAN1 is able to resect the exposed DNA ends and excise stalled replication fork structures. These properties might play a role in the crosslink unhooking step of the ICL repair process by coordinating with other structure-specific nucleases such as XPF-ERCC1 and MUS81-EME1 (Kratz et al.; Liu et al.; MacKay et al.; Smogorzewska et al.). Another nuclease-related factor recruited by ubiquitinated FANCI/D2 is SLX4, or FANCP, which is a docking platform for structure-specific nucleases such as SLX1, XPF-ERCC1, and MUS81-EME1 (Yamamoto et al., 2011).

Transcription-regulatory activity of monoubiquitinated FANCI/D2 complex on tumor suppressor gene has been suggested. TP63, a p53 family member, promotes apoptosis and suppresses tumorigenesis. Monoubiquitinated FANCD2 was found to directly bind to the promoter region of TP63 gene and promotes the transcription of TP63, thus preventing tumorigenesis (Park et al., 2013). The ubiquitination deficient FANCD2 mutant K561R, however, lost its ability to bind to the promoter region and transactivate TP63 upon DNA damage and oncogene stimulation.

Collectively, monoubiquitination of FANCD2 is the central event of the FA pathway activation. Monoubiquitinated FANCD2 can tether the upstream signaling and the downstream effectors for essential cellular response to DNA damage. Thus studying how the FANCD2 is ubiquitinated provides important insight into FA biology and the DNA repair mechanisms.

As mentioned in Chapter I, FANC I/D2 is ubiquitinated by the FA core complex, which consists of A, G, C, E, F, B, L, and two FA associated protein FAAP100 and FAAP20. The relationships between FA core proteins have been shown to be very complicated (Hodson and Walden, 2012). It is generally suggested that FA core proteins form three sub complexes as shown (Fig. 3.2A). FANCA, FANCG, and FAAP20 form a sub complex (Ali et al.; Garcia-Higuera et al., 1999; Kruyt et al., 1999; Reuter et al., 2000; Waisfisz et al., 1999; Yan et al.). FANCB, FANCL, and FAAP100 form another sub complex (Ling et al., 2007; Medhurst et al., 2006). It is still controversial whether FANCL or the B-L-100 sub complex is sufficient for FANCI/D2 ubiquitination or not, as *in vitro* studies indicating that FANCL itself was sufficient to ubiquitinate the FANCD2 (Longerich et al., 2009), whereas most studies showing that loss of the other FA core genes including A, B, C, E, F, G, and FAAP100 abolished the FANCI/D2 ubiquitination (Garcia-Higuera et al., 2001; Howlett et al., 2002; Ling et al., 2007; Meetei et al., 2004; Vandenberg et al., 2003; Yamamoto et al., 2005). Another sub complex is composed of FANCC, FANCE, and FANCF (Leveille et al., 2004; Leveille et al., 2006; Medhurst et al., 2001; Pace et al., 2002; Taniguchi and D'Andrea, 2002). However, the specific roles of each sub complex in the FA core complex are still unclear.

Although there are evidences shown that sub complexes exist in the core complex, understanding of most of the core components is still limited to their presence in the core complex. Except for FANCL which has been shown to have the RING domain bearing the E3 ligase activity (Alpi et al., 2008; Meetei et al., 2003), most of the FA core complex or the sub complexes do not have clearly defined functions contributing to ubiquitination action induced by DNA damage signaling. Therefore, our goal is to study the epistatic relationships among the FA core genes and define functions of each FA core component in the process of FANC I/D2 monoubiquitination and cellular response to DNA damage. Based on these, we hypothesized that the sub complexes exert differential functions contributing to the FANCI/D2 ubiquitination and ICL repair. To test our hypothesis, systematic epistatic analysis and functional studies were conducted to define the roles of the FA core genes especially in resisting against DNA ICL damage and mediating the spatially defined monoubiquitination of FANCI/D2 complex.

Materials and Methods

Cell culture

Human colorectal carcinoma cell line (HCT116) and the derived FA mutant cell lines were all cultured in Dulbecco's Modification of Eagles Medium (DMEM) plus 10% fetal calf serum (FBS) with humidified 5% CO2 at 37°C.

DT40 wild type and knockout cells were generated via published procedures and cultured in RPMI-1640 medium plus 10% FBS, 1% chicken serum, 5µM 2-mercaptoethanol, and 10mM HEPES, at 39.5°C.

Antibodies

Anti-human FANCL, FAAP100, FAAP20, and FANCM antibody, and Anti-chicken FANCD2 was described previously (Ling et al., 2007; Meetei et al., 2003; Wang et al., 2013; Yamamoto et al., 2005; Yan et al.). The commercial antibodies are the following: anti-human FANCD2 (Abcam ab2187, Santa Cruz SC-20022, Novus NB100-182); anti-human FANCI (Bethyl A300-254A); anti-human FANCA (Bethyl A301-980A); anti-human FANCG (Novus NB100-2566); anti-histone H3 (Millipore 05-928); anti-β-tubulin (Sigma-Aldrich T4026); anti-FLAG M2 (Sigma-Aldrich F3165); peroxidase-conjugated rabbit anti-mouse (Jackson ImmunoResearch 315-035-048); peroxidase-conjugated goat anti-rabbit (Jackson ImmunoResearch 111-035-144).

Immunoprecipitation

Whole cell lysates were obtained with NETN buffer. Protein concentration was measured by Bradford's methods. Lysates with equal amount of total protein were incubated with protein G beads (Protein G Sepharose 4 Fast Flow, GE Healthcare 17-0618-01) for 2 hour at 4°C. The precleared sample were obtained by collecting the supernatant after centrifugation and incubated with specific immunoprecipitation antibody over night at 4°C. Then protein G beads were added and rotated for at least 1 hr. at 4°C, after that the beads were washed, boiled with 2× Laemmli SDS sample buffer, and pelleted. The supernatants were collected as immunoprecipitates.

Gel filtration

To obtain the nuclear cell extracts for gel filtration, cells were incubated in hypotonic buffer (10 mM Tris, pH 7.4, 1.5 mM MgCl2, 10 mM KCl, 0.5 mM Dithiothreitol, and protease inhibitors (Roche 04693159001)) on ice. After 10 min, NP-40 (0.1% final concentration) was added and nuclei were pelleted by 10-sec centrifugation at 5,500 × g. After washing three times with hypotonic buffer, the nuclei were lysed in nuclear extract buffer (10 mM Tris, pH 7.4, 150 mM NaCl, 1% NP40, 0.5% sodium deoxycholate, 1 mM EDTA, 1 mM Dithiothreitol , and protease inhibitors). Subsequently, the nuclear extract (about 2 mg total protein) was applied directly to a Superose 6 10/300 GL column (GE Healthcare 17-5172-01). The fractions of 0.4ml were collected and analyzed by western blot.

Chromatin fractionation

To obtain chromatin-bound protein fraction, cells were lysed with NETN buffer (100 mM NaCl, 20 mM Tris-HCl, pH 8.0, 0.5 mM EDTA, 0.5% Nonidet P-40, with cOmplete Mini Protease Inhibitor Cocktail Tablet (Roche Applied Science 11836153001)) at 4 °C for 30 min and centrifuged for 30 min at 14,000 rpm for collection of the insoluble pellet. The soluble fraction was collected as the soluble fraction. The insoluble fraction was then lysed with 0.2 N HCl for 30 min on ice and centrifuged for 30 min at 14,000 rpm. The supernatant was later neutralized with 1 N Tris-HCl (pH 8.0) and collected as the chromatin fraction.

Western blot

Cells were lysed by NETN buffer (150 mM NaCl, 20 mM Tris-HCl, pH 8.0, 1 mM EDTA, 0.5% Nonidet P-40, with complete Mini Protease Inhibitor Cocktail (Roche 04693159001)) on ice for 30min. After centrifuging at 4°C, 14,000 rpm for 5min, the supernatants were collected as whole cell extracts. Protein concentration was measured by Bradford's methods. The whole cell extracts with equal amount of total protein were boiled with SDS 2×loading buffer, boiled at 100°C heat block for 10min, short spun, brief vortexed, and loaded to SDS-PAGE gel for electrophoresis. Semi-dry transfer was applied with nitrocellulose membrane afterwards. The blots were blocked and incubated with primary antibody over night at 4°C. After washing, HRP-conjugated secondary antibody was applied at room temperature for 1 hr. And then wash the membrane before exposure to enhanced chemiluminescence reagent (Amershanm Biosciences) and film development.

Clonogenic survival assay

Equal amount of cells were seeded in 100 mm culture plate. The next day, cells were exposed to ICL damage agents at different dosages for 1 hr. After that, cells were washed, trypsinized, and seeded with appropriate cell number in 100 mm culture plates, by triplicates per dosage per cell line. After grown for approximately 14 days, colonies were fixed by glutaraldehyde 6.0% (v/v) and stained with 0.5% crystal violet (w/v) in ethanol. Colonies about 50-200 per plate were counted and used to calculate the relative survival with the following equation: % survival = # of colonies counted / (# of cells plated × plating efficiency) × 100.

Mitotic spread and cytogenetic analysis

For spontaneous and MMC-induced chromosomal abnormality analysis, cells were grown in low density and mocked treated or treated with 20 ng/ml MMC for 18 hrs. Cells were collected after colcemid treatment (0.1 μg/ml) for 1 hr. Cells were then swelled in hypotonic solution (0.075M KCl) at RT for 15 min and then fixed by methanol: acetic acid (3:1). The fixed cells were dropped into slides and stained with 4% Giemsa. Chromosomal abnormalities were quantified under bright field microscope by scoring more than 50 metaphases per sample.

Results

Confirmation of sub complexes in the FA core complex

To investigate the function of each protein in cellular response to ICL DNA damage, we created *FANCG*$^{-/-}$ and *FANCB*$^{-}$ knockout mutants via homology-mediated replacement targeting in HCT116 cell line as mentioned in Chapter II. The strict isogenicity among these knockout mutants allows direct comparison of protein functions.

To further verify the existence of the sub complexes in the FA core complex, protein-protein interdependency and interaction were analyzed with the *FANCG*$^{-/-}$, *FANCB*$^{-}$, *FANCL*$^{-/-}$, and *FAAP20*$^{-/-}$ cell lines. As shown in Fig 3.1A, FANCG knockout significantly reduced the level of FANCA and FAAP20, and FAAP20 deficiency decreased the level of FANCA. On the other hand, FANCL and FAAP100 level was greatly reduced in *FANCB*$^{-}$ cells. Immunoprecipitation studies showed that the A-G-20 sub complex still existed in the absence of FANCB or FANCL, in that the interaction between FANCA and FANCG or FANCA and FAAP20 remained in FANCB and FANCL null cells (Fig. 3.1B). On the other hand, the B-L-100 sub complex remains intact in the absence of FANCG or FAAP20, in that the interaction between FANCL and FAAP100 remained in FANCG and FAAP20 null cells (Fig. 3.1C). Similar results were obtained in the condition of MMC treatment (data not shown). In summary, our study demonstrated that the A-G-20 and B-L-100 sub complexes physically presented in the human cells. If one of the sub complexes collapsed, the other still existed and might function in the ICL induced cellular response.

Fig. 3.1 Formation of sub modules within the FA core complex.

(***A***) Immunoblot detecting FA core complex protein levels in *FANCG*$^{-/-}$, *FANCB*$^{-}$, *FANCL*$^{-/-}$, and *FAAP20*$^{-/-}$ knockout mutant cells. Whole cell extracts were prepared from unperturbed mutant cell lines in human HCT116 background. Protein stability interdependencies are observed in the *FANCG*$^{-/-}$, *FANCB*$^{-}$, and *FANCL*$^{-/-}$ mutants.

(***B***) Co-immunoprecipitation of FANCA in *FANCG*$^{-/-}$, *FANCB*$^{-}$, *FANCL*$^{-/-}$, and *FAAP20*$^{-/-}$ mutants, indicating the presence of the A-G-20 sub module.

(***C***) Co-immunoprecipitation of FANCL in *FANCG*$^{-/-}$, *FANCB*$^{-}$, *FANCL*$^{-/-}$, and *FAAP20*$^{-/-}$ mutants, indicating the presence of the B-L-100 module.

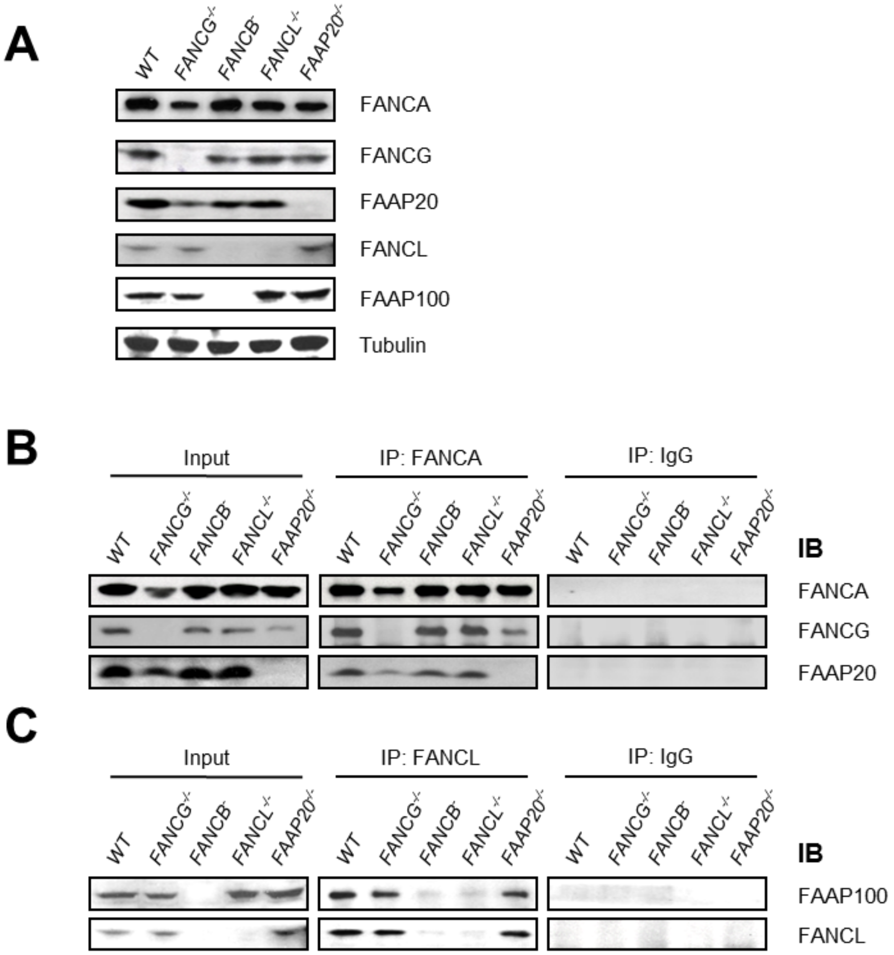
A
WT
FANCG-/-
FANCB-
FANCL-/-
FAAP20-/-
FANCA
FANCG
FAAP20
FANCL
FAAP100
Tubulin
B
Input
IP: FANCA
IP: IgG
IB
FANCA
FANCG
FAAP20
C
Input
IP: FANCL
IP: IgG
IB
FAAP100
FANCL

FA core complex is not an integral complex

Previous literatures and our protein-protein inter-dependency and interaction studies in the knockout mutant have collectively defined the three sub complexes inside the FA core complex (Fig. 3.2A). To verify whether deletion of individual core component impact the overall integrity of the core, gel filtration chromatography was carried out and determined the size of the core. As shown (Fig. 3.2B), deletion of FANCG and FANCL did not result in a gross disruption of the core complex, as reflected by the similar elution positions of the mutant core components to that of the wild type FA core complex (670kD). Nevertheless, it cannot be excluded that certain core component(s) may be accounted for retaining the overall complex integrity (Gordon et al., 2005). To verify the presence of such structural component(s), additional studies are required.

Fig. 3.2 FA core complex is not an integral complex.

(***A***) Depiction of three modules inside the FA core complex.

(***B***) Superose 6 gel filtration profiling of the core complex in *WT*, *FANCL*$^{-/-}$, and *FANCG*$^{-/-}$ mutants. Immunoblotting of FAAP100 and FANCL in the indicated fractions shows that the elution volumes of the core complex in wild type and mutant cells are largely consistent, suggesting that the integrity of the core complex is not overly disrupted by the deletion of *FANCG* or *FANCL*. Fraction 21 marks the void.

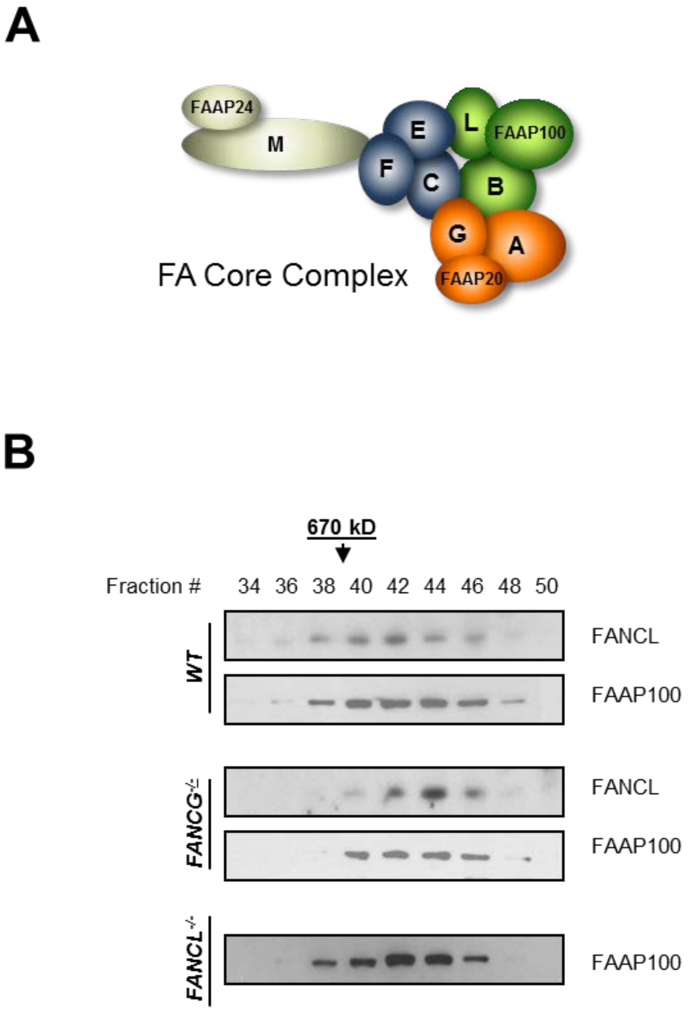
A
FAAP24
M
E
L
FAAP100
F
C
B
G
A
FAAP20
FA Core Complex
B
670 kD
Fraction #
34 36 38 40 42 44 46 48 50
WT
FANCL
FAAP100
FANCG-/-
FANCL
FAAP100
FANCL-/-
FAAP100

Identification of the B-L-100 catalytic module in the FA core complex

Loss of FANCB leads to marked decreased protein level of FANCL (Fig. 3.1A), which is previously shown to bear the E3 ligase activity for FANCD2 monoubiquitination. Thus it is plausible that FANCB also plays a more essential role than FANCG in impacting the level of FANCD2 monoubiquitination. To evaluate this hypothesis, we examined a panel of human cellular knockout mutants for DNA damage-induced FANCD2 monoubiquitination from whole cell extracts, except for FAAP20, most mutant showed a significantly reduced FANCD2 monoubiquitination. However, in the chromatin fractions prepared from cells exposed to mitomycin C where ubiquitinated form of FANCD2 is enriched, mutants devoid of FANCL, and FANCB exhibited complete loss of FANCD2 and FANCI monoubiquitination, whereas loss of G, and FAAP20 showed readily detectable levels of FANCD2 and FANCI monoubiquitination (Fig.3.3A). This was consistent in cisplatin treated cells (Fig.3.3B).

To confirm this result, DT40 FA mutant cells were tested for FANCD2 ubiquitination. As shown (Fig. 3.3C), FANCL and FAAP100 knockout led to complete ablation of monoubiquitinated FANCD2, while FANCA, G, E, and FAAP20 deficiency did not completely abolish the ubiquitination. This result suggests that FANCL, B, and FAAP100 constitute a catalytic core, which is absolutely essential for the E3 ligase activity of the FA core complex.

To exclude the possibility of differential FANCD2 total protein loss in the knockout mutants, chromatin-bound, soluble protein fractions, and whole cell extracts were tested for their FANCD2 levels and confirmed that each contained the same amount of total FANCD2 as the parental HCT116 or DT40 cells (Fig. 3.4). Thus FANCB, FANCL, and FAAP100 most likely form a highly integrated module as demonstrated by a strong interdependency of protein stabilities. On the other hand, the A-G-20 and C-E-F modules appear to play auxiliary roles in FA core complex function.

Fig. 3.3 FANCL, FANCB, and FAAP100 form the catalytic module of the FA core complex. (***A***) Immunoblot detecting MMC-induced monoubiquitination of FANCD2 and FANCL in wild type (*WT*) and the indicated knockout mutants in human HCT116 background.

(***B***) Immunoblot detecting cisplatin-induced monoubiquitination of FANCD2 in wild type (*WT*) and indicated knockout mutants in human HCT116 background.

(***C***) Immunoblot detecting MMC- and cisplatin-induced monoubiquitination of FANCD2 in wild type (*WT*) and indicated knockout mutants in chicken DT40 background.

**FANCG* gene localizes in the single Z chromosome and thus DT40 cell only have one *FANCG* allele.

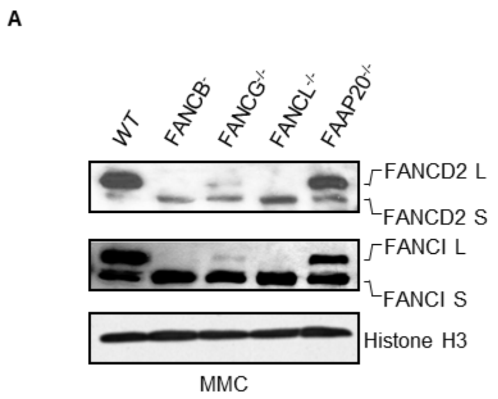
A
WT
FANCB-
FANCG-/-
FANCL-/-
FAAP20-/-
FANCD2 L
FANCD2 S
FANCI L
FANCI S
Histone H3
MMC

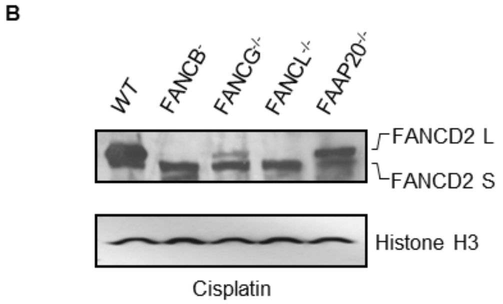
B
WT
FANCB-
FANCG-/-
FANCL-/-
FAAP20-/-
FANCD2 L
FANCD2 S
Histone H3
Cisplatin

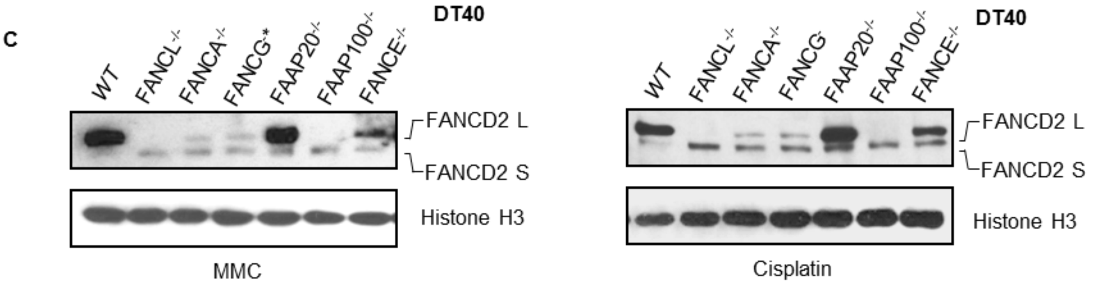
C
DT40
WT
FANCL-/-
FANCA-/-
FANCG*
FAAP20-/-
FAAP100-/-
FANCE-/-
FANCD2 L
FANCD2 S
Histone H3
MMC
DT40
WT
FANCL-/-
FANCA-/-
FANCG-
FAAP20-/-
FAAP100-/-
FANCE-/-
FANCD2 L
FANCD2 S
Histone H3
Cisplatin

Fig. 3.4 FANCD2 levels in HCT116 and DT40 knockout mutants

(***A***) Immunoblot detecting MMC-induced monoubiquitination of FANCD2 in wild type (*WT*) and the indicated knockout mutants in human HCT116 background.

(***B***) Immunoblot detecting cisplatin-induced monoubiquitination of FANCD2 in wild type (*WT*) and indicated knockout mutants in human HCT116 background.

(***C***) Immunoblot detecting MMC-induced monoubiquitination of FANCD2 in wild type (*WT*) and indicated knockout mutants in chicken DT40 background.

(***D***) Immunoblot detecting cisplatin-induced monoubiquitination of FANCD2 in wild type (*WT*) and indicated knockout mutants in chicken DT40 background.

Tubulin and Histone H3 are used as loading and extraction controls.

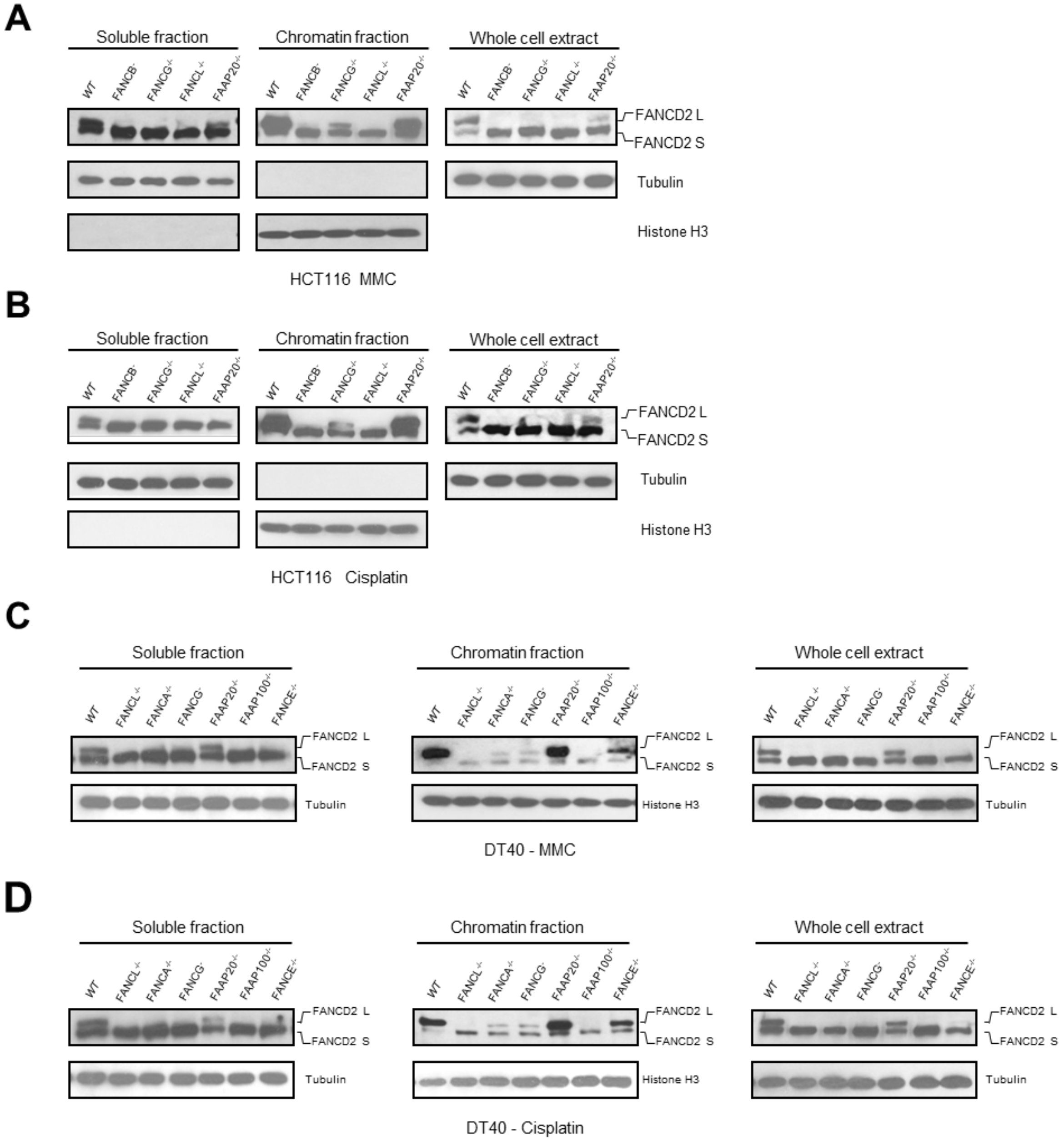
A
Soluble fraction
Chromatin fraction
Whole cell extract
WT
FANCB-
FANCG-/-
FANCL-/-
FAAP20-/-
FANCD2 L
FANCD2 S
Tubulin
Histone H3
HCT116 MMC
B
Soluble fraction
Chromatin fraction
Whole cell extract
WT
FANCB-
FANCG-/-
FANCL-/-
FAAP20-/-
FANCD2 L
FANCD2 S
Tubulin
Histone H3
HCT116 Cisplatin
C
Soluble fraction
Chromatin fraction
Whole cell extract
WT
FANCL-/-
FANCA-/-
FANCG-
FAAP20-/-
FAAP100-/-
FANCE-/-
FANCD2 L
FANCD2 S
Tubulin
Histone H3
DT40 - MMC
D
Soluble fraction
Chromatin fraction
Whole cell extract
WT
FANCL-/-
FANCA-/-
FANCG-
FAAP20-/-
FAAP100-/-
FANCE-/-
FANCD2 L
FANCD2 S
Tubulin
Histone H3
DT40 - Cisplatin

B-L-100 sub complex is more critical for cellular resistance to MMC than the A-G-20 sub complex

Since FANCD2 monoubiquitination is the central event for the FA pathway activation, which functions in the cellular resistance to ICL DNA damage, and B-L-100 is the catalytic core module of the FA core complex, it is predicted that mutants from this module leads to stronger damage sensitivity compared with other mutants from FA core complex. To test this premise, we compared four isogenic knockout mutants (Fig. 3.5A) for their crosslinking damage sensitivity and observed that loss of FANCL or FANCB rendered comparable but much more severe phenotypes than loss of FANCG or FAAP20. The variant degree of sensitivities from distinct components of the core complex seems to indicate distinct functions executed by the two different protein modules in maintaining genomic integrity of the cells in response to DNA damage. Indeed, the chromosomal analysis showed that FANCL or FANCB was more important in protecting cells from genomic instability than FANCG or FAAP20 as expected (Fig. 3.5B).

Fig. 3.5 B-L-100 sub complex is more essential for the cellular resistance to MMC than A-G-20 sub complex.

(***A***) Clonogenic survival of *FAAP20*$^{-/-}$, *FANCG*$^{-/-}$, *FANCB*$^{-}$, and *FANCL*$^{-/-}$ mutants treated with mitomycin C. Error bars were derived from SDs from 4-6 independent experiments with triplicated plates.

(***B***) Chromosomal aberration counts in *FAAP20*$^{-/-}$, *FANCG*$^{-/-}$, *FANCB*$^{-}$, and *FANCL*$^{-/-}$ mutants treated with mitomycin C. Error bars are derived from DSs from more than 50 counts per cell line.

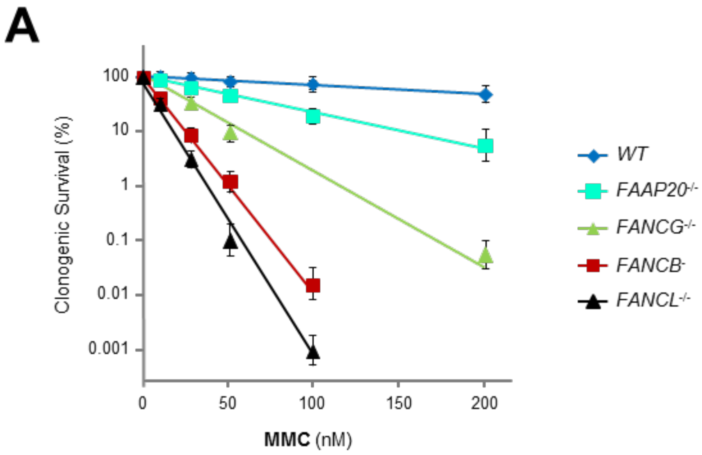
A
100
10
1
0.1
0.01
0.001
Clonogenic Survival (%)
0
50
100
150
200
MMC (nM)
WT
FAAP20-/-
FANCG-/-
FANCB-
FANCL-/-

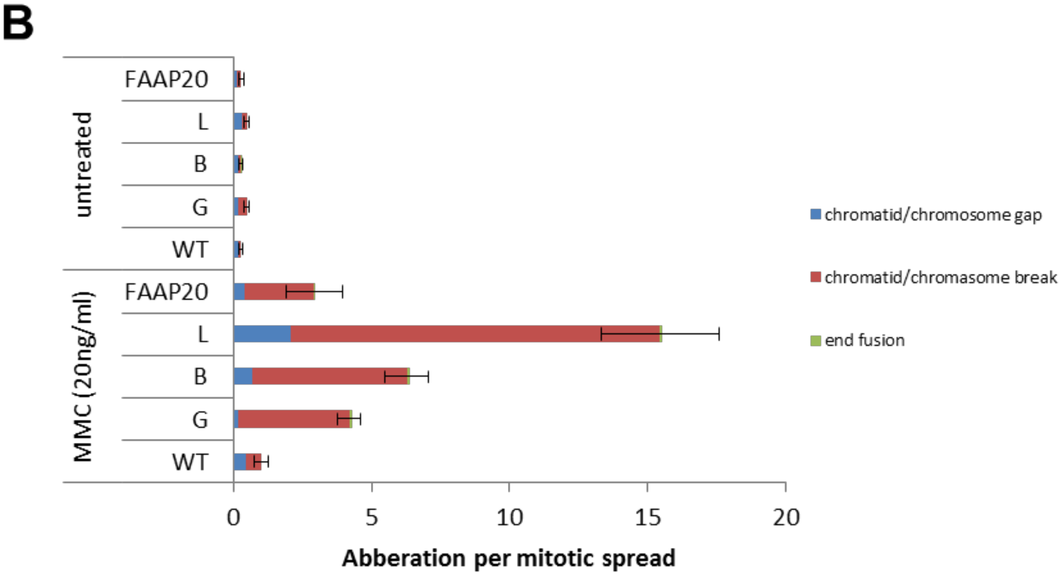
B
untreated
FAAP20
L
B
G
WT
MMC (20ng/ml)
FAAP20
L
B
G
WT
0
5
10
15
20
Abberation per mitotic spread
chromatid/chromosome gap
chromatid/chromasome break
end fusion

B-L-100 sub complex is epistatic to A-G-20 sub complex in cellular resistance to ICLs

To test the epistatic relationship among the FA core genes, clonogenic survival assay was carried out. As shown (Fig. 3.6A), the *FANCG*$^{-/-}$ mutant is significantly more resistant than *FANCB*$^{-}$ to crosslinking DNA damage, while deletion of both genes did not acquire any additional sensitivity compared to *FANCB*$^{-}$. The differential sensitivities suggest that FANCB plays an epistatic yet more important role than FANCG in cellular resistance to crosslinking DNA damage. This is also confirmed in other crosslinking agent treatment experiment such as cisplatin and formaldehyde (Fig. 3.6C and D). Given that FANCG and FAAP20 reside in the same module, we tested *FAAP20*$^{-/-}$*FANCB*$^{-}$ knockout mutants (Fig. 3.6B) and observed a similar survival profile, which implicates an epistatic but more essential function of FANCB in cellular resistance to crosslinking reagents.

Fig. 3.6 B-L-100 sub complex is epistatic to A-G-20 sub complex in cellular resistance to ICLs.

(***A***) Clonogenic survival of *FANCB*-, *FANCG*$^{-/-}$, and *FANCB*$^{-}$G$^{-/-}$ mutants treated with mitomycin C.

(***B***) Clonogenic survival of isogenic *FANCB*$^{-}$, *FAAP20*$^{-/-}$, and *FANCB-FAAP20*$^{-/-}$ mutants treated with mitomycin.

(***C***) Clonogenic survival of *FANCB*$^{-}$, *FANCG*$^{-/-}$, and *FANCB*$^{-}$*FANCG*$^{-/-}$ mutants treated with cisplatin.

(***D***) Clonogenic survival of *FANCB*$^{-}$, *FANCG*$^{-/-}$, and *FANCB*$^{-}$*FANCG*$^{-/-}$ mutants treated with formaldehyde.

Error bars were derived from SDs from four independent experiments with triplicated plates.

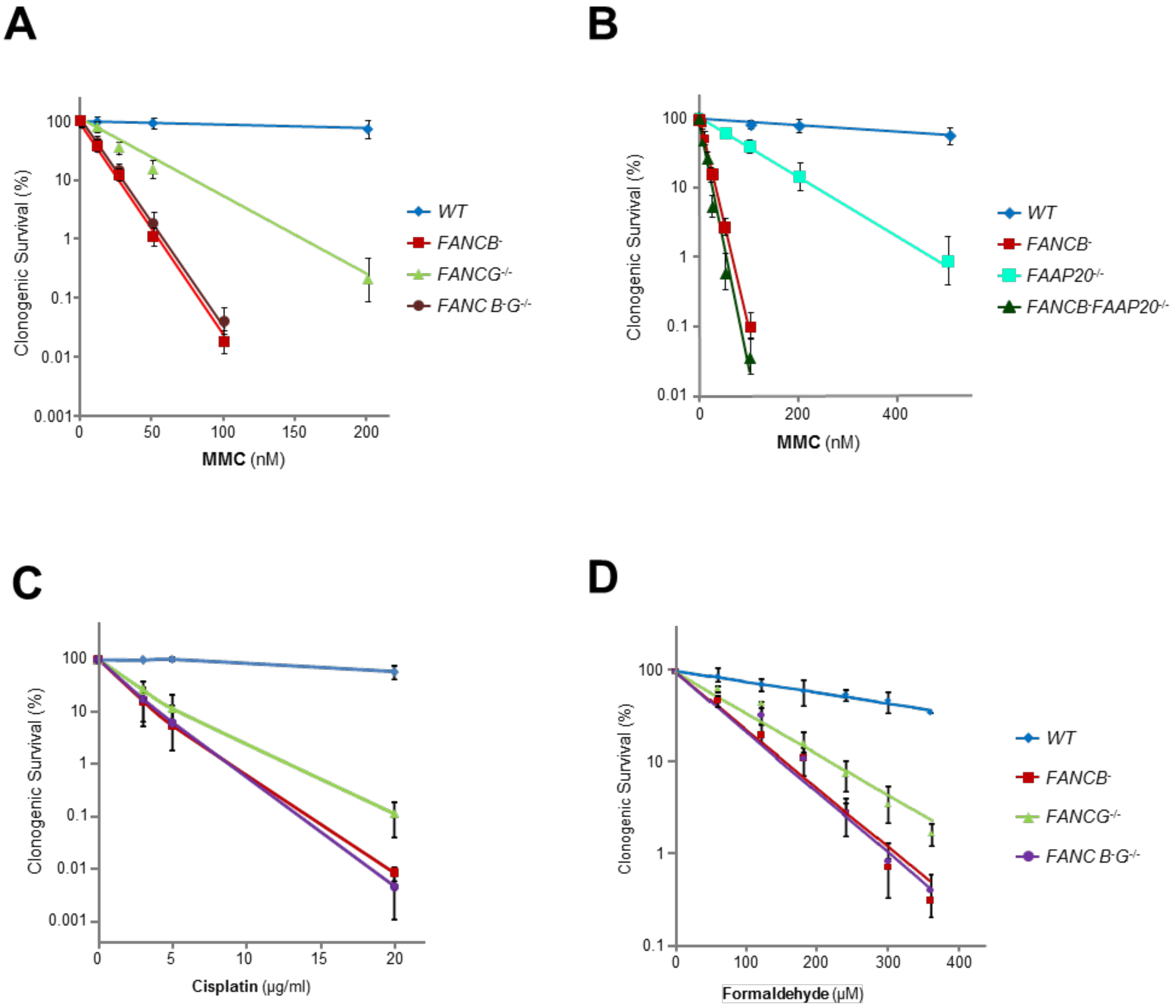
A
Clonogenic Survival (%)
100
10
1
0.1
0.01
0.001
0
50
100
150
200
MMC (nM)
WT
FANCB-
FANCG-/-
FANC B-G-/-
B
Clonogenic Survival (%)
100
10
1
0.1
0.01
0
200
400
MMC (nM)
WT
FANCB-
FAAP20-/-
FANCB-FAAP20-/-
C
Clonogenic Survival (%)
100
10
1
0.1
0.01
0.001
0
5
10
15
20
Cisplatin (μg/ml)
D
Clonogenic Survival (%)
100
10
1
0.1
0
100
200
300
400
Formaldehyde (μM)
WT
FANCB-
FANCG-/-
FANC B-G-/-

Discussion

In conclusion, our study showed that FA core genes play differential roles in ICL damage resistance based on their presence in different sub complexes. This is the first study to demonstrate that FA core complex is not working as an integral complex. Instead, it can be dissected into sub complexes/modules according to protein interaction and functional differences. Specifically, B-L-100 sub module is indispensable for FANCI/D2 ubiquitination while A-G-20 and C-E-F are less important. In addition, genetic study also defined that A-G-20 is epistatic with B-L-100 sub module.

Our study is consistent with previous *in vitro* studies that FANCL is essential to ubiquitinate the FANCD2, while the intactness of the core complex is not essential (Longerich et al., 2009). The essential role of FANCB and FAAP100 in FA pathway activation lies in the fact that they stabilize the E3 ligase FANCL by forming a sub complex to maintain a stable level of FANCL. Our finding diverged from the current paradigm that each of the core complex submit is absolutely essential for the E3 ligase of the core. This is achieved from using epistasis analyses and functional readout of cell survival.

Furthermore, our study further validated the notion that functional sub complexes exist in the core complex, A-G-20, B-L-100, and C-E-F sub complexes (Leveille et al., 2004; Ling et al., 2007; Medhurst et al., 2006; Yan et al.). B-L-100 sub complex is identified as the catalytic core module of the FA core complex. The accessory roles of A-G-20 and C-E-F sub complexes play in the FA pathway are addressed in the following Chapter IV.

As to the study of sub complex, we notice that even in the same sub complexes the binding strength and dependence among components varies. For example, FANCG and FANCA are more tightly bound compared with FAAP20 and FANCG or FAAP20 and

FANCA. The effect of FAAP20 knockout on FANCA level is intermediate compared with *FANCG* knockout, while FANCG level is not affected apparently by FAAP20 deficiency (Fig. 3.1A). This indicates that FANCA and FANCG consists the core of the sub complex. Similarly, FANCB-FANCL and FANCB-FAAP100 are more closely bound compared with FANCL-FAAP100, as FAAP100 level is not significantly affected by FANCL depletion (Fig. 3.1C).

Our study also shed new light on the disease etiology and biology of FA in different subtypes. The differential sensitivities of different FA core subunit genes may explain the different prevalence of the corresponding gene mutation among FA patients. In FA complementation subtypes, FANCA, FANCG, and FANCC have high frequency distribution, as 63%, 9%, and 12% respectively among all the FA patients genetically defined while FANCB and FANCL mutations accounts for less and 2% and 0.1%, respectively (Table 1.1 in Chapter I). Such a profound variation in complementation group distribution may be a strong reflection of their functions in FANCD2 monoubiquitination and cellular sensitivity against DNA crosslinking agents.

CHAPTER IV

Chromatin Anchoring and Loading Modules Are Required For Full Function of FA Core Complex

Introduction

The major role of the core complex in FA pathway is to catalyze the monoubiquitination of the FANCI/D2 complex. FANCI/D2 complex ubiquitination is the core of the FA pathway activation. The function of the monoubiquitinated FANCI/D2 complex is thought to recruit downstream factors to execute DNA damage repair process in response to ICL DNA damage, such as nucleases to repair ICLs (Liu et al.; MacKay et al.). However, how each of the core complex subunit functions in the ubiquitination reaction remains unclear except for the FANCL protein.

As shown in the previous Chapter (Chapter III, Fig. 3.1 & 3.2), we have found that the FA core complex that the formation of one sub complex, which depends on protein-protein interaction, does not depend on other FA core components. Moreover, in the FA core complex, only the B-L-100 sub complex is essential for the catalytic activity and more crucial for the cellular resistance to ICL DNA damage compared to the other two sub complexes. This is consistent with previous findings that FANCL with a RING domain bears E3 ligase activity and is essential to ubiquitinate the FANCI/D2 complex *in vitro* (Longerich et al., 2009). Then the next question is why vertebrate system needs many other components to execute the function.

Our previous results show that the A-G-20 and C-E-F sub complexes likely provide accessory role in the FA pathway. This is reflected by not only the residual levels of

FANCD2 ubiquitination but also the less severe ICL DNA damage sensitivity in the FANCA, FANCG, FAAP20, and FANCE deficient cell lines (Chapter III, Fig. 3.3 & 3.4). Therefore, this Chapter focuses on deciphering the functions of A-G-20 and C-E-F complexes in the FA pathway activation and ICL DNA response, specifically how they facilitate FANCI/D2 ubiquitination.

A major unanswered question in the FA pathway is how the FA core complex is recruited to the damaged site to initiate the ubiquitination reaction. FANCM has been showed by our group to play a role in loading the core complex to the damaged DNA site (Wang et al., 2013). FANCM was initially named FAAP250, as an FA associated protein during FANCA tandem affinity purification. It was first found to be mutated in a Fanconi anemia patient in 2005 and therefore identified as a FA gene (Meetei et al., 2005). It has highly conserved helicase domain with DNA translocase activity (Meetei et al., 2005). FANCM forms a complex with another FA associated protein, FAAP24 and the MHF1/MHF2 histone-fold complex.

It is proposed that FANCM complex interacts with and targets the FA core complex to chromatin (Thompson and Hinz, 2009). This model is supported by the DNA binding activities of FAAP24 and MHF complex. Indeed, FANCM is demonstrated *in vivo* to constitutively associates with chromatin, and the FANCM/FAAP24 complex can load the FA core complex to chromatin together with FAAP24, in response to DNA damage (Kim et al., 2008). The MHF proteins are also shown to possess DNA binding activity, thus they facilitate the DNA interaction of FANCM and promote the FA pathway activation (Singh et al., 2010; Yan et al.). Together, FANCM appears important for the FANCD2 ubiquitination as other FA core genes by controlling the chromatin-loading of the whole core complex.

However, results from our lab and others showed that FANCM is not essential in the activation of the FA pathway which is indicated by the considerate amount of ubiquitinated FANCD2 and the very mild phenotype in the deficient cell lines (Bakker et al., 2009; Wang et al., 2013). This indicates that additional factors may be involved in the recruitment of the FA core especially the catalytic B-L-100 sub complex to the damaged site for the full function of the FA core complex. The C-E-F sub complex is closely associated with FANCM, the MM2 motif of FANCM binds to the N-terminal 158 aa motif of FANCF (Deans and West, 2009). This is consistent with the previous finding that FANCF serves as an adapter for the core complex function (Leveille et al., 2004) and that FANCE is not essential for FANCD2 ubiquitination as shown in Chapter III. Thus it is likely that C-E-F is at least involved in the FANCM mediated initial loading of the FA core complex and there should be other factors functioning independently with FANCM.

In the A-G-20 sub complex. FAAP20 is an FA associated protein discovered that contribute to the stabilization of the FANCA and its UBZ domain has been shown to binding to DNA damage-induced H2A polyubiquitination (Ali et al.; Leung et al.; Yan et al.). FANCA has direct DNA binding affinity (Yuan et al., 2012). Thus we hypothesized that A-G-20 together also play a role in recruiting FANCL to the chromatin and the DNA damaged site independently of FANCM and the C-E-F sub complex. To test the hypothesis, chromatin-bound FANCL and the enrichment of FANCL to the ICL sites were analyzed in FA knockout and knockdown cells.

Materials and Methods

Cell culture

Human embryonic kidney cell line HEK293T, human colorectal carcinoma cell line HCT116 and the derived FA mutant cell lines were all cultured in Dulbecco's Modification of Eagles Medium (DMEM) plus 10% fetal calf serum (FBS) with humidified 5% CO2 at 37°C.

shRNA

GIPZ lentiviral shRNA plasmids were purchased from the ShRNA and ORFeome Core, the University of Texas MD Anderson Cancer Center. The mature antisense sequences of FANCF shRNAs are ACTTCAAAATCTCCATCCT (#1), TGGGTTCTCTCTATAGCCA (#2), TTCTGAAGGTCATAGTGCA (#3), and TGGAGTGTCTCCTCATCGG (#4). Lentiviruses were packaged in HEK293T cells and then used to transduce cells. Stable cell lines were obtained after puromycin selection (2ug/ml).

Antibodies

Antibodies against human FANCL and FANCM and chicken FANCD2 were described previously (Meetei et al., 2003; Wang et al., 2013; Yamamoto et al., 2005). The commercial antibodies are from the following sources: anti-human FANCD2 (Abcam ab2187, Santa Cruz SC-20022); anti-human FANCI (Bethyl A300-254A); anti-human FANCG (Novus NB100-2566); anti-histone H3 (Millipore 05-928); anti-β-tubulin (Sigma-Aldrich T4026); anti-FLAG M2 (Sigma-Aldrich F3165); anti-Myc (Santa Cruz SC-40); peroxidase-conjugated rabbit anti-mouse (Jackson ImmunoResearch 315-035-048); peroxidase-conjugated goat anti-rabbit (Jackson ImmunoResearch 111-035-144).

Chromatin fractionation

To obtain chromatin-bound protein fraction, cells were lysed with NETN buffer (100 mM NaCl, 20 mM Tris-HCl, pH 8.0, 0.5 mM EDTA, 0.5% Nonidet P-40, with cOmplete Mini Protease Inhibitor Cocktail Tablet (Roche Applied Science 11836153001)) at 4 °C for 30 min and centrifuged for 30 min at 14,000 rpm for collection of the insoluble pellet. The soluble fraction was collected as the cytosol and soluble nuclear part. The insoluble fraction was then lysed with 0.2 N HCl for 30 min on ice and centrifuged for 30 min at 14,000 rpm. The supernatant containing chromatin-bound proteins was neutralized with 1 N Tris-HCl (pH 8.0).

Streptavidin Sepharose pull-down assay

Whole cell lysates were obtained with NETN buffer. Protein concentration was measured by the Bradford assay. Lysates with equal amount of total protein were incubated with protein G beads (Protein G Sepharose 4 Fast Flow, GE Healthcare 17-0618-01) for 2 hour at 4°C. The precleared sample were then obtained by collecting the supernatant after centrifugation and incubated with Streptavidin Sepharose® High Performance Beads (GE Healthcare 17-5113-01) over night at 4°C. After that, the beads were washed, boiled with 2× Laemmli SDS sample buffer, and pelleted. The supernatants were collected for western blot.

Western blot

Cells were lysed by NETN buffer (150 mM NaCl, 20 mM Tris-HCl, pH 8.0, 1 mM EDTA, 0.5% Nonidet P-40, with complete Mini Protease Inhibitor Cocktail (Roche 04693159001)) on ice for 30min. After centrifuging at 4°C, 14,000 rpm for 5min, the supernatants were collected as whole cell extracts. Protein concentration was measured by Bradford's methods. The whole cell extracts with equal amount of total protein were boiled with SDS 2×loading buffer, boiled at 100°C heat block for 10min, short spun, brief vortexed, and loaded to SDS-PAGE gel for electrophoresis. Semi-dry transfer was applied with nitrocellulose membrane afterwards. The blots were blocked and incubated with primary antibody over night at 4°C. After washing, HRP-conjugated secondary antibody was applied at room temperature for 1 hr. And then wash the membrane before exposure to enhanced chemiluminescence reagent (Amershanm Biosciences) and film development.

Clonogenic survival assay

Equal amount of cells were seeded in 100 mm culture plate. The next day, cells were exposed to ICL damage agents at different dosages for 1 hr. After that, cells were washed, trypsinized, and seeded with appropriate cell number in 100 mm culture plates, by triplicates per dosage per cell line. After grown for approximately 14 days, colonies were fixed by glutaraldehyde 6.0% (v/v) and stained with 0.5% crystal violet (w/v) in ethanol. Colonies about 50-200 per plate were counted and used to calculate the relative survival with the following equation: % survival = # of colonies counted / (# of cells plated × plating efficiency) × 100.

eChIP assay

The eChIP assay was done as previously described (Shen et al., 2009). Briefly, cells are transfected by electroporation with control, psoralen-induced ICL- or cisplatin-induced ICL- containing plasmid. 4-6 hours later, the attached cells were lysed, sonicated, and preceded to immunoprecipitation with specific antibody. The precipitates were used for DNA extraction and real-time PCR to detect the enrichment of specific protein at the ICL site. The cisplatin-adducted plasmid substrate was prepared by incubating with 15 μM cisplatin at 37°C in the dark for 3 hrs. The cisplatin treatment induced on average 3 ICL/kb.

Results

FANCG is important for FANCL chromatin loading

To examine if A-G-20 sub complex is required for FANCL chromatin recruitment, we performed chromatin fractionation in *FANCB*$^{-}$, FANCG$^{-/-}$, and FANCL$^{-/-}$ mutant cells (Fig. 4.1A). As expected, there was much reduced FANCL chromatin loading in *FANCB*$^{-}$ mutant because of its reduced FANCL protein level as shown before. However, despite normal FANCL protein abundance, chromatin bound FANCL level in FANCG$^{-/-}$ was drastically reduced. Quantitative analysis showed that it was approximately 10% of the wild type cells (Fig. 4.1B). This result indicates that the chromatin retention of the E3 ligase FANCL relies largely on FANCG. Knockout of *FAAP20* led to partial loss of FANCL chromatin binding, suggesting a minor role of FAAP20 in FANCL chromatin association. Conversely, the chromatin binding of FANCG maintained a significant level in *FANCB*$^{-}$ and FANCL$^{-/-}$ mutant cells, although a bit weakened compared to wild type cells (Fig. 4.1A, C). Therefore, it appears that the A-G-20 module plays a role s in the binding of the FANCL-based catalytic sub complex to chromatin and anchors it to the site of DNA lesions.

Fig. 4.1 FANCG is important for FANCL chromatin loading.

(***A***) Immunoblot detects the FANCL and FANCG protein in chromatin fractions in wild type (*WT*) and indicated mutants exposed to mitomycin C. Histone H3 serves as a loading control for chromatin-bound protein fractions.

(***B***) Quantification of chromatin-bound FANCG in *FANCB*$^{-}$, *G*$^{-/-}$, *L*$^{-/-}$, and *FAAP20*$^{-/-}$ knockout mutants.

(***C***) Quantification of chromatin-bound FANCL in *FANCB*$^{-}$, *G*$^{-/-}$, *L*$^{-/-}$, and *FAAP20*$^{-/-}$ knockout mutants. Error bars for chromatin fraction represent SDs derived from three independent experiments.

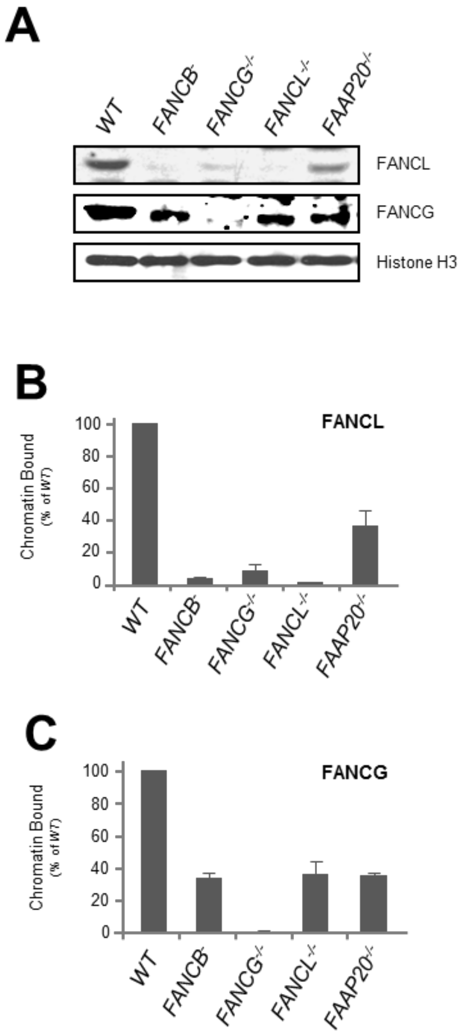
A
WT
FANCB-
FANCG-/-
FANCL-/-
FAAP20-/-
FANCL
FANCG
Histone H3
B
FANCL
Chromatin Bound
(% of WT)
100
80
60
40
20
0
WT
FANCB-
FANCG-/-
FANCL-/-
FAAP20-/-
C
FANCG
Chromatin Bound
(% of WT)
100
80
60
40
20
0
WT
FANCB-
FANCG-/-
FANCL-/-
FAAP20-/-

FANCG is important for FANCL recruitment to ICL sites

To investigate the recruitment of FANCL and FANCG to the ICL sites, we performed the eChIP (Shen et al., 2009) assay with psoralen-induced DNA ICL substrates in the FANCL$^{-/-}$ and *FANCG*$^{-/-}$ mutants, respectively. Consistent with the chromatin fractionation results, we found that ICL-induced FANCG enrichment did not require FANCL (Fig. 4.2A), while enrichment of FANCL strongly depended on FANCG (Fig. 4.2C). To confirm this finding, cisplatin-induced ICL substrate was used in the eChIP assay and a similar result was obtained (Fig. 4.2B, D). These results collectively support that the A-G-20 module anchors the FA core complex to the DNA damaged sites. Moreover, the residual FANCL chromatin loading in the *FANCG*$^{-/-}$ mutant also implicates that, aside from FANCG, a separate factor, most likely FANCM, acts in the chromatin recruitment of FANCL.

Fig. 4.2 FANCG is important for FANCL recruitment to ICL sites.

(***A***) eChIP analysis of FANCG enrichment to a defined psoralen lesion in wild type (*WT*) and *FANCL*$^{-/-}$ mutant.

(***B***) eChIP analysis of FANCG enrichment to a cisplatin-adducted plasmid substrate in wild type (*WT*) and *FANCL*$^{-/-}$ mutant.

(***C***) eChIP analysis of FANCL enrichment to a defined psoralen lesion in wild type (*WT*) and *FANCG*$^{-/-}$ mutant.

(***D***) eChIP analysis of FANCL enrichment to a cisplatin-adducted plasmid substrate in wild type (*WT*) and *FANCG*$^{-/-}$ mutant.

Error bars for eChIP analyses represent SDs derived from three independent experiments.

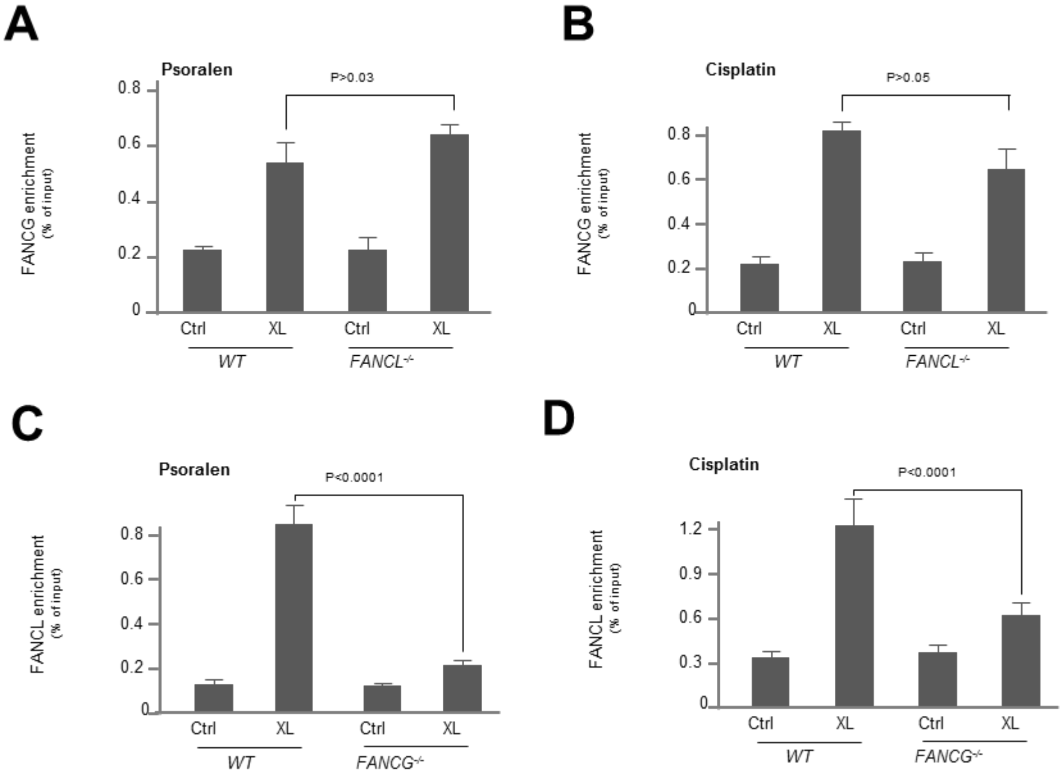
A
Psoralen
P>0.03
FANCG enrichment (% of input)
0.8
0.6
0.4
0.2
0
Ctrl
XL
Ctrl
XL
WT
FANCL-/-
B
Cisplatin
P>0.05
FANCG enrichment (% of input)
0.8
0.6
0.4
0.2
0
Ctrl
XL
Ctrl
XL
WT
FANCL-/-
C
Psoralen
P<0.0001
FANCL enrichment (% of input)
0.8
0.6
0.4
0.2
0
Ctrl
XL
Ctrl
XL
WT
FANCG-/-
D
Cisplatin
P<0.0001
FANCL enrichment (% of input)
1.2
0.9
0.6
0.3
0
Ctrl
XL
Ctrl
XL
WT
FANCG-/-

Generation of FANCF stable knockdown cell lines

Previous studies have implied that C-E-F may function in placing the FA catalytic core to the chromatin, since FANCF interacts with the FANCM/FAAP24 complex, C-E-F may serve as a chromatin-loading element for the FA core complex (Deans and West, 2009). To test this hypothesis functionally, a cell line with disrupted C-E-F module is necessary. Despite repeated efforts on targeting FANCC, I was unable to delete the second allele of FANCC in HCT116 cells. Thus, I employed the lentivirus-mediated shRNA technology to knockdown FANCF.

As shown (Fig. 4.3A), four lentiviral shRNAs with different targeting sequences were screened and the one with the highest efficiency of knockdown was used to generate the FANCF stable knockdown cell in HCT116 cells. To confirm the specificity of this shRNA and exclude off-target effects, complementation experiments were carried by introducing full length human myc-tagged FANCF into the knockdown cell lines to show rescue of FANCD2/I ubiquitination and cellular sensitivity to ICL reagents (Fig. 4.3B-E). In order to study the epistatic relationship between C-E-F and A-G-20 or C-E-F and FANCM, FANCF was also stably knocked down in the FANCG and FANCM mutants (Fig. 4.3D-E).

Fig. 4.3 Generation of FANCF shRNA knockdown cell lines.

(***A***) Screening of FANCF shRNAs. Four Lentivirus (#1 to #4) shRNA to FANCF were used to infect 293T cells stably expressing Myc-tagged FANCF. The Myc-tagged FANCF stable line was constructed to circumvent the lack of effective FANCF antibody. Immunoblotting with Myc antibody identifies the most effective shRNA (#1), which was used in all subsequent experiment.

(***B***) Immunoblot detecting MMC-induced monoubiquitination of FANCD2 and FANCI in parental HCT116 (*WT*) and indicated FANCF knockdown mutants complemented stably with shRNA-resistant Myc-tagged FANCF.

(***C***) Clonogenic survival of wild type (WT), shFANCF stable knockdown cell line, and two complemented cell lines (#6 and #9) against mitomycin C. Error bars for clonogenic survival are derived from SDs from three independent tests with triplications.

(***D***) Reverse transcription/Q-PCR measuring stable FANCF knockdown in the indicated mutant cell lines.

(***E***) Immunoblotting with Myc antibody testing FANCF knockdown efficiency in the indicated stable cell lines transiently transfected with wild type Myc-FANCF.

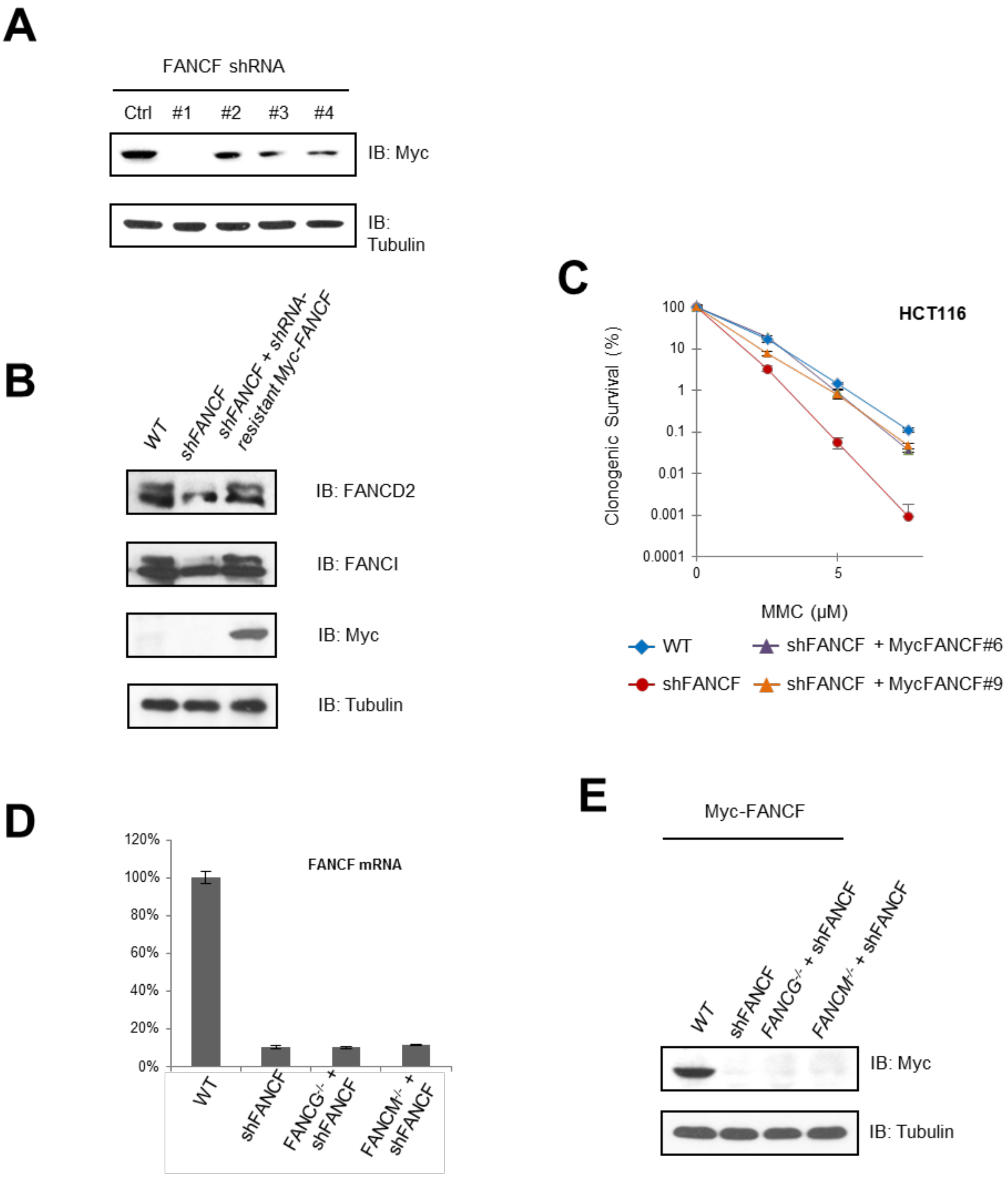
A
FANCF shRNA
Ctrl #1 #2 #3 #4
IB: Myc
IB: Tubulin
B
WT
shFANCF
shFANCF + shRNA-resistant Myc-FANCF
IB: FANCD2
IB: FANCI
IB: Myc
IB: Tubulin
C
HCT116
Clonogenic Survival (%)
100
10
1
0.1
0.01
0.001
0.0001
0
5
MMC (μM)
WT
shFANCF
shFANCF + MycFANCF#6
shFANCF + MycFANCF#9
D
FANCF mRNA
120%
100%
80%
60%
40%
20%
0%
WT
shFANCF
FANCG-/- + shFANCF
FANCM-/- + shFANCF
E
Myc-FANCF
WT
shFANCF
FANCG-/- + shFANCF
FANCM-/- + shFANCF
IB: Myc
IB: Tubulin

A-G-20 and C-E-F are required for the full function of FA core complex

To test whether the C-E-F module functions independently for the full extent of FANCD2 ubiquitination, FANCF was knocked down in the *FANCG*$^{-/-}$ mutant by shRNA (Fig. 4.3D-E). As shown (Fig. 4.4A), loss of both FANCF and FANCG completely eliminated FANCI/D2 monoubiquitination upon MMC or cisplatin exposure, suggesting that FANCG and FANCF provide distinct functions in the FA core complex. The complete loss of FANCD2 monoubiquitination resulted from compromised loading/anchoring of FANCL at the site of DNA damage, as shown (Fig. 4.4A and B). Consistently, cells deficient of both FANCG and FANCF exhibited much more severe sensitivity to MMC than single mutants, which is comparable to that of the FANCL mutant (Fig. 4.4C).

In order to test if FANCF as an initial loading module act independently of the anchoring module A-G-20, FANCF chromatin-binding was analyzed in FANCG knockout background and found that chromatin-bound FANCF was not affected by FANCG deficiency (Fig. 4.4D). Together, these results suggest that the A-G-20 and C-E-F modules can act independently to position the catalytic module at the site of DNA damage.

Fig. 4.4 A-G-20 and C-E-F modules are required for the full function of FA core complex.

(***A***) Immunoblot detecting MMC and cisplatin-induced monoubiquitination of FANCD2 and FANCL in wild type (*WT*) and the indicated knockout/knockdown mutant cells.

(***B***) Quantification of chromatin-bound FANCL (left panel of B) in wild type HCT116 (*WT*) and indicated mutants exposed to mitomycin C.

(***C***) Clonogenic survival of parental HCT116 (*WT*), *FANCG*$^{-/-}$ + *Ctrl shRNA*, *FANCG*$^{-/-}$ + *shFANCF*, and *FANCL*$^{-/-}$ cells treated with mitomycin C.

(***D***) Immunoblot detecting chromatin-bound Myc-tagged FANCF in *FANCG*$^{+/+}$ and *FANCG*$^{-/-}$ cells with stable knockdown of endogenous FANCF and complemented with shRNA-resistant Myc-tagged FANCF.

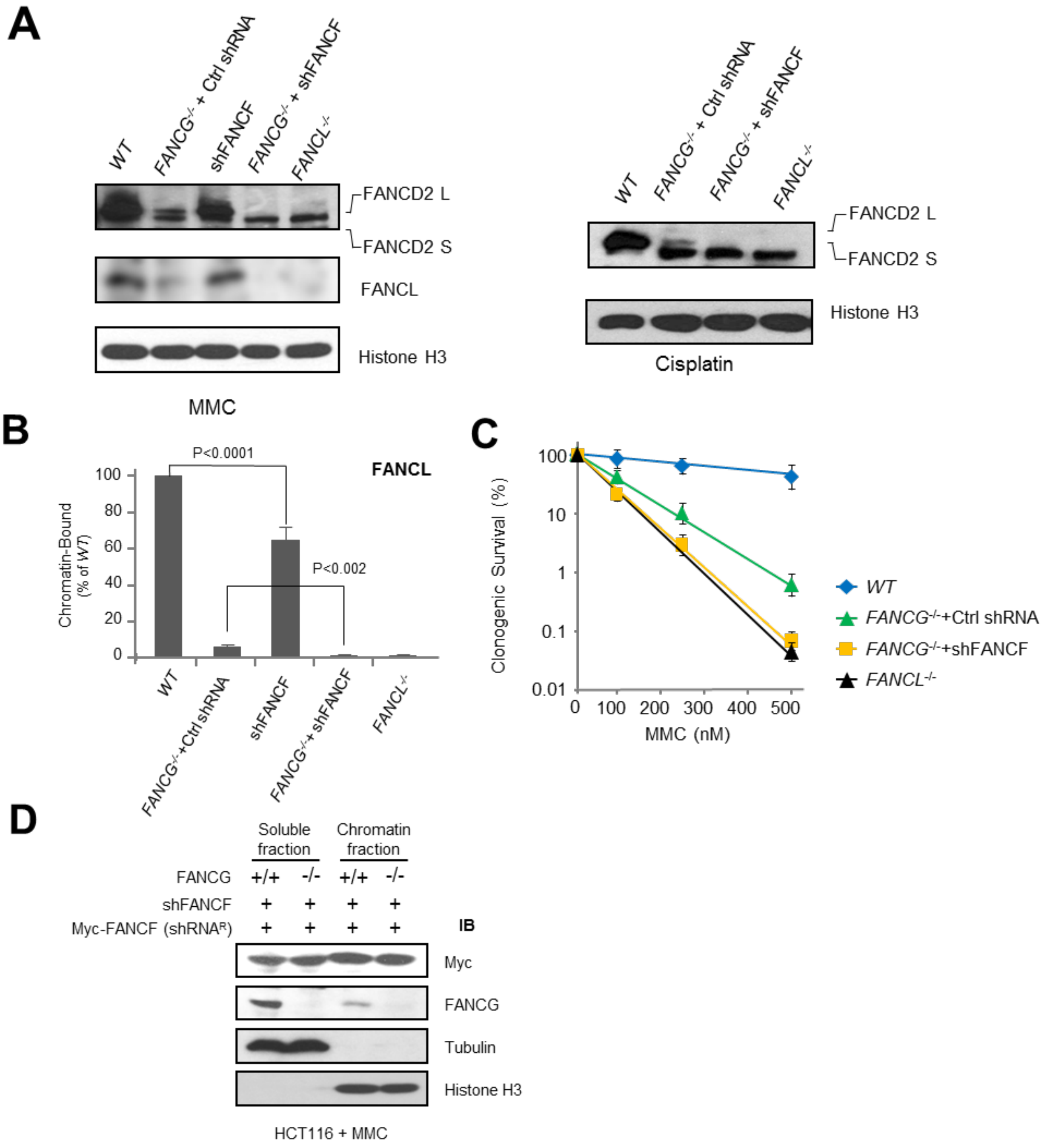
A
WT
FANCG-/- + Ctrl shRNA
shFANCF
FANCG-/- + shFANCF
FANCL-/-
FANCD2 L
FANCD2 S
FANCL
Histone H3
MMC
WT
FANCG-/- + Ctrl shRNA
FANCG-/- + shFANCF
FANCL-/-
FANCD2 L
FANCD2 S
Histone H3
Cisplatin
B
FANCL
Chromatin-Bound (% of WT)
P<0.0001
P<0.002
100
80
60
40
20
0
WT
FANCG-/-+Ctrl shRNA
shFANCF
FANCG-/-+shFANCF
FANCL-/-
C
Clonogenic Survival (%)
100
10
1
0.1
0.01
0
100
200
300
400
500
MMC (nM)
WT
FANCG-/-+Ctrl shRNA
FANCG-/-+shFANCF
FANCL-/-
D
Soluble fraction
Chromatin fraction
FANCG +/+ -/- +/+ -/-
shFANCF + + + +
Myc-FANCF (shRNAR) + + + +
IB
Myc
FANCG
Tubulin
Histone H3
HCT116 + MMC

FANCG and FANCM are required for the full function of FA core complex in recruiting FANCL into ICL sites

The above results suggest that FANCF acts as a loading factor for the FA core complex via interacting with FANCM, thus deletion of both FANCM and FANCG is expected to completely eliminate the FANCI/D2 ubiquitination by compromising both chromatin loading and anchoring machineries of FANCL. To confirm the interaction between FANCF and FANCM, immunoprecipitation experiment was performed and we found that FANCF indeed binds to FANCM (Fig. 4.5A). Subsequently, we tested FANCD2 ubiquitination in the *FANCG* and *FANCM* knockout mutants. As shown (Fig. 4.5B), only loss of both FANCG and FANCM yielded complete loss of FANCD2 monoubiquitination compared with the single knockout mutants, further suggesting that the chromatin anchoring module and FANCM-dependent loading provide a combined function of placing FANCL to the damaged site for ubiquitination action.

To further verify this notion, FANCL chromatin loading was analyzed in the FANCG and FANCM single and double knockout cells. Indeed, either FANCG or FANCM depletion results in partial removal of chromatin-bound FANCL, while double depletion completely comprised the chromatin recruitment of FANCL (Fig. 4.5B, C). MMC survival assay was conducted to test the functional consequence of removing both FANCG and FANCM. The results showed that DNA damage sensitivity of the FANCG- FANCM double mutant was much more severe than each single mutant (Fig. 4.5D), implying that depleting both loading and anchoring factors of the FA catalytic FANCL severely impact the cellular survival.

Fig. 4.5 FANCG and FANCM are required for the full function of FA core complex in recruiting FANCL into ICL sites.

(***A***) Co-immunoprecipitation between FANCF and FANCM. S-tag-Flag-Biotin (SFB) – tagged FANCF or the empty vector was stably expressed in 293T cells. Protein extracts prepared from both cell lines were subjected to streptavidin beads pull down and bound proteins were immunoblotted by FANCM or Flag antibodies.

(***B***) Immunoblot detecting MMC- and cisplatin-induced monoubiquitination of FANCD2 and chromatin loading of FANCL in wild type (*WT*) and *FANCG*$^{-/-}$, *FANCM*$^{-/-}$, and *FANCG*$^{-/-}$ *FANCM*$^{-/-}$ double mutants.

(***C***) Quantification of (C) - chromatin-bound FANCL in *FANCG*$^{-/-}$, *FANCM*$^{-/-}$, and *FANCG*$^{-/-}$ M$^{-/-}$ double mutants. Error bars for chromatin fraction represent SDs derived from three independent experiments.

(***D***) Clonogenic survival of *FANCM*$^{-/-}$, *FANCG*$^{-/-}$, *FANCL*$^{-/-}$, and *FANCG*$^{-/-}$ *FANCM*$^{-/-}$ mutants treated with mitomycin C. Error bars for clonogenic survival are derived from DSs from four independent tests with triplications.

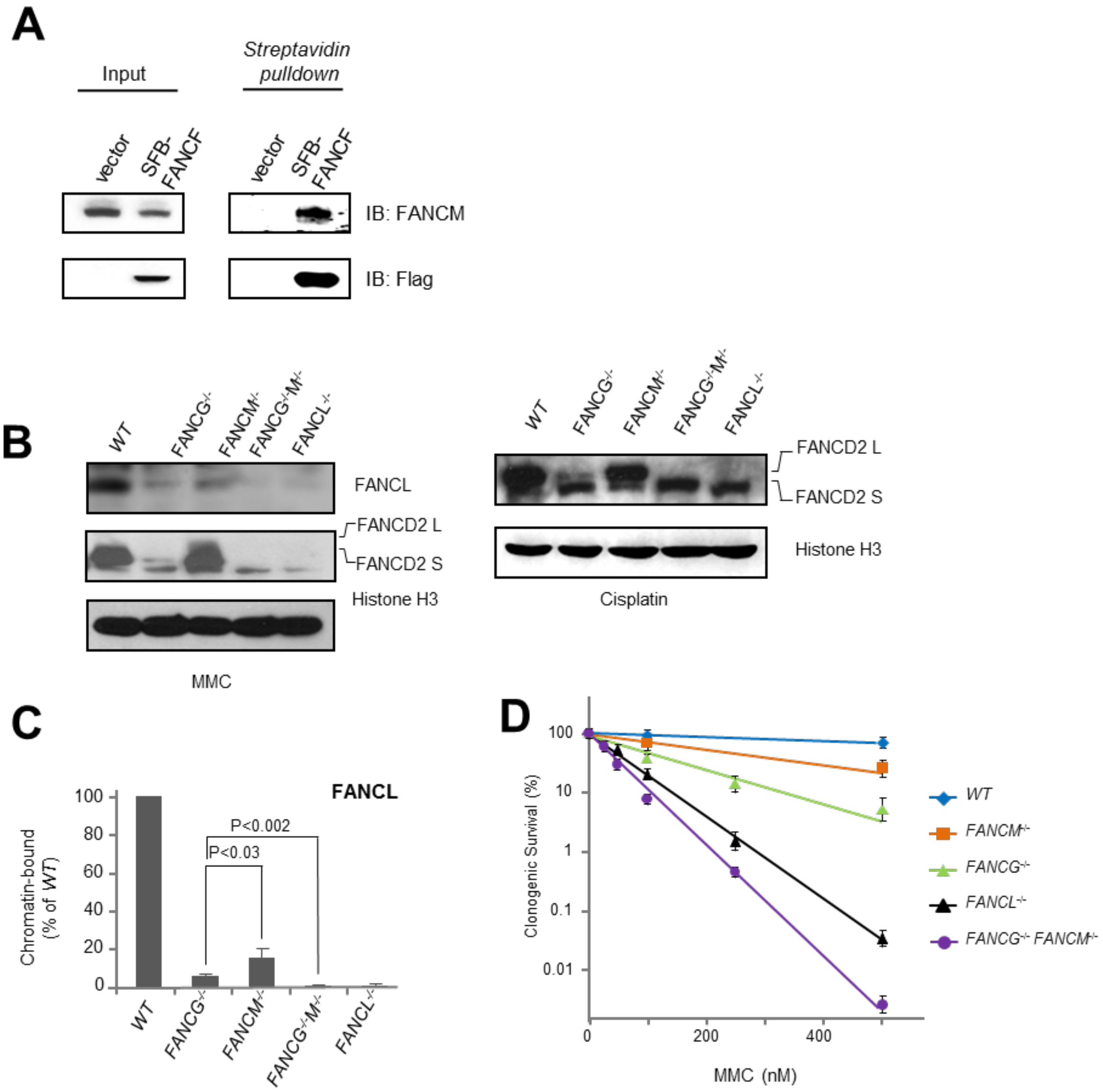
A
Input
Streptavidin pulldown
vector
SFB-FANCF
vector
SFB-FANCF
IB: FANCM
IB: Flag
B
WT
FANCG-/-
FANCM-/-
FANCG-/-M-/-
FANCL-/-
FANCL
FANCD2 L
FANCD2 S
Histone H3
MMC
WT
FANCG-/-
FANCM-/-
FANCG-/-M-/-
FANCL-/-
FANCD2 L
FANCD2 S
Histone H3
Cisplatin
C
FANCL
Chromatin-bound (% of WT)
100
80
60
40
20
0
P<0.002
P<0.03
WT
FANCG-/-
FANCM-/-
FANCG-/-M-/-
FANCL-/-
D
Clonogenic Survival (%)
100
10
1
0.1
0.01
0
200
400
MMC (nM)
WT
FANCM-/-
FANCG-/-
FANCL-/-
FANCG-/- FANCM-/-

FANCM functions epistatically with the chromatin loading module

The above results have depicted a model that C-E-F and A-G-20 sub complexes act together for the full function of FA core complex in ubiquitination of FANCI/D2 complex. As such, it is expected that knockout both FANCM and FANCF would not yield additional phenotype than loss of FANCM alone due to the fact that loss of either protein lead to the same disruption of the loading module. To test this hypothesis, we analyzed FANCD2 monoubiquitination in FANCM deficient cells with stable knockdown of FANCF. As shown (Fig. 4.6A, B), loss of FANCF in *FANCM*$^{-/-}$ cells did not generate any additional loss of FANCD2 or FANCI monoubiquitination upon ICL damage. Consistently, loss of both FANCM and FANCF failed to show further increased sensitivity to mitomycin C than the FANCM mutant alone (Fig. 4.6C). Therefore, FANCM and FANCF function epistatically in the initial chromatin loading of the FA core complex.

Fig. 4.6 FANCM functions epistatically with the chromatin loading module.

(***A***) Immunoblot detecting MMC-induced monoubiquitination of FANCD2 and FANCI in wild type HCT116 (*WT*) and the indicated knockout/knockdown mutant cells.

(***B***) Immunoblot detecting cisplatin-induced monoubiquitination of FANCD2 in wild type HCT116 (*WT*) and the indicated knockout/knockdown mutant cells.

(***C***) Clonogenic survival of HCT116 FANCF knockdown alone (*shFANCF*), *FANCM*$^{-/-}$ *+shFANCF*, and *FANCM*$^{-/-}$*+Ctrl shRNA* mutants treated with mitomycin C.

Error bars for clonogenic survival are derived from DSs from four independent tests with triplications.

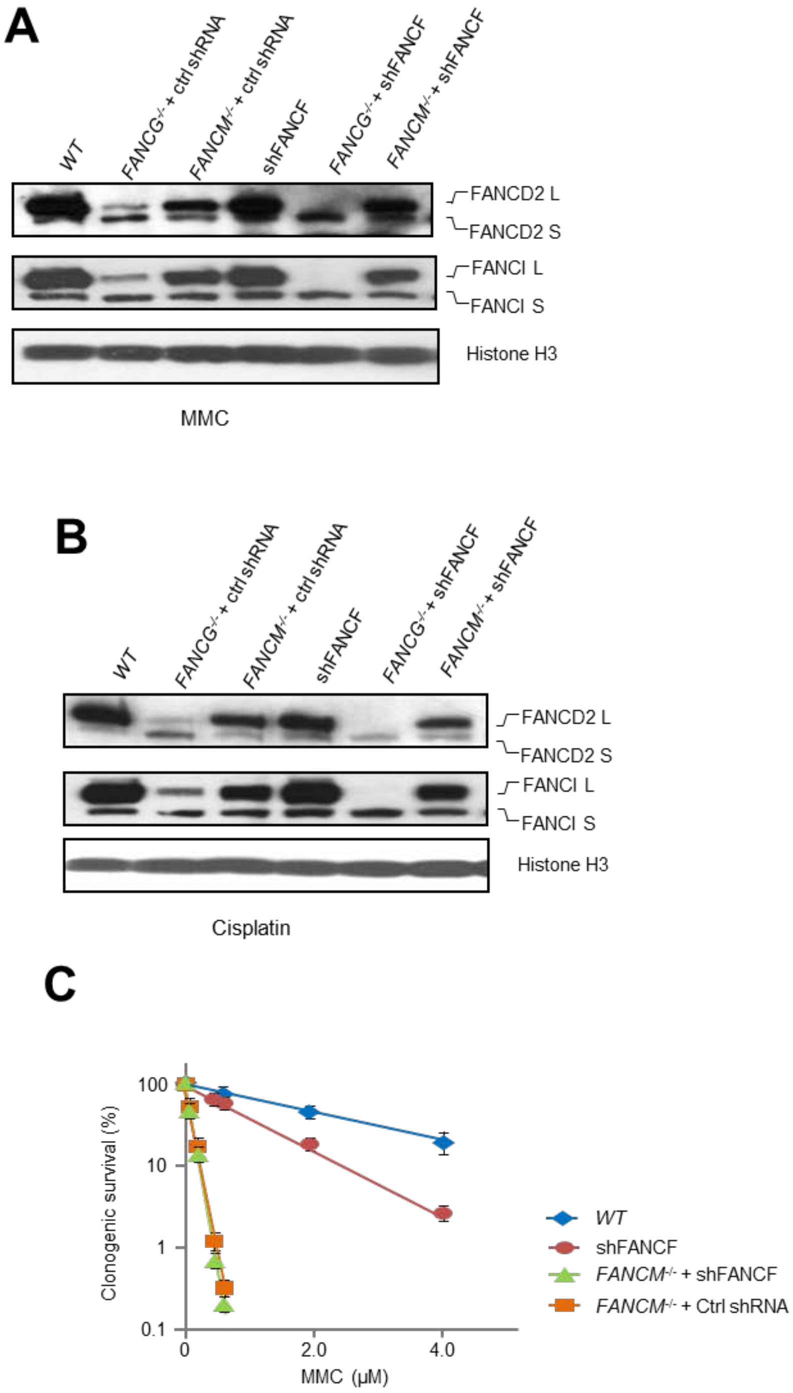
A
WT
FANCG-/- + ctrl shRNA
FANCM-/- + ctrl shRNA
shFANCF
FANCG-/- + shFANCF
FANCM-/- + shFANCF
FANCD2 L
FANCD2 S
FANCI L
FANCI S
Histone H3
MMC
B
WT
FANCG-/- + ctrl shRNA
FANCM-/- + ctrl shRNA
shFANCF
FANCG-/- + shFANCF
FANCM-/- + shFANCF
FANCD2 L
FANCD2 S
FANCI L
FANCI S
Histone H3
Cisplatin
C
Clonogenic survival (%)
100
10
1
0.1
0
2.0
4.0
MMC (μM)
WT
shFANCF
FANCM-/- + shFANCF
FANCM-/- + Ctrl shRNA

Discussion

Results presented in this chapter define the redundant functions of the A-G-20 sub complex and C-E-F sub complex in the damage-specific loading of the FA catalytic core activity. The function of A-G-20 as DNA/chromatin anchoring module is independent of FANCM mediated chromatin loading mechanism. On the other hand, the C-E-F sub complex as a loading module works with FANCM which most likely provides the initial loading of the FA core complex. The two modules enable the FA core complex to be positioned to DNA damage site, so that FANCL is able to monoubiquitinate FANCD2/I complex in a spatially-defined fashion. With the capability to recognize stalled forks or processed lesion (Joo et al.) and to recruit downstream effectors, including endonucleases (Knipscheer et al., 2009; Kratz et al.; Liu et al.; MacKay et al.; Smogorzewska et al.), the ubiquitinated FANCI/D2 therefore can tether the upstream DNA damage signaling and the downstream effectors for repair purpose.

Both of the loading and the anchoring modules are important for the full function of the FA core complex. With either A-G-20 sub complex or C-E-F sub complex disrupted, the phenotype is relatively mild by showing diminished but not fully abolished FANCI/D2 ubiquitination, and less severe ICL-induced DNA damage killing. Disruption of both, however, impedes the essential recruitment of the catalytic FANCL to the damaged site and thus fully compromises the monoubiquitination and causes hypersensitivity to ICL reagents. This model also explains why the *Fancc and Fancg* double knockout mice showed more severe phenotype than single knockout mice (Pulliam-Leath et al.). In this mouse model study, disruption of both *Fancc* and *Fancg* led to bone marrow failure, acute myeloid leukemia, and myelodysplasia, which recapitulated the hematologic symptoms of FA patients, while the single knockout mice did not.

A question remains as how A-G-20 sub complex is able to anchor the E3 ligase FANCL to the chromatin or DNA damaged site. FANCA has been demonstrated to possess DNA binding affinity *in vitro* (Yuan et al., 2012). Also FAAP20 has been shown to bind to ubiquitinated forms of H2A (Yan et al.), although FAAP20 is likely to play a minor role in chromatin association of the E3 ligase which is indicated by the weak phenotypes of FAAP20 mutant. Potentially, these DNA/chromatin affinity features of the A-G-20 sub complex may contribute to their chromatin anchoring role in FA core complex. Nevertheless, further study is needed to fully define biochemical properties of the A-G-20 sub complex responsible for damage DNA association.

FANCM has been shown to constitutively bind to the chromatin and is important for the chromatin association of the core complex (Kim et al., 2008). Deletion of FANCM results in substantial loss of the chromatin-bound FA core proteins, and moderate defects of FANCD2 monoubiquitination (Wang et al., 2013). Thus it is likely that in the absence of FANCM-mediated initial loading, the chromatin anchoring module is still able to retain certain amount of the E3 ligase at the site of DNA damage, which is sufficient to keep a detectable level of FA pathway activation.

This model explains why FANCG deficient cell line showed more severe phenotype than FANCM knockout cells but not a complete loss of FANCD2/I monoubiquitination and less severe sensitivity than FANCL. This also explains why only by knocking out both FANCG and FANCM, FANCD2 monoubiquitination is completely eliminated and hypersensitivity to ICL agents even surpassed that of the *FANCL*$^{-/-}$ mutant. The additional sensitivity of the FANCG and FANCM double mutant over the FANCL mutant (Fig. 4.5D) is most likely attributed to the FA pathway- independent function of FANCM as suggested by previous studies (Huang et al.; Wang et al., 2013).

In summary, our study has delineated the chromatin loading module C-E-F and anchoring module A-G-20 for the damage-specific recruitment of the FA core complex E3 ligase to the ICLs. The epistatic relationships among the FA genes are much more clearly-defined. This not only accelerates the elucidation of the ICL repair mechanism but also enhances the understanding of the disease biology of Fanconi Anemia.

CHAPTER V

Conclusion and Future Directions

Conclusion

Monoubiquitination of FANCD2 is a central event of the FA pathway activation. Studying the mechanism on how the FANCD2 is ubiquitinated is important to dissect the FA pathway and DNA repair mechanisms. The goal of our study was to analyze the epistatic relationship between FA core genes and elucidate the functions of the FA core components in FA pathway activation and DNA interstrand crosslinking damage resistance. Based on the modularized FA core complex hypothesis, we tested how the three sub complexes exert differential functions contributing to the FANCI/D2 ubiquitination and ICL repair. Our main approach is epistatic analysis and functional studies using a panel of isogenic human cellular knockout mutants.

In this study, I found that FA core genes showed variant sensitivity to DNA ICL damage. FANCG and FAAP20 null cells were less sensitive than FANCB and FANCL null cells to DNA ICLs. Epistatic analyses showed that FANCG and FAAP20 were epistatic to FANCB and FANCL, but have less severe phenotypes. This result suggested that B-L-100 sub complex plays a more important role in ICL repair, although they function in the same pathway. Moreover, disruption of genes from the B-L-100 sub complex completely disabled the core complex to ubiquitinate the FANCI/D2 complex, while the deficiency of the genes from the A-G-20 and C-E-F sub complex only partially reduced the ubiquitination activity. Therefore, B-L-100 acts as the E3 catalytic core module in the FA core complex, whereas other components play secondary roles.

FANCM has been shown to constitutively bind to chromatin and is believed to initiate the chromatin loading of the core complex through interacting with FANCF (Deans and West, 2009; Kim et al., 2008). By analyzing the chromatin fractions and enrichment of the FA core genes at the ICL site in the mutant cells, I found that the A-G-20 acted as a chromatin anchoring module for the catalytic core contain FANCL. The removal of either FANCG or FANCF resulted in partial reduction of the FANCL chromatin loading and FANCI/D2 ubiquitination, while removing both led to additional impact in FANCL chromatin loading, abolished FANCI/D2 ubiquitination, and heightened sensitivity to ICL reagents comparable to FANCL mutant. In addition, the interaction between FANCM and FANCF was also found by my study to support the recruitment of the core complex. ICL survival assays, on the other hand, revealed non-redundant functions of the A-G-20 and C-E-F complexes in ICL repair, most likely reflecting the cooperative nature of core complex recruitment.

Collectively, my studies defined that FA core complex mediate the ubiquitination of FANCI/D2 ubiquitination through an assembly of different functional modules, the B-L-100 catalytic core module, the C-E-F chromatin loading module, and the A-G-20 chromatin anchoring module. These findings provided novel mechanistic insights into how FA core genes contribute to the FA pathway activation and genomic integrity.

Proposed Model

Based on our findings, a model is proposed to depict the functional modules of FA core complex in its DNA damage-specific recruitment (Fig 5.1). The FA core complex is assembled with three functional modules, the catalytic module (B-L-100 sub complex), the chromatin loading module (C-E-F sub complex), and the chromatin anchoring module (A-G-20 sub complex). FANCM complex constitutively binds to chromatin, when forming a complex with FAAP24, exhibit DNA damage binding property (Gari et al., 2008a; Gari et al., 2008b; Singh et al., 2010). Upon DNA damage, C-E-F sub complex initiates the transient recruitment of FA core complex to the lesion site through interaction between FANCM and FANCF, while the A-G-20 complex anchors the FA core complex to the chromatin/lesion sites, so that the core complex is stably located at the damaged site to catalyze the FANCI/D2 ubiquitination reaction. When cells are devoid of either chromatin loading or chromatin anchoring module, the FA pathway activation is only partially disabled with intermediate hypersensitivity to ICLs. When both chromatin loading and anchoring module are defective, the catalytic module fails to be stabilized to the DNA damaged site, leading to complete inability of FA pathway activation and high sensitivity to ICLs, which is comparable to deficiency of the E3 ligase FANCL.

Fig. 5.1 Working model for FA core genes in activating FA pathway.

FANCM constitutively binds to chromatin and DNA. Upon DNA damage, C-E-F sub complex initiates the recruitment of FA core complex to the lesion site through interaction with FANCM. After initial loading, A-G-20 anchors the FA core complex to the chromatin/lesion sites, where B-L-100 catalyzes the FANCI/D2 ubiquitination reaction.

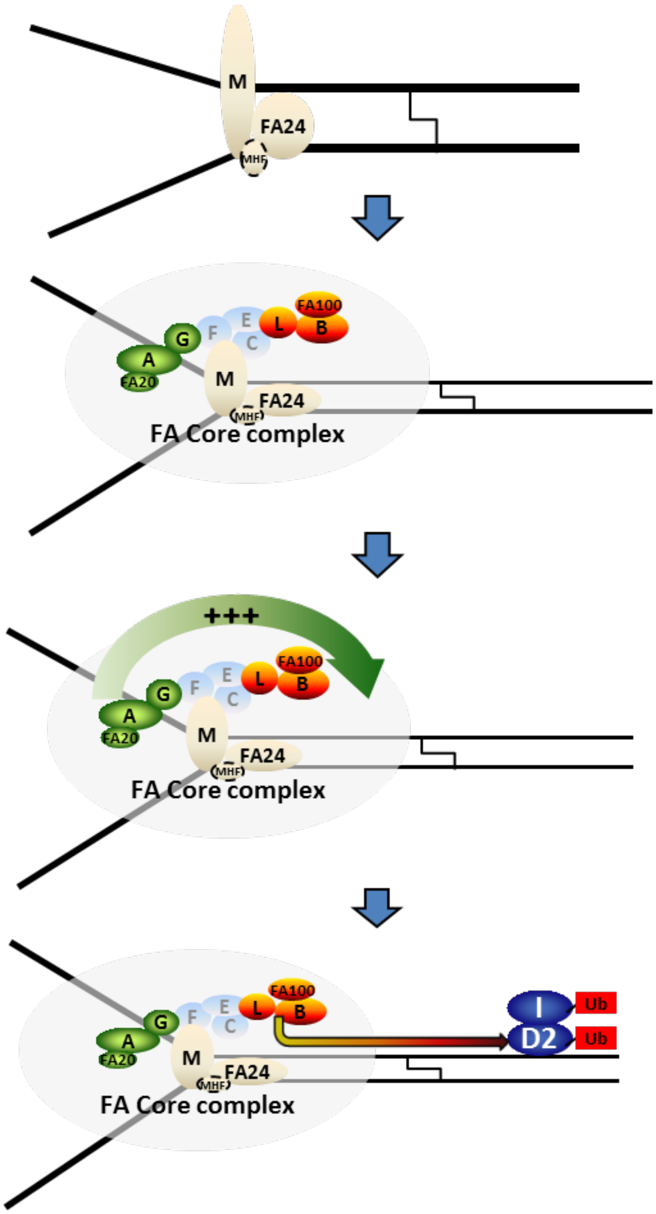
M
FA24
MHF
G
F
E
C
L
FA100
B
A
FA20
M
FA24
MHF
FA Core complex
+++
G
F
E
C
L
FA100
B
A
FA20
M
FA24
MHF
FA Core complex
G
F
E
C
L
FA100
B
A
FA20
M
FA24
MHF
FA Core complex
I
D2
Ub
Ub

Future Directions

Chromatin/DNA anchoring machinery of A-G-20 sub complex

As shown in Chapter IV, A-G-20 sub complex plays a role in anchoring the FA core complex at the damaged site. Although a previous study suggested that FANCA had DNA binding affinity, no clear DNA- or chromatin-interacting domain was defined (Yuan et al., 2012). Thus, it would be important to determine how the A-G-20 sub complex retains the core complex. To this end, I am planning to perform a structure-function analysis of FANCA.

By aligning the amino acid sequence of FANCA with known chromatin or DNA binding domain, I found that FANCA has a near C-terminal domain which displays similarity to the PWWP motif (Fig. 5.2). The PWWP domain is a protein-protein interaction domain and some of these domains have been shown to mediate interaction with modified histones. For example, the PWWP domain of the MutSα was found to mediate the chromatin binding of mismatch repair machinery to the tri-methylated histone H3 (Li et al., 2013). Other PWWP domain proteins have been shown to mediate the binding of proteins to the histone for the regulation of histone modifications and the downstream DNA damage repair signaling (Wang et al., 2009).

Fig. 5.2 Sequence alignment of the PWWP domain-containing proteins and FANCA. Homozygous mutation sites found in FA patients are indicated by red arrows. The upper panel is for the alignment of the core portion of the PWWP domain and the lower panel is for the alignment of FFS portion of the PWWP domain.

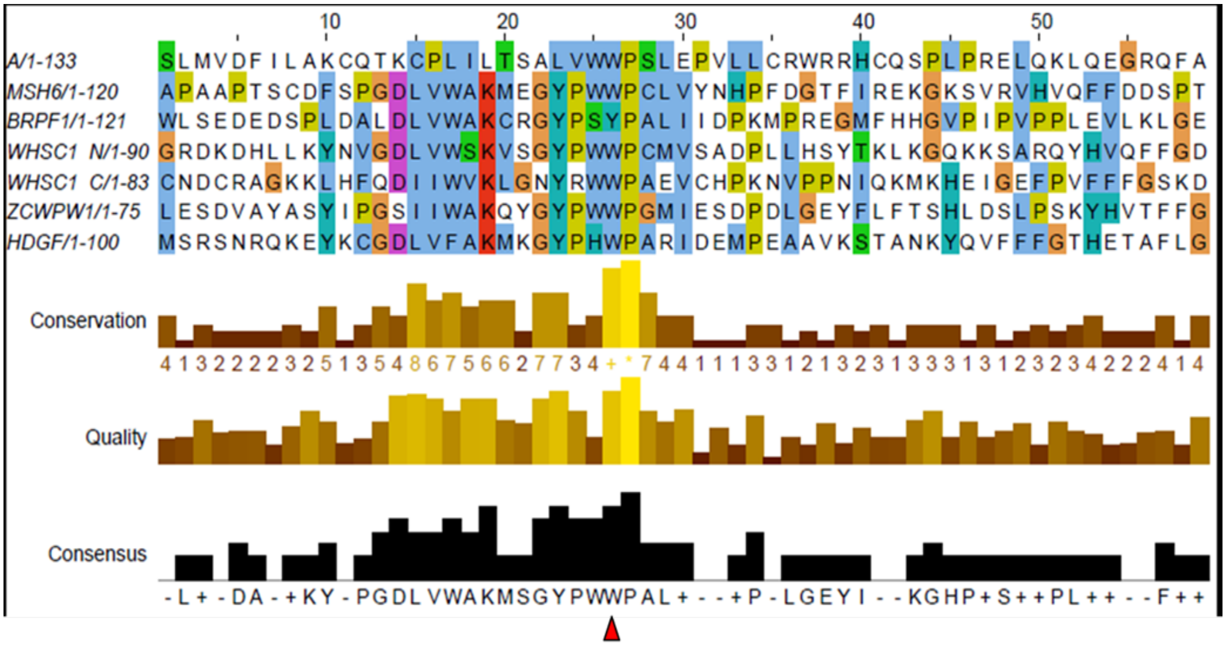

W1174del

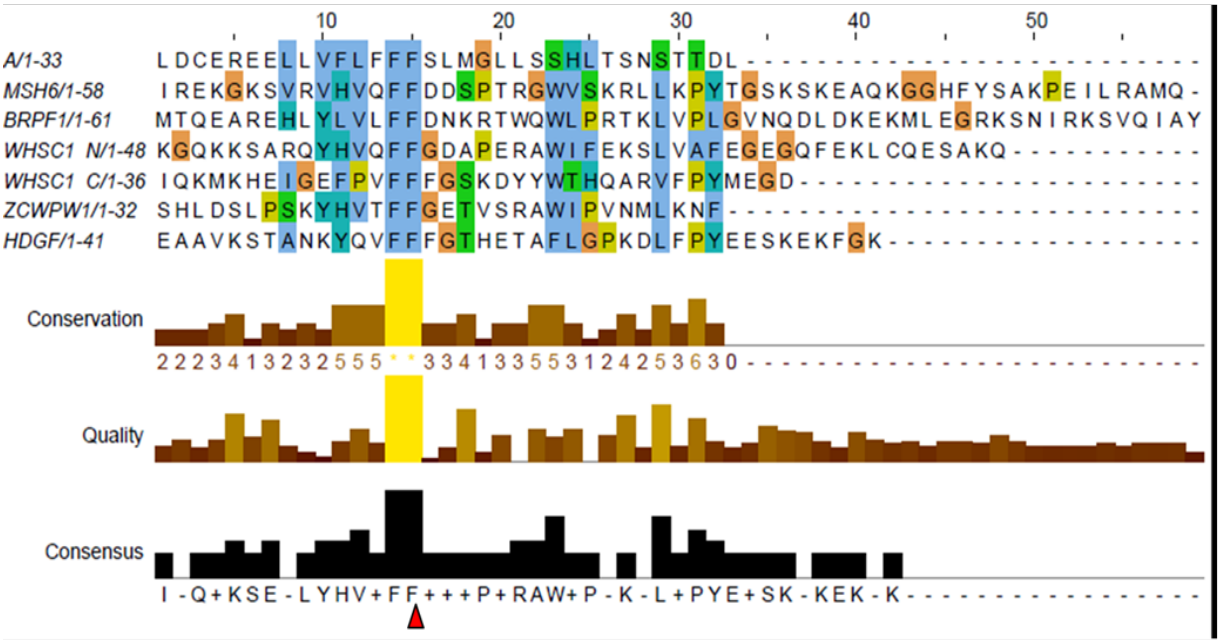

F1263del

By aligning the sequences of FANCA cross species, I found that this “PWWP-like” domain is highly conserved among the homologs, as shown (Fig. 5.3). Furthermore, homozygous deletions of the highly conserved core amino acids W1174 or F1263 has been found in FANCA complementation group patients, which underscores the importance of the two residues in FANCA function (Adachi et al., 2002). In addition, this “PWWP-like” domain does not overlap with the N-terminal NLS domain which is responsible for FANCG interaction (Garcia-Higuera et al., 2000), or the FAAP20 interacting motif of FANCA which includes residues 674-1032 (Leung et al.).

Fig. 5.3 Sequence alignment of the “PWWP-like” domain of FANCA homologs across species.

Homozygous single amino acid deletions in FA patients are indicated by red rectangles.

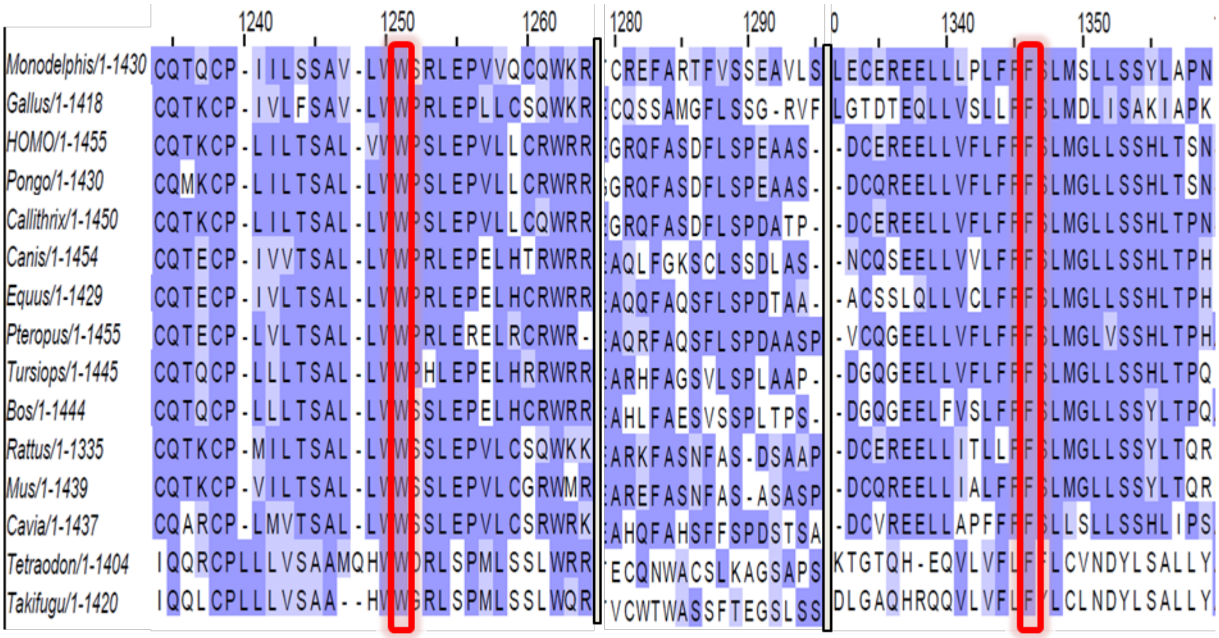

```
Monodelphis/1-1430  CQTQCP-IILSSAV-LVWSRLEPVVQCQWKR  CREFARTFVSSEAVLS  LECEREELLLPLFFFSLMSLLSSYLAPN
Gallus/1-1418       CQTKCP-IVLFSAV-LVWPRLEPLLCSQWKR  CQSSAMGFLSSG-RVF  LGTDTEQLLVSLLFFSLMDLISAKIAPK
HOMO/1-1455         CQTKCP-LILTSAL-VVWPSLEPVLLCRWRR  GRQFASDFLSPEAAS-  -DCEREELLVFLFFFSLMGLLSSHLTSN
Pongo/1-1430        CQMKCP-LILTSAL-LVWPSLEPVLLCRWRR  GRQFASDFLSPEAAS-  -DCQREELLVFLFFFSLMGLLSSHLTSN
Callithrix/1-1450   CQTKCP-LILTSAL-LVWPSLEPVLLCQWRR  GRQFASDFLSPDATP-  -DCEREELLVFLFFFSLMGLLSSHLTPN
Canis/1-1454        CQTECP-IVVTSAL-LVWPRLEPELHTRWRR  AQLFGKSCLSSDLAS-  -NCQSEELLVVLFFFSLMGLLSSHLTPH
Equus/1-1429        CQTECP-IVLTSAL-LVWPRLEPELHCRWRR  AQQFAQSFLSPDTAA-  -ACSSLQLLVCLFFFSLMGLLSSHLTPH
Pteropus/1-1455     CQTECP-LVLTSAL-LVWPRLERELRCRWR-  AQRFAQSFLSPDAASP  -VCQGEELLVFLFFFSLMGLVSSHLTPH
Tursiops/1-1445     CQTQCP-LLLTSAL-LVWPHLEPELHRRWRR  ARHFAGSVLSPLAAP-  -DGQGEELLVFLFFFSLMGLLSSHLTPQ
Bos/1-1444          CQTQCP-LLLTSAL-LVWSSLEPELHCRWRR  AHLFAESVSSPLTPS-  -DGQGEELFVSLFFFSLMGLLSSYLTPQ
Rattus/1-1335       CQTKCP-MILTSAL-LVWSSLEPVLCSQWKK  ARKFASNFAS-DSAAP  -DCEREELLITLLFFSLMGLLSSYLTQR
Mus/1-1439          CQTKCP-VILTSAL-LVWSSLEPVLCGRWMR  AREFASNFAS-ASASP  -DCQREELLIALFFFSLMGLLSSYLTQR
Cavia/1-1437        CQARCP-LMVTSAL-LVWSSLEPVLCSRWRK  AHQFAHSFFSPDSTSA  -DCVREELLAPFFFFSLLSLLSSHLIPS
Tetraodon/1-1404    IQQRCPLLLVSAAMQHVWDRLSPMLSSLWRR  ECQNWACSLKAGSAPS  KTGTQH-EQVLVFLFFLCVNDYLSALLY
Takifugu/1-1420     IQQLCPLLLVSAA--HVWGRLSPMLSSLWQR  VCWTWASSFTEGSLSS  DLGAQHRQQVLVFLFYLCLNDYLSALLY
```

The alignment results suggest the existence of a functional “PWWP-like” domain in FANCA. Thus we hypothesize that the PWWP domain of FANCA plays a role of anchoring the FA core complex to damaged marked histone. To test this hypothesis, the following specific aims are planned.

Specific Aim 1, To determine whether the FANCA PWWP domain is important for the chromatin anchoring of the FA core complex upon DNA damage.

For this purpose, FANCA null cell line will be established with Cas9 targeting technology. FANCA PWWP domain mutants will be introduced into a *FANCA* null cell line for chromatin fractionation and eChIP analyses of the FA core proteins. In addition, FANCD2 ubiquitination will be examined with chromatin fractionation and cellular resistance to ICLs will be assayed with clonogenic assay under ICL treatment. The positive control will be wild type FANCA complemented cell line and the negative control will be the FANCA null cell line with empty vector introduced.

It is expected that the chromatin-bound and the lesion-enriched FANCL is significantly reduced in the PWWP domain mutants of FANCA compared with the wild type FANCA group. The mutants are expected to exhibit less FANCD2 ubiquitination and higher sensitivity to ICLs than positive control cell. If the reduction level is comparable to the negative control, the mutated region or residue is essential to the function of FANCA. However, if the phenotype is milder than the negative control, the mutated region or residue is important but not crucial for FANCA function. Under this scenario, combined mutation such as multiple residue mutation or truncation can be generated to study the essential domains required for the full function of FANCA.

Specific Aim 2, To investigate the histone target of the FANCA PWWP domain upon DNA damage.

For this purpose, the recombinant peptide of FANCA PWWP domain will be produced and purified for modified histone peptide array to screen for positive histone binding target (Paul et al., 2013; Rothbart et al., 2012). The interaction between FANCA PWWP domain and the potential modified histone target will be verified both *in vitro* by pull down assay and *in vivo* by immunoprecipitation. Furthermore, PWWP domain mutants of FANCA will be investigated for their binding ability to the histone target *in vitro* with the recombinant peptides and *in vivo* with the cell lines generated in specific aim 1.

If the FANCA PWWP domain possesses modified histone binding affinity, such as H3K36me3, the wild type PWWP domain should bind to the target in the array blotting while the mutants are deficient. The histone target is expected to be pulled down by the wild type PWWP domain peptide but not the mutants. Immunoprecipitation analysis is expected to show that, the endogenous FANCA interacts with histone target in the wild type cell line, while the mutants have impaired affinity. If the modified histone peptide array fails to work due to sensitivity or specificity issue, recombinant FANCA PWWP domain can be conjugated onto column to capture and enrich the target peptide from a library of modified histones.

Specific Aim 3, To establish the co-crystal structure of FANCA PWWP domain and the target histone.

For this purpose, collaboration will be needed. This study is expected to gain structural validation into how FANCA PWWP domain interacts with the target histone. It also explains why certain residues are important for the interaction.

Epistatic analysis of FA genes

Most of the FA genes involved in FANCD2/I monoubiquitination exist only in vertebrate, which makes it difficult to conduct epistatic analysis, since common genetic platforms such as yeast and drosophila cannot be used. On the other hand, the delineation of the epistatic correlations between the FA genes is important to genetically define the FA pathway. As shown in Chapter II-IV, *FANCG*$^{-/-}$, *FANCB*$^{-}$, *FANCG*$^{-/-}$*FANCB*$^{-}$, *FAAP20*$^{-/-}$*FANCB*$^{-}$, and *FANCG*$^{-/-}$*FANCM*$^{-/-}$ cell lines were constructed through rAAV-based recombination targeting for ICL repair functional analysis. With the same technology, I also made *FANCM*$^{-/-}$*FANCB*$^{-}$, *FANCI*$^{-/-}$*FANCB*$^{-}$ cell lines as shown (Fig. 5.4). To make more single and double knockout cell lines to systematically analyze the epistatic relationships between FA genes, it would be more efficient to use the newly established Cas9 knockout technology, since the rAAV-based recombination targeting is a lengthy and laborious procedure. With the generated isogenic mutant cell lines, the function of each gene can be further dissected through characterizing these mutant cell lines and performing DNA damage functional assays.

Fig. 5.4 Construction of human cellular knockout mutants.

(***A***) PCR genotyping of the *FANCM*$^{-/-}$*B*$^{-}$ double knockout mutant.

(***B***) PCR genotyping of the *FANCI*$^{-/-}$*FANCB*$^{-}$ double knockout mutant.

(***C***) Immunoblot detects the indicated FA core protein in whole cell extracts of wild type (*WT*) and indicated mutants.

Δ, knockout allele. wt, wild type allele. MW, molecular weight size marker.

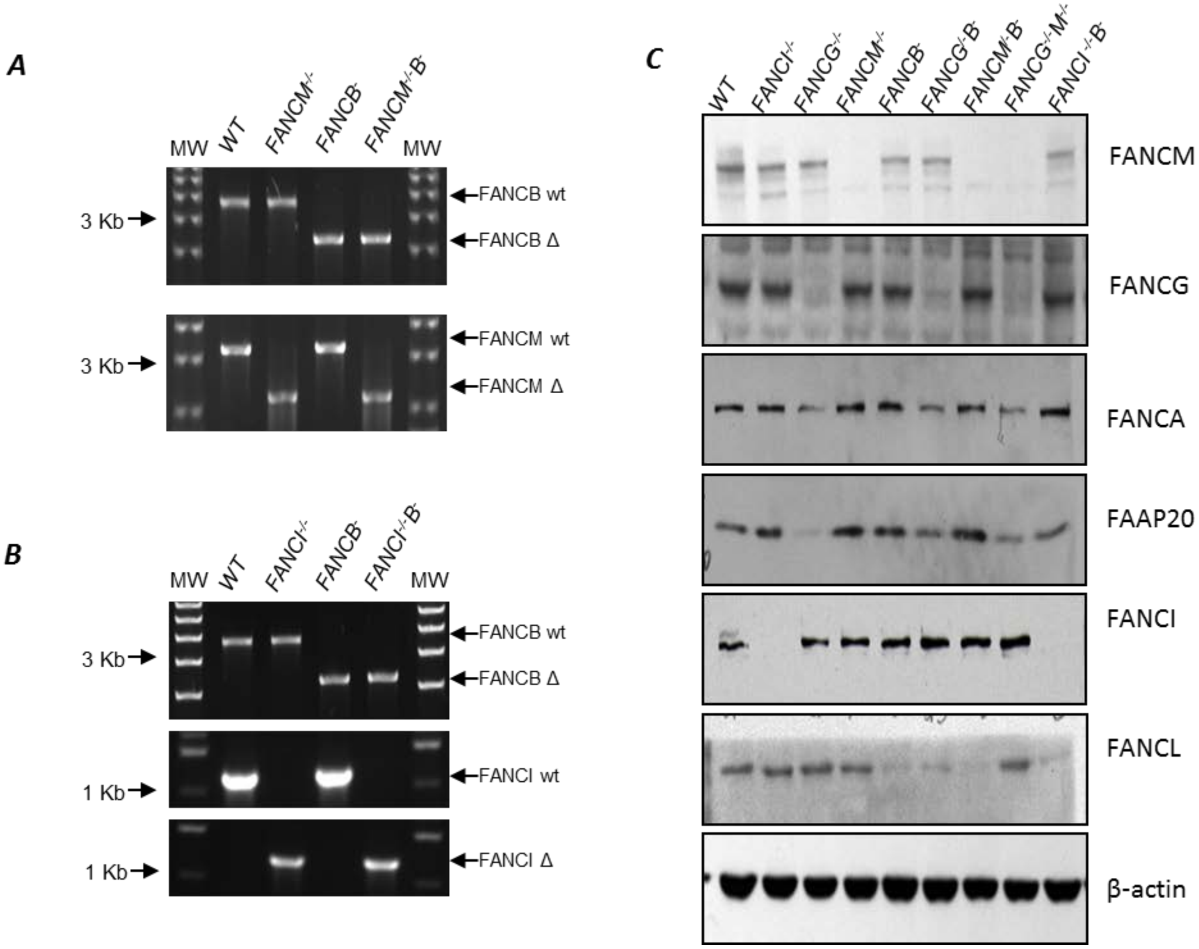
A
MW
WT
FANCM$^{-/-}$
FANCB^{-}
FANCM$^{-/-}$B^{-}
MW
3 Kb
FANCB wt
FANCB Δ
3 Kb
FANCM wt
FANCM Δ
B
MW
WT
FANCI$^{-/-}$
FANCB^{-}
FANCI$^{-/-}$B^{-}
MW
3 Kb
FANCB wt
FANCB Δ
1 Kb
FANCI wt
1 Kb
FANCI Δ
C
WT
FANCI$^{-/-}$
FANCG$^{-/-}$
FANCM$^{-/-}$
FANCB^{-}
FANCG$^{-/-}$B^{-}
FANCM$^{-/-}$B^{-}
FANCG$^{-/-}$M$^{-/-}$
FANCI$^{-/-}$B^{-}
FANCM
FANCG
FANCA
FAAP20
FANCI
FANCL
β-actin

With the current single and double knockout cell lines (*FANCG*$^{-/-}$, *FANCB*$^{-}$, *FANCM*$^{-/-}$, *FANCI*$^{-/-}$, *FANCG*$^{-/-}$*FANCB*$^{-}$, *FAAP20*$^{-/-}$*FANCB*$^{-}$, *FANCG*$^{-/-}$*FANCM*$^{-/-}$, *FANCM*$^{-/-}$*FANCB*$^{-}$, and *FANCI*$^{-/-}$*FANCB*$^{-}$), clonogenicity was tested for their ability of proliferation and survival. As shown (Fig. 5.5), all FA single mutants showed reduced clonogenic ability compared with wild-type HCT116 cells. *FANCM*$^{-/-}$*FANCB*$^{-}$ and *FANCG*$^{-/-}$*FANCM*$^{-/-}$ showed further decrease of clonogenic ability compared with single mutants. *FANCG*$^{-/-}$*FANCB*$^{-}$ cell and *FANCI*$^{-/-}$*FANCB*$^{-}$ cell didn’t show additionally reduced clonogenic ability compared with single mutants. In all, FA genes play a role in cell survival and/or proliferation. These observations also indicate that FANCB, FANCG and FANCI functionally overlap for cell survival and/or proliferation, while *FANCM* has extra function that is not overlapping with the core complex gene FANCB or FANCG.

Fig. 5.5 Clonogenicity of the FA mutants.

(***A***) Plating efficiency of wild type (*WT*) and *FANCI*$^{-/-}$, *FANCG*$^{-/-}$, *FANCM*$^{-/-}$, and *FANCB*$^{-}$ mutants.

(***B***) Plating efficiency of wild type (*WT*) and *FANCM*$^{-/-}$, *FANCB*-, and *FANCM*$^{-/-}$*FANCB*$^{-}$ mutants.

(***C***) Plating efficiency of wild type (*WT*) and *FANCG*$^{-/-}$, *FANCM*$^{-/-}$, and *FANCG*$^{-/-}$*FANCM*$^{-/-}$ mutants.

(***D***) Plating efficiency of wild type (*WT*) and *FANCG*$^{-/-}$, *FANCB*$^{-}$, and *FANCG*$^{-/-}$*FANCB*$^{-}$ mutants.

(***E***) Plating efficiency of wild type (*WT*) and *FANCI*$^{-/-}$, *FANCB*$^{-}$, and *FANCI*$^{-/-}$*FANCB*$^{-}$ mutants.

Error bars represent SDs derived from three independent experiments. One-way ANOVA analysis and Bonferroni multiple comparison tests was used for statistical analysis. *, $p<0.05$; **, $p<0.01$; ***, $p<0.001$; ns, not statistically significant.

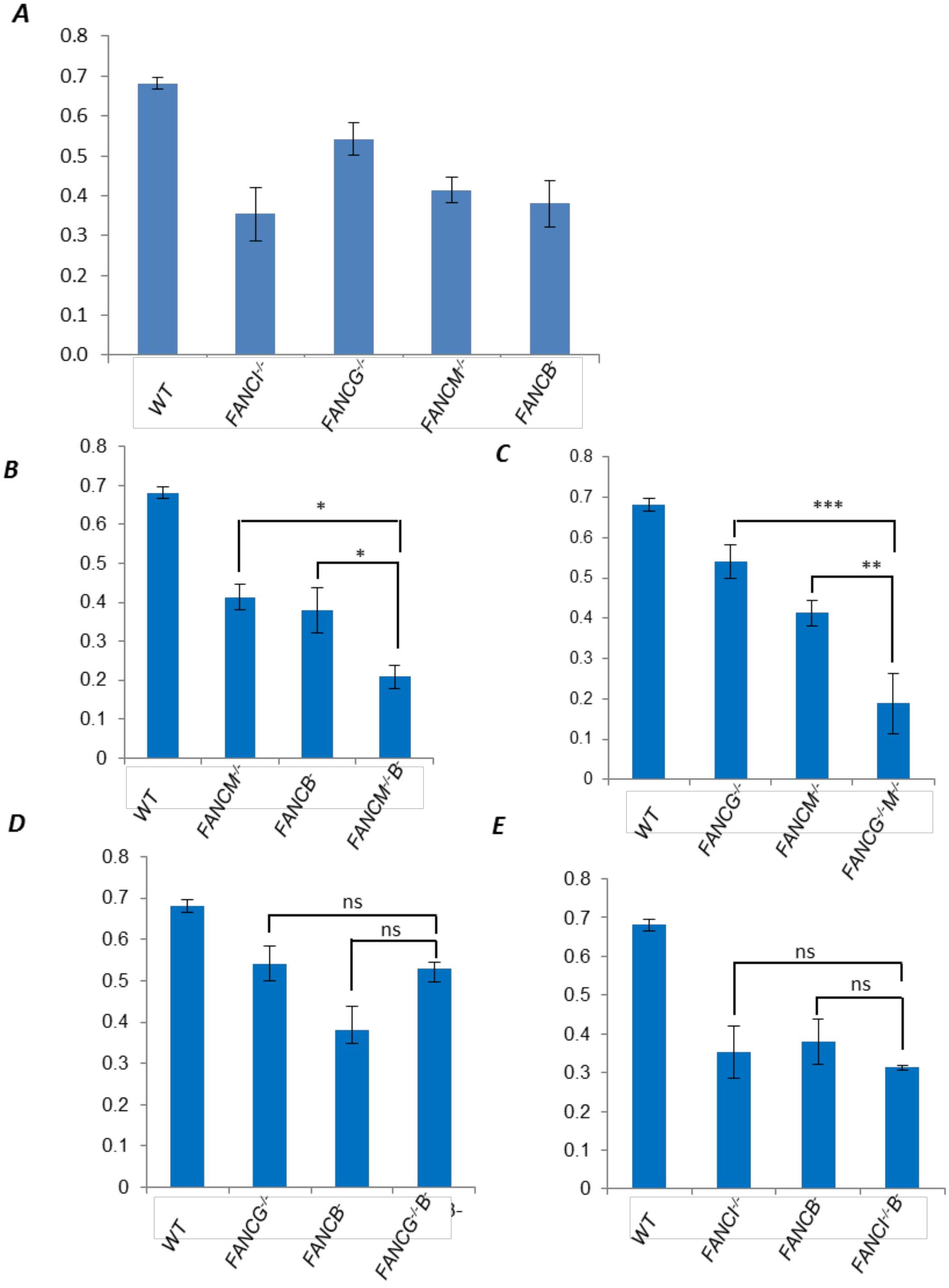
A
0.8
0.7
0.6
0.5
0.4
0.3
0.2
0.1
0.0
WT
FANCI-/-
FANCG-/-
FANCM-/-
FANCB-
B
0.8
0.7
0.6
0.5
0.4
0.3
0.2
0.1
0
*
*
WT
FANCM-/-
FANCB-
FANCM-/-B-
C
0.8
0.7
0.6
0.5
0.4
0.3
0.2
0.1
0
***
**
WT
FANCG-/-
FANCM-/-
FANCG-/-M-/-
D
0.8
0.7
0.6
0.5
0.4
0.3
0.2
0.1
0
ns
ns
WT
FANCG-/-
FANCB-
FANCG-/-B-
E
0.8
0.7
0.6
0.5
0.4
0.3
0.2
0.1
0
ns
ns
WT
FANCI-/-
FANCB-
FANCI-/-B-

As for cell cycle progression, upon MMC treatment, all FA mutants showed G2/M arrest (Fig. 5.6). *FANCG*$^{-/-}$*FANCM*$^{-/-}$ showed highly-increased population in G0/G1 phase compared with single mutants and *FANCM*$^{-/-}$*FANCB*$^{-}$ showed mildly-increased population in G0/G1 phase, while *FANCG*$^{-/-}$*FANCB*$^{-}$ and *FANCI*$^{-/-}$*FANCB*$^{-}$ didn’t showed more population in G0/G1 phase compared with single mutants. All these are consistent with the cell clonogenicity results that FANCB, FANCG and FANCI overlap functionally for cell cycle progression in response to replication stress, while FANCM has extra functions.

Fig. 5.6 Cell cycle profiles of the FA mutants with or without mitomycin C treatment.

To analyze the cell cycle progression profile, cells were treated with or without MMC for 16 hours and pelleted after trypsinization and neutralization. The cell pellets were then suspended in PBS buffer and fixed with ethanol. The fixed cells were then suspended in propidium iodide (PI) staining buffer (5 µg/ml PI in PBS plus 0.2 mg/ml RNase A) in the dark for 30 min at room temperature. Then samples were transferred into FACS tubes and cell cycle was analyzed by flow cytometry. I, *FANCI*$^{-/-}$; G, *FANCG*$^{-/-}$; M, *FANCM*$^{-/-}$; B, *FANCB*$^{-}$; GB, *FANCG*$^{-/-}$ *B*$^{-}$; MB, *FANCM*$^{-/-}$ *B*$^{-}$; GM, *FANCG*$^{-/-}$ *M*$^{-/-}$; IB, *FANCG*$^{-/-}$*M*$^{-}$.

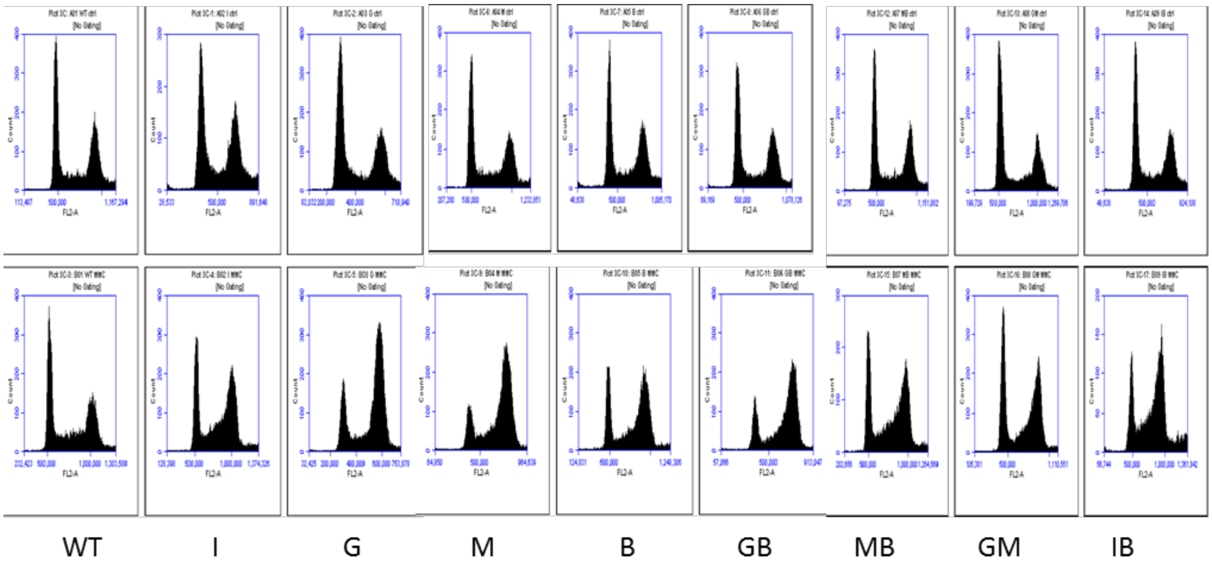

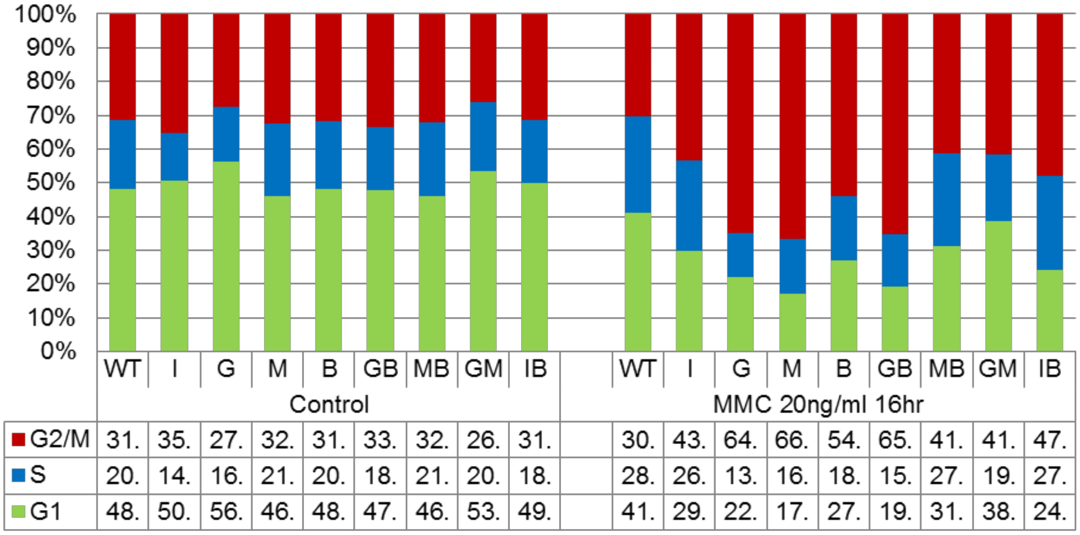

	Control									MMC 20ng/ml 16hr								
	WT	I	G	M	B	GB	MB	GM	IB	WT	I	G	M	B	GB	MB	GM	IB
🟥 G2/M	31.	35.	27.	32.	31.	33.	32.	26.	31.	30.	43.	64.	66.	54.	65.	41.	41.	47.
🟦 S	20.	14.	16.	21.	20.	18.	21.	20.	18.	28.	26.	13.	16.	18.	15.	27.	19.	27.
🟩 G1	48.	50.	56.	46.	48.	47.	46.	53.	49.	41.	29.	22.	17.	27.	19.	31.	38.	24.

In order to study the epistatic relationship between FA genes especially in response to ICL-induced DNA damage, MMC survival assay was carried on these mutants (Fig. 5.7). In general, single knockout cells were hyper-sensitive to MMC. *FANCI*$^{-/-}$ and *FANCB*$^{-}$ showed the highest sensitivity followed by *FANCG*$^{-/-}$, *FANCM*$^{-/-}$ showed the mildest sensitivity to MMC. Double knockout cell lines, *FANCM*$^{-/-}$*FANCB*$^{-}$, showed increased sensitivity to MMC compared with single mutants, indicating that FANCM and core components only have partially overlapping function. On the other hand, *FANCB* knockout on top of *FANCI*$^{-/-}$ cells didn’t show additional increased sensitivity to MMC, suggesting that FA core component genes and I/D2 complex genes are epistatic in ICL resistance. Other DNA damage treatment will be applied for a more comprehensive understanding of the function of the FA genes in response to various DNA damage stress.

Fig. 5.7 Cellular resistance of the FA mutants to mitomycin C.

(***A***) Clonogenic survival curves of wild type (*WT*) and *FANCI*$^{-/-}$, *FANCG*$^{-/-}$, *FANCM*$^{-/-}$, and *FANCB*$^{-}$ mutants under MMC treatment.

(***B***) Clonogenic survival curves of wild type (*WT*) and *FANCM*$^{-/-}$, *FANCB*$^{-}$, and *FANCM*$^{-/-}$ *FANCB*$^{-}$ mutants in MMC treatment.

(***C***) Clonogenic survival curves of wild type (*WT*) and *FANCI*$^{-/-}$, *FANCB*$^{-}$, and *FANCI*$^{-/-}$ *FANCB*$^{-}$ mutants. Error bars for clonogenic survival are derived from DSs from four independent tests with triplications.

A

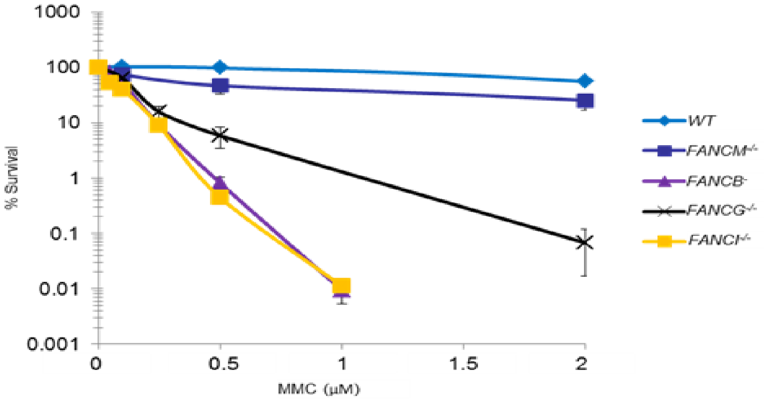
1000
100
10
1
0.1
0.01
0.001
% Survival
0
0.5
1
1.5
2
MMC (µM)
WT
FANCM-/-
FANCB-
FANCG-/-
FANCI-/-

B

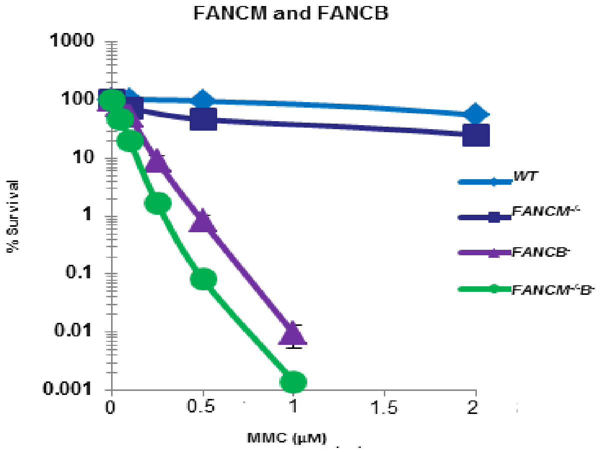
FANCM and FANCB
1000
100
10
1
0.1
0.01
0.001
% Survival
0
0.5
1
1.5
2
MMC (µM)
WT
FANCM-/-
FANCB-
FANCM-/-B-

C

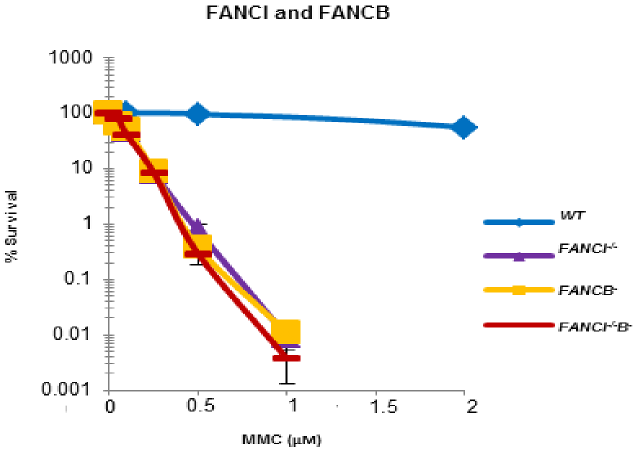
FANCI and FANCB
1000
100
10
1
0.1
0.01
0.001
% Survival
0
0.5
1
1.5
2
MMC (µM)
WT
FANCI-/-
FANCB-
FANCI-/-B-

To investigate the FA function on genomic stability, cytogenetic analysis was performed. FA genes were shown to be important for maintaining genomic integrity upon MMC treatment (Fig. 5.8). The abnormal chromosome were counted, the results was consistent with MMC survivals, in that *FANCG*$^{-/-}$*FANCM*$^{-/-}$ and *FANCM*$^{-/-}$*FANCB*$^{-}$ showed the highest degree of genomic instability, followed by *FANCI*$^{-/-}$*FANCB*$^{-}$ (and *FANCB*$^{-}$, *FANCI*$^{-/-}$), *FANCG*$^{-/-}$, and *FANCM*$^{-/-}$ cell lines. Radial chromosomes were also counted, showing significantly increased counts in the FA deficient cells than wild type cells, but there was no statistically significant difference among the FA mutant cells. This result suggests that radial chromosome counts, as a common phenotype of FA cells, is not able to differentiate the importance of the different FA genes in ICL resistance.

Fig. 5.8 Cytogenetic characterization of the FA mutants with or without mitomycin C treatment.

(***A***) Radial chromosomal counts of wild type and indicated mutants treated with mitomycin C. Error bars are derived from DSs from two independent tests with triplications.

(***B***) Chromosomal aberration counts in wild type and indicated mutants treated with or without mitomycin C. Error bars are derived from DSs from more than 50 counts per cell line.

I, *FANCI*$^{-/-}$; G, *FANCG*$^{-/-}$; M, *FANCM*$^{-/-}$; B, *FANCB*$^{-}$; GB, *FANCG*$^{-/-}$ *B*$^{-}$; MB, *FANCM*$^{-/-}$ *B*$^{-}$; GM, *FANCG*$^{-/-}$ *M*$^{-/-}$; IB, *FANCG*$^{-/-}$*M*$^{-}$.

A

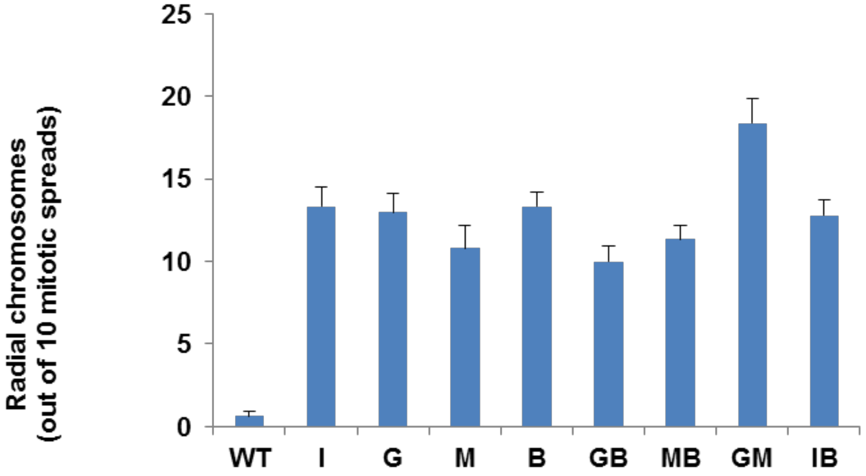
Radial chromosomes
(out of 10 mitotic spreads)
25
20
15
10
5
0
WT
I
G
M
B
GB
MB
GM
IB

B

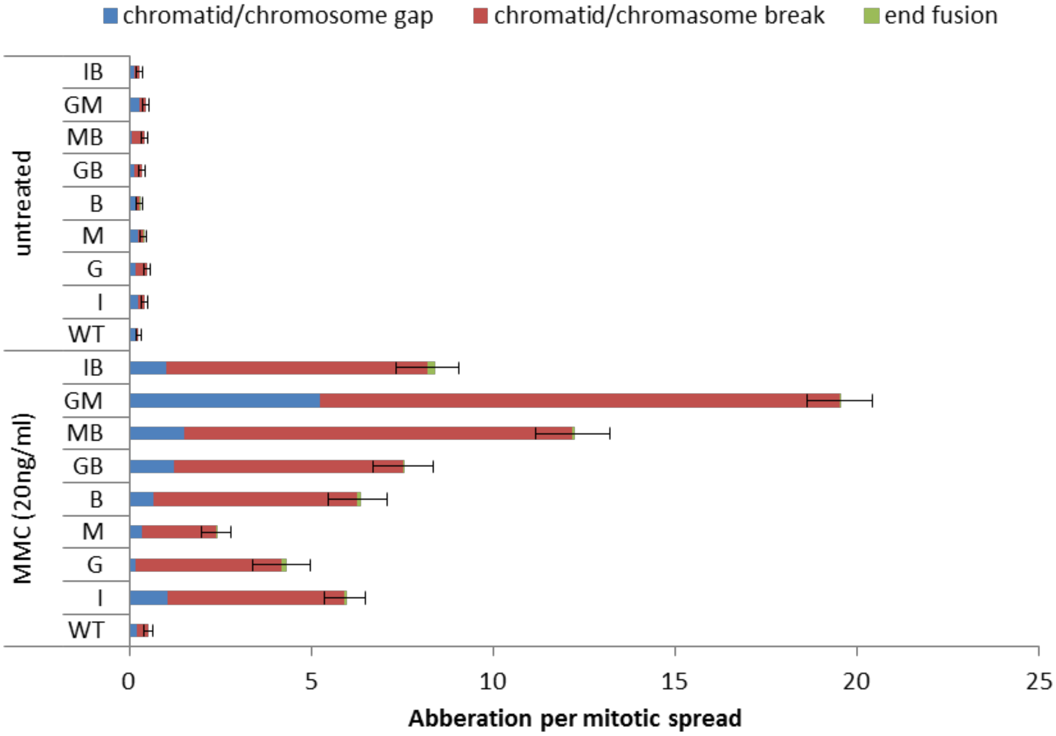
chromatid/chromosome gap
chromatid/chromasome break
end fusion
untreated
MMC (20ng/ml)
IB
GM
MB
GB
B
M
G
I
WT
IB
GM
MB
GB
B
M
G
I
WT
0
5
10
15
20
25
Abberation per mitotic spread

To further analyze these cell lines in response to ICL, G0/G1 phase ICL repair was examined on these mutants. As shown (Fig. 5.9), *FANCI*$^{-/-}$, *FANCM*$^{-/-}$ had impaired replication independent ICL repair, while *FANCG*$^{-/-}$ had increased repair. *FANCM* knockout on top of *FANCG*$^{-/-}$ negatively affected the recombination-independent ICL repair, which indicated that FANCM counteracted with FANCG in G0/G1 phase ICL repair. This could be the reason why FANCG and FANCM show severe phenotype in MMC survival assay. It is interesting that *FANCB* knockout didn't affect this repair, neither did *FANCB* knockout on top of *FANCG*$^{-/-}$, *FANCI*$^{-/-}$ or *FANCM*$^{-/-}$ affect the G0/G1 phase ICL repair significantly. Further mutagenesis assay will be performed to analyze the results of this affected ICL repair efficiency which may provide insight into how FA genes functions in this G0/G1 phase recombination-independent ICL repair and the overall impact of FA gene defects on G0/G1 phase cells.

Fig. 5.9 Recombination-independent repair efficiency of the FA mutants.

(***A***) Recombination independent repair activity analysis of wild type (*WT*) and *FANCI*$^{-/-}$, *FANCG*$^{-/-}$, *FANCM*$^{-/-}$, and *FANCB*$^{-}$ mutants.

(***B***) Recombination independent repair activity analysis of wild type (*WT*) and *FANCM*$^{-/-}$, *FANCB*$^{-}$, and *FANCM*$^{-/-}$*FANCB*$^{-}$ mutants.

(***C***) Recombination independent repair activity analysis of wild type (*WT*) and *FANCG*$^{-/-}$, *FANCM*$^{-/-}$, and *FANCG*$^{-/-}$*FANCM*$^{-/-}$ mutants.

(***D***) Recombination independent repair activity analysis of wild type (*WT*) and *FANCG*$^{-/-}$, *FANCB*$^{-}$, and *FANCG*$^{-/-}$*FANCB*$^{-}$ mutants.

(***E***) Recombination independent repair activity analysis of wild type (*WT*) and *FANCI*$^{-/-}$, *FANCB*$^{-}$, and *FANCI*$^{-/-}$*FANCB*$^{-}$ mutants.

XL, stands for interstrand crosslink. Error bars represent SDs derived from three independent experiments. The luciferase reporter reactivation assay was performed according to previously described protocol to test the recombination-independent ICL repair efficiency (Shen et al., 2009). Briefly, an ICL reporter substrate which blocks transcription of luciferase or an undamaged reporter substrate as control (1ng/each) was transfected into each cell line together with β-galactosidase plasmid as internal control (50ng). Luciferase assay was conducted as standard procedures. The luciferase activity was normalized against the β-galactosidase activity. The relative luciferase activity of the crosslinked reporter to that of the undamaged reporter was calculated as the recombination-independent ICL repair efficiency. One-way ANOVA analysis and Bonferroni multiple comparison tests was used for statistical analysis. **, $p<0.01$; ns, not statistically significant.

A

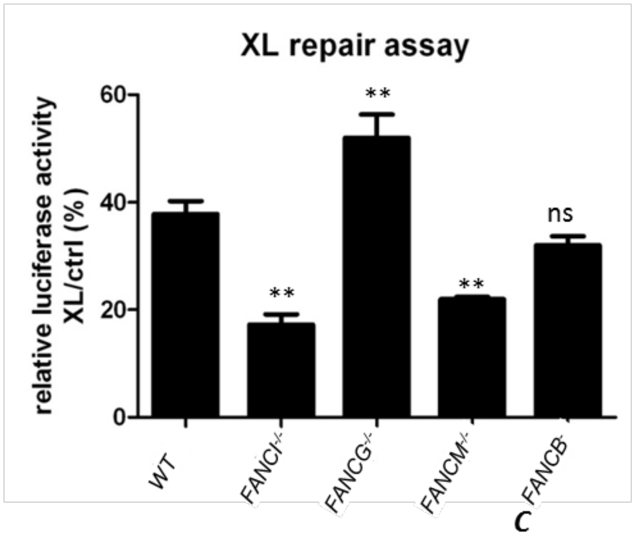
XL repair assay
relative luciferase activity XL/ctrl (%)
60
40
20
0
**
**
**
ns
WT
FANCI-/-
FANCG-/-
FANCM-/-
FANCB-

B

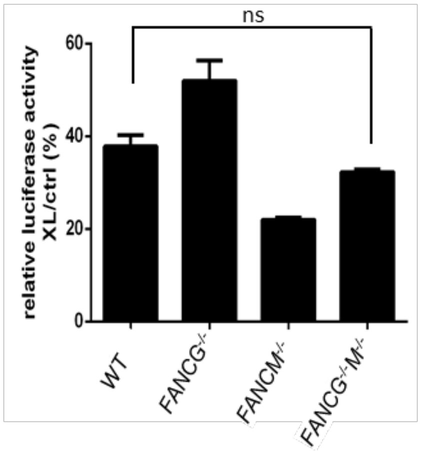
ns
relative luciferase activity XL/ctrl (%)
60
40
20
0
WT
FANCG-/-
FANCM-/-
FANCG-/-M-/-

C

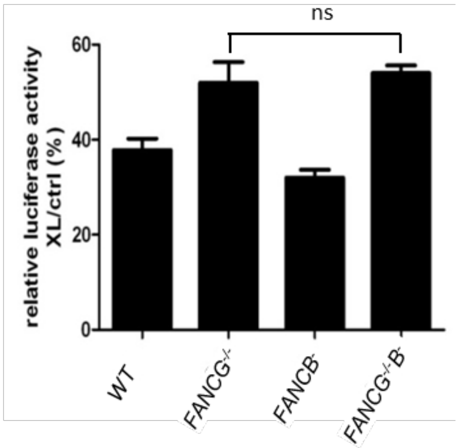
ns
relative luciferase activity XL/ctrl (%)
60
40
20
0
WT
FANCG-/-
FANCB-
FANCG-/-B-

D

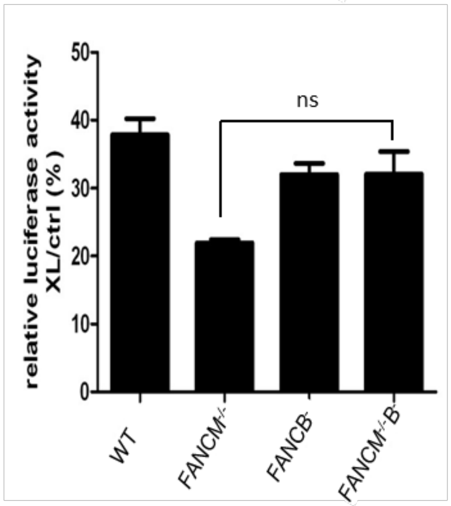
ns
relative luciferase activity XL/ctrl (%)
50
40
30
20
10
0
WT
FANCM-/-
FANCB-
FANCM-/-B-

E

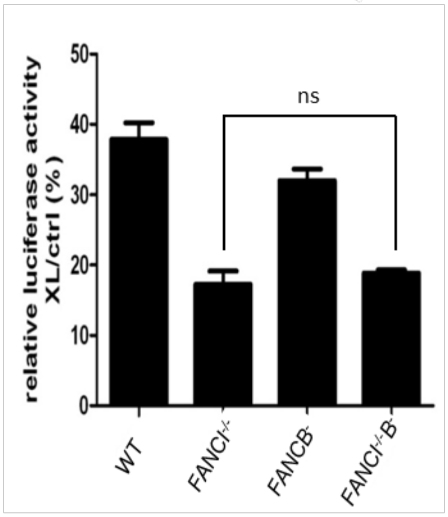
ns
relative luciferase activity XL/ctrl (%)
50
40
30
20
10
0
WT
FANCI-/-
FANCB-
FANCI-/-B-

In conclusion, a series of single and double FA gene knockout cell lines were established. The characterization of the cell lines and DNA repair related functional assay were initiated in these cell lines. In the future, more knockout cell lines will be established to undergo functional assays. Therefore, a more systematic genetic relationship network of the FA genes will be depicted, and functions of each FA genes will be further clarified.

Role of FA genes in DNA-protein crosslink (DPC) repair

Hypersensitivity to DNA interstrand crosslinking agents with increased genomic instability is the standard diagnostic indicator of FA patient and a cellular hallmark for FA pathway deficiency. However, it is still not clear about the nature and the source of endogenous crosslinking lesion. In addition to DNA interstrand crosslinks, recent studies showed a likely role of the FA pathway in repairing DNA-protein crosslinking (DPC) lesions arisen from intrinsic metabolites, acetaldehyde, and formaldehyde (Langevin et al.; Rosado et al.). Interestingly, DPC can also induced by ionizing radiation with a relatively high frequency (>150/cell/Gy) (Frankenberg-Schwager, 1990). Thus FA genes may play a substantial role in countering the replication-blocking damage of DNA-protein crosslinks resulting from ionizing radiation during radiation therapy.

In recent mouse genetic studies from the Patel laboratory, reactive aldehydes have been suggested to constitute a key source of the endogenous crosslinking damage (Langevin et al.). The *Fand2* knockout leads to lethality when combining with the knockout of *Aldh5*, a formaldehyde dehydrogenase gene, which encodes the primary detoxifying enzyme for reactive formaldehyde in cells (Rosado et al.). This may also provide a mechanistic explanation for the progressive hematopoietic stem cells depletion manifested in FA patient (Boulad et al., 2000; Garaycoechea et al., 2012).

Besides ethanol and food preservative consumption, another source of endogenous aldehyde is histone demethylation, which occurs when cells undergo epigenetic changes. The elevated levels of formaldehyde resulting from extensive histone demethylation will immediately spread to the DNA and proteins. Since formaldehyde is also an effective DNA-protein crosslinking agents, the DPCs could be a major kind of endogenous lesion caused by formaldehyde. This reaction is extremely possible where proteins such as histones and transcription factors are in close contact with chromosomal DNA. Although DPCs have been known for a long time, how cells deal with them is poorly understood. In this study, we will explore DPC repair mechanism and possible roles of the FA pathway in this repair.

To analyze the DPC repair mechanism, an *in vivo* system based on our previous ICL-repair system (Shen et al., 2006) is being constructed in our lab, and will be used in this study. To precisely assess the functions of each FA gene group, a panel of isogenic null single and double mutants will be created by homologous replacement targeting mediated targeting in somatic cells. Although patient mutants are available, most of them carry mutations such as hypomorphic alleles making it complicated to explain the phenotypes. Also the individuality makes it very difficult to quantitatively compare cellular phenotypes of the patient cells and the non-patient cells. The somatic cellular knockout models, however, have the advantage over the patient cells, in that the somatic knockout is isogenic. This strict isogenicity allows more accurate functional definition of each gene. Compared with the recent short homology-based gene editing technology such as TALEN and the CAS9 systems, the rAAV-based knockout platform also have the advantage in minimizing off-target events which ensures a more unambiguous conclusion (Fu et al., 2013). With the DPC repair assay and the isogenic cellular models, investigation will be carried out to fulfill the following specific aims.

Specific Aim 1: To study the role of FA genes in the *in vivo* repair of DPCs with the FA gene deficient cells.

For this purpose, luciferase expression plasmid containing site-specific DPC lesion, which blocks the transcription of the firefly luciferase gene, will be constructed and validated. The DPC lesion containing plasmid together with the internal control β-galactosidase will be transfected into various FA null cells and wild type control cells. Luciferase and β-galactosidase dual reporter assay will be performed. The DPC lesion repair efficiency will be tested using the relative luciferase activity as readout to determine whether cells defective in the FA pathway are particularly vulnerable in response to DPCs.

It is expected that FA deficient cell lines have significantly decreased DPC lesion repair efficiency compared with the wild type control cells, demonstrating that FA genes play a role in DPC repair. Different FA mutant cells may show various DPC repair efficiency defect. This will suggest FA genes have various roles in DPC repair.

Specific Aim 2: To detect the physical recruitment of FA proteins to the DPC site.

To do this, eChIP plasmid containing site-specific DPC lesion will be generated to study the recruitment of FA proteins to the lesion site. This eChIP assay will be performed in HEK293 and HEK293-EBNA1cell lines. Since the eChIP plasmid contains an Epstein-Barr virus replication origin (EBV-OriP), the HEK293-EBNA1 cell lines with stably expressed Epstein-Barr nuclear antigen 1 (EBNA-1) will allow the EBNA-1/ori-P based unidirectional replication, while the HEK293 does not (Shen et al., 2006). Therefore, replication-independent and replication-dependent recruitments of FA genes to the DPC site are measurable.

Result from the eChIP assay is expected to show significant enrichment of FA proteins to the damaged site if the function of the FA pathway is directly involved in DPC removal. The enrichment fold of the FA proteins to DPC site may be higher in HEK293-EBNA1 cell than HEK293 cell. This indicates the presence of replication-dependent recruitment mechanism of FA proteins.

Specific Aim 3: To test the epistatic relationship between FA pathway and the formaldehyde detoxifying pathway when encountering DPCs in human cell line.

Although previous mouse study has already shown that the *Fand2* and *Aldh5* double knockout leads to lethality (Rosado et al.), studies of epistatic relationship between FA pathway and the formaldehyde detoxifying pathway are still needed. The reason lies in the probability of different etiology between human and mouse due to the facts that FA knockout mice was not able to recapitulate the phenotype of the FA patients (Koomen et al., 2002; Yang et al., 2001). To this end, *FA-ALDH5* double knockout cells will be generated through Cas9 target strategy. Clonogenic assay will be performed and chromosomal aberration will be counted with the single and double knockout cell lines and the wild type control cell line under the treatment of formaldehyde or other acetaldehyde. This study can also be extended to test the genetic interaction of FA genes with ALDH5 in response to other genotoxins.

It is expected that defects in both cellular protection pathways will lead to substantially increased chromosomal abnormality and impaired cell survival. The cell lines defective in either FA pathway or ALDH5 detoxify pathway may not show severe phenotype to aldehyde comparable to the double deficient cell line, which indicates redundant functions between the two pathways in response to DPCs. All these results will lead to the conclusion that DPCs is an important endogenous lesion endangering genomic integrity and cell survival of humans.

In summary, my thesis study and future studies provide novel mechanistic insights into how FA genes coordinately contribute to resist against crosslinking damage and mediate the spatially defined monoubiquitination of FANCI/D2 complex. It also shed light on the disease biological features in different subtypes. These findings can help to identify the disease characteristics of different subtypes and develop personalized and more effective therapy for FA patients.

References

Adachi, D., Oda, T., Yagasaki, H., Nakasato, K., Taniguchi, T., D'Andrea, A.D., Asano, S., and Yamashita, T. (2002). Heterogeneous activation of the Fanconi anemia pathway by patient-derived FANCA mutants. Hum Mol Genet *11*, 3125-3134.

Akbari, M.R., Tonin, P., Foulkes, W.D., Ghadirian, P., Tischkowitz, M., and Narod, S.A. (2010). RAD51C germline mutations in breast and ovarian cancer patients. Breast Cancer Res *12*, 404.

Ali, A.M., Pradhan, A., Singh, T.R., Du, C., Li, J., Wahengbam, K., Grassman, E., Auerbach, A.D., Pang, Q., and Meetei, A.R. FAAP20: a novel ubiquitin-binding FA nuclear core-complex protein required for functional integrity of the FA-BRCA DNA repair pathway. Blood *119*, 3285-3294.

Alpi, A.F., Pace, P.E., Babu, M.M., and Patel, K.J. (2008). Mechanistic insight into site-restricted monoubiquitination of FANCD2 by Ube2t, FANCL, and FANCI. Mol Cell *32*, 767-777.

Auerbach, A.D., Rogatko, A., and Schroeder-Kurth, T.M. (1989). International Fanconi Anemia Registry: relation of clinical symptoms to diepoxybutane sensitivity. Blood *73*, 391-396.

Bakker, S.T., van de Vrugt, H.J., Rooimans, M.A., Oostra, A.B., Steltenpool, J., Delzenne-Goette, E., van der Wal, A., van der Valk, M., Joenje, H., te Riele, H., *et al.* (2009). Fancm-deficient mice reveal unique features of Fanconi anemia complementation group M. Hum Mol Genet *18*, 3484-3495.

Blom, E., van de Vrugt, H.J., de Vries, Y., de Winter, J.P., Arwert, F., and Joenje, H. (2004). Multiple TPR motifs characterize the Fanconi anemia FANCG protein. DNA Repair (Amst) *3*, 77-84.

Bogliolo, M., Schuster, B., Stoepker, C., Derkunt, B., Su, Y., Raams, A., Trujillo, J.P., Minguillon, J., Ramirez, M.J., Pujol, R., *et al.* (2013). Mutations in ERCC4, encoding the DNA-repair endonuclease XPF, cause Fanconi anemia. American journal of human genetics *92*, 800-806.

Boulad, F., Gillio, A., Small, T.N., George, D., Prasad, V., Torok-Castanza, J., Regan, A.D., Collins, N., Auerbach, A.D., Kernan, N.A., *et al.* (2000). Stem cell transplantation for the treatment of Fanconi anaemia using a fludarabine-based cytoreductive regimen and T-cell-depleted related HLA-mismatched peripheral blood stem cell grafts. Br J Haematol *111*, 1153-1157.

Ciccia, A., Ling, C., Coulthard, R., Yan, Z., Xue, Y., Meetei, A.R., Laghmani el, H., Joenje, H., McDonald, N., de Winter, J.P., *et al.* (2007). Identification of FAAP24, a Fanconi anemia core complex protein that interacts with FANCM. Mol Cell *25*, 331-343.

Collis, S.J., Ciccia, A., Deans, A.J., Horejsi, Z., Martin, J.S., Maslen, S.L., Skehel, J.M., Elledge, S.J., West, S.C., and Boulton, S.J. (2008). FANCM and FAAP24 function in ATR-mediated checkpoint signaling independently of the Fanconi anemia core complex. Mol Cell *32*, 313-324.

D'Andrea, A.D. Susceptibility pathways in Fanconi's anemia and breast cancer. N Engl J Med *362*, 1909-1919.

Deans, A.J., and West, S.C. (2009). FANCM connects the genome instability disorders Bloom's Syndrome and Fanconi Anemia. Mol Cell *36*, 943-953.

Frankenberg-Schwager, M. (1990). Induction, repair and biological relevance of radiation-induced DNA lesions in eukaryotic cells. Radiation and environmental biophysics *29*, 273-292.

Fu, Y., Foden, J.A., Khayter, C., Maeder, M.L., Reyon, D., Joung, J.K., and Sander, J.D. (2013). High-frequency off-target mutagenesis induced by CRISPR-Cas nucleases in human cells. Nature biotechnology *31*, 822-826.

Futaki, M., Igarashi, T., Watanabe, S., Kajigaya, S., Tatsuguchi, A., Wang, J., and Liu, J.M. (2002). The FANCG Fanconi anemia protein interacts with CYP2E1: possible role in protection against oxidative DNA damage. Carcinogenesis *23*, 67-72.

Garaycoechea, J.I., Crossan, G.P., Langevin, F., Daly, M., Arends, M.J., and Patel, K.J. (2012). Genotoxic consequences of endogenous aldehydes on mouse haematopoietic stem cell function. Nature *489*, 571-575.

Garcia-Higuera, I., Kuang, Y., Denham, J., and D'Andrea, A.D. (2000). The fanconi anemia proteins FANCA and FANCG stabilize each other and promote the nuclear accumulation of the Fanconi anemia complex. Blood *96*, 3224-3230.

Garcia-Higuera, I., Kuang, Y., Naf, D., Wasik, J., and D'Andrea, A.D. (1999). Fanconi anemia proteins FANCA, FANCC, and FANCG/XRCC9 interact in a functional nuclear complex. Mol Cell Biol *19*, 4866-4873.

Garcia-Higuera, I., Taniguchi, T., Ganesan, S., Meyn, M.S., Timmers, C., Hejna, J., Grompe, M., and D'Andrea, A.D. (2001). Interaction of the Fanconi anemia proteins and BRCA1 in a common pathway. Mol Cell *7*, 249-262.

Gari, K., Decaillet, C., Delannoy, M., Wu, L., and Constantinou, A. (2008a). Remodeling of DNA replication structures by the branch point translocase FANCM. Proc Natl Acad Sci U S A *105*, 16107-16112.

Gari, K., Decaillet, C., Stasiak, A.Z., Stasiak, A., and Constantinou, A. (2008b). The Fanconi anemia protein FANCM can promote branch migration of Holliday junctions and replication forks. Mol Cell *29*, 141-148.

Gordon, S.M., Alon, N., and Buchwald, M. (2005). FANCC, FANCE, and FANCD2 form a ternary complex essential to the integrity of the Fanconi anemia DNA damage response pathway. J Biol Chem *280*, 36118-36125.

Hoadley, K.A., Xue, Y., Ling, C., Takata, M., Wang, W., and Keck, J.L. Defining the molecular interface that connects the Fanconi anemia protein FANCM to the Bloom syndrome dissolvasome. Proc Natl Acad Sci U S A *109*, 4437-4442.

Hodson, C., and Walden, H. (2012). Towards a molecular understanding of the fanconi anemia core complex. Anemia *2012*, 926787.

Howlett, N.G., Taniguchi, T., Olson, S., Cox, B., Waisfisz, Q., De Die-Smulders, C., Persky, N., Grompe, M., Joenje, H., Pals, G., *et al.* (2002). Biallelic inactivation of BRCA2 in Fanconi anemia. Science *297*, 606-609.

Huang, J., Liu, S., Bellani, M.A., Thazhathveetil, A.K., Ling, C., de Winter, J.P., Wang, Y., Wang, W., and Seidman, M.M. (2013). The DNA translocase FANCM/MHF promotes replication traverse of DNA interstrand crosslinks. Mol Cell *52*, 434-446.

Huang, M., Kim, J.M., Shiotani, B., Yang, K., Zou, L., and D'Andrea, A.D. The FANCM/FAAP24 complex is required for the DNA interstrand crosslink-induced checkpoint response. Mol Cell *39*, 259-268.

Huang, Y., and Li, L. (2013). DNA crosslinking damage and cancer - a tale of friend and foe. Translational Cancer Research *2*, 144-154.

Hussain, S., Wilson, J.B., Blom, E., Thompson, L.H., Sung, P., Gordon, S.M., Kupfer, G.M., Joenje, H., Mathew, C.G., and Jones, N.J. (2006). Tetratricopeptide-motif-mediated interaction of FANCG with recombination proteins XRCC3 and BRCA2. DNA Repair (Amst) *5*, 629-640.

Joo, W., Xu, G., Persky, N.S., Smogorzewska, A., Rudge, D.G., Buzovetsky, O., Elledge, S.J., and Pavletich, N.P. Structure of the FANCI-FANCD2 complex: insights into the Fanconi anemia DNA repair pathway. Science *333*, 312-316.

Kim, J.M., Kee, Y., Gurtan, A., and D'Andrea, A.D. (2008). Cell cycle-dependent chromatin loading of the Fanconi anemia core complex by FANCM/FAAP24. Blood *111*, 5215-5222.

Knipscheer, P., Raschle, M., Smogorzewska, A., Enoiu, M., Ho, T.V., Scharer, O.D., Elledge, S.J., and Walter, J.C. (2009). The Fanconi anemia pathway promotes replication-dependent DNA interstrand cross-link repair. Science *326*, 1698-1701.

Koomen, M., Cheng, N.C., van de Vrugt, H.J., Godthelp, B.C., van der Valk, M.A., Oostra, A.B., Zdzienicka, M.Z., Joenje, H., and Arwert, F. (2002). Reduced fertility and hypersensitivity to mitomycin C characterize Fancg/Xrcc9 null mice. Hum Mol Genet *11*, 273-281.

Kratz, K., Schopf, B., Kaden, S., Sendoel, A., Eberhard, R., Lademann, C., Cannavo, E., Sartori, A.A., Hengartner, M.O., and Jiricny, J. Deficiency of FANCD2-associated nuclease KIAA1018/FAN1 sensitizes cells to interstrand crosslinking agents. Cell *142*, 77-88.

Kruyt, F.A., Abou-Zahr, F., Mok, H., and Youssoufian, H. (1999). Resistance to mitomycin C requires direct interaction between the Fanconi anemia proteins FANCA and FANCG in the nucleus through an arginine-rich domain. J Biol Chem *274*, 34212-34218.

Kutler, D.I., Singh, B., Satagopan, J., Batish, S.D., Berwick, M., Giampietro, P.F., Hanenberg, H., and Auerbach, A.D. (2003). A 20-year perspective on the International Fanconi Anemia Registry (IFAR). Blood *101*, 1249-1256.

Langevin, F., Crossan, G.P., Rosado, I.V., Arends, M.J., and Patel, K.J. Fancd2 counteracts the toxic effects of naturally produced aldehydes in mice. Nature *475*, 53-58.

Lawley, P.D., and Phillips, D.H. (1996). DNA adducts from chemotherapeutic agents. Mutat Res *355*, 13-40.

Leung, J.W., Wang, Y., Fong, K.W., Huen, M.S., Li, L., and Chen, J. Fanconi anemia (FA) binding protein FAAP20 stabilizes FA complementation group A (FANCA) and participates in interstrand cross-link repair. Proc Natl Acad Sci U S A *109*, 4491-4496.

Leveille, F., Blom, E., Medhurst, A.L., Bier, P., Laghmani el, H., Johnson, M., Rooimans, M.A., Sobeck, A., Waisfisz, Q., Arwert, F., *et al.* (2004). The Fanconi anemia gene product FANCF is a flexible adaptor protein. J Biol Chem *279*, 39421-39430.

Leveille, F., Ferrer, M., Medhurst, A.L., Laghmani el, H., Rooimans, M.A., Bier, P., Steltenpool, J., Titus, T.A., Postlethwait, J.H., Hoatlin, M.E., *et al.* (2006). The nuclear accumulation of the Fanconi anemia protein FANCE depends on FANCC. DNA Repair (Amst) *5*, 556-565.

Li, F., Mao, G., Tong, D., Huang, J., Gu, L., Yang, W., and Li, G.M. (2013). The histone mark H3K36me3 regulates human DNA mismatch repair through its interaction with MutSalpha. Cell *153*, 590-600.

Ling, C., Ishiai, M., Ali, A.M., Medhurst, A.L., Neveling, K., Kalb, R., Yan, Z., Xue, Y., Oostra, A.B., Auerbach, A.D., *et al.* (2007). FAAP100 is essential for activation of the Fanconi anemia-associated DNA damage response pathway. EMBO J *26*, 2104-2114.

Liu, T., Ghosal, G., Yuan, J., Chen, J., and Huang, J. FAN1 acts with FANCI-FANCD2 to promote DNA interstrand cross-link repair. Science *329*, 693-696.

Lobitz, S., and Velleuer, E. (2006). Guido Fanconi (1892-1979): a jack of all trades. Nat Rev Cancer *6*, 893-898.

Longerich, S., San Filippo, J., Liu, D., and Sung, P. (2009). FANCI binds branched DNA and is monoubiquitinated by UBE2T-FANCL. J Biol Chem *284*, 23182-23186.

MacKay, C., Declais, A.C., Lundin, C., Agostinho, A., Deans, A.J., MacArtney, T.J., Hofmann, K., Gartner, A., West, S.C., Helleday, T., *et al.* Identification of KIAA1018/FAN1, a DNA repair nuclease recruited to DNA damage by monoubiquitinated FANCD2. Cell *142*, 65-76.

Magana-Schwencke, N., Henriques, J.A., Chanet, R., and Moustacchi, E. (1982). The fate of 8-methoxypsoralen photoinduced crosslinks in nuclear and mitochondrial yeast DNA: comparison of wild-type and repair-deficient strains. Proc Natl Acad Sci U S A *79*, 1722-1726.

Medhurst, A.L., Huber, P.A., Waisfisz, Q., de Winter, J.P., and Mathew, C.G. (2001). Direct interactions of the five known Fanconi anaemia proteins suggest a common functional pathway. Hum Mol Genet *10*, 423-429.

Medhurst, A.L., Laghmani el, H., Steltenpool, J., Ferrer, M., Fontaine, C., de Groot, J., Rooimans, M.A., Scheper, R.J., Meetei, A.R., Wang, W., *et al.* (2006). Evidence for subcomplexes in the Fanconi anemia pathway. Blood *108*, 2072-2080.

Meetei, A.R., de Winter, J.P., Medhurst, A.L., Wallisch, M., Waisfisz, Q., van de Vrugt, H.J., Oostra, A.B., Yan, Z., Ling, C., Bishop, C.E., *et al.* (2003). A novel ubiquitin ligase is deficient in Fanconi anemia. Nat Genet *35*, 165-170.

Meetei, A.R., Levitus, M., Xue, Y., Medhurst, A.L., Zwaan, M., Ling, C., Rooimans, M.A., Bier, P., Hoatlin, M., Pals, G., *et al.* (2004). X-linked inheritance of Fanconi anemia complementation group B. Nat Genet *36*, 1219-1224.

Meetei, A.R., Medhurst, A.L., Ling, C., Xue, Y., Singh, T.R., Bier, P., Steltenpool, J., Stone, S., Dokal, I., Mathew, C.G., *et al.* (2005). A human ortholog of archaeal DNA repair protein Hef is defective in Fanconi anemia complementation group M. Nat Genet *37*, 958-963.

Metzger, M.B., Hristova, V.A., and Weissman, A.M. (2012). HECT and RING finger families of E3 ubiquitin ligases at a glance. Journal of cell science *125*, 531-537.

Pace, P., Johnson, M., Tan, W.M., Mosedale, G., Sng, C., Hoatlin, M., de Winter, J., Joenje, H., Gergely, F., and Patel, K.J. (2002). FANCE: the link between Fanconi anaemia complex assembly and activity. EMBO J *21*, 3414-3423.

Pace, P., Mosedale, G., Hodskinson, M.R., Rosado, I.V., Sivasubramaniam, M., and Patel, K.J. (2010). Ku70 corrupts DNA repair in the absence of the Fanconi anemia pathway. Science *329*, 219-223.

Papadopoulos, N., Nicolaides, N.C., Wei, Y.F., Ruben, S.M., Carter, K.C., Rosen, C.A., Haseltine, W.A., Fleischmann, R.D., Fraser, C.M., Adams, M.D., *et al.* (1994). Mutation of a mutL homolog in hereditary colon cancer. Science *263*, 1625-1629.

Park, E., Kim, H., Kim, J.M., Primack, B., Vidal-Cardenas, S., Xu, Y., Price, B.D., Mills, A.A., and D'Andrea, A.D. (2013). FANCD2 Activates Transcription of TAp63 and Suppresses Tumorigenesis. Mol Cell *50*, 908-918.

Paul, S., Kuo, A., Schalch, T., Vogel, H., Joshua-Tor, L., McCombie, W.R., Gozani, O., Hammell, M., and Mills, A.A. (2013). Chd5 requires PHD-mediated histone 3 binding for tumor suppression. Cell reports *3*, 92-102.

Pulliam-Leath, A.C., Ciccone, S.L., Nalepa, G., Li, X., Si, Y., Miravalle, L., Smith, D., Yuan, J., Li, J., Anur, P., *et al.* Genetic disruption of both Fancc and Fancg in mice recapitulates the hematopoietic manifestations of Fanconi anemia. Blood *116*, 2915-2920.

Rago, C., Vogelstein, B., and Bunz, F. (2007). Genetic knockouts and knockins in human somatic cells. Nat Protoc *2*, 2734-2746.

Raschle, M., Knipscheer, P., Enoiu, M., Angelov, T., Sun, J., Griffith, J.D., Ellenberger, T.E., Scharer, O.D., and Walter, J.C. (2008). Mechanism of replication-coupled DNA interstrand crosslink repair. Cell *134*, 969-980.

Reuter, T., Herterich, S., Bernhard, O., Hoehn, H., and Gross, H.J. (2000). Strong FANCA/FANCG but weak FANCA/FANCC interaction in the yeast 2-hybrid system. Blood *95*, 719-720.

Rosado, I.V., Langevin, F., Crossan, G.P., Takata, M., and Patel, K.J. Formaldehyde catabolism is essential in cells deficient for the Fanconi anemia DNA-repair pathway. Nat Struct Mol Biol.

Roschke, A.V., Stover, K., Tonon, G., Schaffer, A.A., and Kirsch, I.R. (2002). Stable karyotypes in epithelial cancer cell lines despite high rates of ongoing structural and numerical chromosomal instability. Neoplasia *4*, 19-31.

Rosenberg, P.S., Greene, M.H., and Alter, B.P. (2003). Cancer incidence in persons with Fanconi anemia. Blood *101*, 822-826.

Rosenberg, P.S., Tamary, H., and Alter, B.P. (2011). How high are carrier frequencies of rare recessive syndromes? Contemporary estimates for Fanconi Anemia in the United States and Israel. Am J Med Genet A *155A*, 1877-1883.

Rothbart, S.B., Krajewski, K., Nady, N., Tempel, W., Xue, S., Badeaux, A.I., Barsyte-Lovejoy, D., Martinez, J.Y., Bedford, M.T., Fuchs, S.M., *et al.* (2012). Association of UHRF1 with methylated H3K9 directs the maintenance of DNA methylation. Nat Struct Mol Biol *19*, 1155-1160.

Sarkar, S., Davies, A.A., Ulrich, H.D., and McHugh, P.J. (2006). DNA interstrand crosslink repair during G1 involves nucleotide excision repair and DNA polymerase zeta. EMBO J *25*, 1285-1294.

Sato, K., Ishiai, M., Toda, K., Furukoshi, S., Osakabe, A., Tachiwana, H., Takizawa, Y., Kagawa, W., Kitao, H., Dohmae, N., *et al.* (2012). Histone chaperone activity of Fanconi anemia proteins, FANCD2 and FANCI, is required for DNA crosslink repair. EMBO J *31*, 3524-3536.

Schwab, R.A., Blackford, A.N., and Niedzwiedz, W. ATR activation and replication fork restart are defective in FANCM-deficient cells. EMBO J *29*, 806-818.

Shen, X., Do, H., Li, Y., Chung, W.H., Tomasz, M., de Winter, J.P., Xia, B., Elledge, S.J., Wang, W., and Li, L. (2009). Recruitment of fanconi anemia and breast cancer proteins to DNA damage sites is differentially governed by replication. Mol Cell *35*, 716-723.

Shen, X., Jun, S., O'Neal, L.E., Sonoda, E., Bemark, M., Sale, J.E., and Li, L. (2006). REV3 and REV1 play major roles in recombination-independent repair of DNA interstrand cross-links mediated by monoubiquitinated proliferating cell nuclear antigen (PCNA). J Biol Chem *281*, 13869-13872.

Singh, T.R., Saro, D., Ali, A.M., Zheng, X.F., Du, C.H., Killen, M.W., Sachpatzidis, A., Wahengbam, K., Pierce, A.J., Xiong, Y., *et al.* (2010). MHF1-MHF2, a histone-fold-containing protein complex, participates in the Fanconi anemia pathway via FANCM. Mol Cell *37*, 879-886.

Smogorzewska, A., Desetty, R., Saito, T.T., Schlabach, M., Lach, F.P., Sowa, M.E., Clark, A.B., Kunkel, T.A., Harper, J.W., Colaiacovo, M.P., *et al.* A genetic screen identifies FAN1, a Fanconi anemia-associated nuclease necessary for DNA interstrand crosslink repair. Mol Cell *39*, 36-47.

Smogorzewska, A., Matsuoka, S., Vinciguerra, P., McDonald, E.R., 3rd, Hurov, K.E., Luo, J., Ballif, B.A., Gygi, S.P., Hofmann, K., D'Andrea, A.D., *et al.* (2007). Identification of the FANCI protein, a monoubiquitinated FANCD2 paralog required for DNA repair. Cell *129*, 289-301.

Taniguchi, T., and D'Andrea, A.D. (2002). The Fanconi anemia protein, FANCE, promotes the nuclear accumulation of FANCC. Blood *100*, 2457-2462.

Thompson, L.H., and Hinz, J.M. (2009). Cellular and molecular consequences of defective Fanconi anemia proteins in replication-coupled DNA repair: mechanistic insights. Mutat Res *668*, 54-72.

Umar, A., Boyer, J.C., Thomas, D.C., Nguyen, D.C., Risinger, J.I., Boyd, J., Ionov, Y., Perucho, M., and Kunkel, T.A. (1994). Defective mismatch repair in extracts of colorectal and endometrial cancer cell lines exhibiting microsatellite instability. J Biol Chem *269*, 14367-14370.

Vandenberg, C.J., Gergely, F., Ong, C.Y., Pace, P., Mallery, D.L., Hiom, K., and Patel, K.J. (2003). BRCA1-independent ubiquitination of FANCD2. Mol Cell *12*, 247-254.

Waisfisz, Q., de Winter, J.P., Kruyt, F.A., de Groot, J., van der Weel, L., Dijkmans, L.M., Zhi, Y., Arwert, F., Scheper, R.J., Youssoufian, H., *et al.* (1999). A physical complex of the Fanconi anemia proteins FANCG/XRCC9 and FANCA. Proc Natl Acad Sci U S A *96*, 10320-10325.

Wang, L.C., and Gautier, J. (2010). The Fanconi anemia pathway and ICL repair: implications for cancer therapy. Critical reviews in biochemistry and molecular biology *45*, 424-439.

Wang, W. (2007). Emergence of a DNA-damage response network consisting of Fanconi anaemia and BRCA proteins. Nat Rev Genet *8*, 735-748.

Wang, Y., Leung, J.W., Jiang, Y., Lowery, M.G., Do, H., Vasquez, K.M., Chen, J., Wang, W., and Li, L. (2013). FANCM and FAAP24 maintain genome stability via cooperative as well as unique functions. Mol Cell *49*, 997-1009.

Wang, Y., Reddy, B., Thompson, J., Wang, H., Noma, K., Yates, J.R., 3rd, and Jia, S. (2009). Regulation of Set9-mediated H4K20 methylation by a PWWP domain protein. Mol Cell *33*, 428-437.

Yamamoto, K., Hirano, S., Ishiai, M., Morishima, K., Kitao, H., Namikoshi, K., Kimura, M., Matsushita, N., Arakawa, H., Buerstedde, J.M., *et al.* (2005). Fanconi anemia protein FANCD2 promotes immunoglobulin gene conversion and DNA repair through a mechanism related to homologous recombination. Mol Cell Biol *25*, 34-43.

Yamamoto, K.N., Kobayashi, S., Tsuda, M., Kurumizaka, H., Takata, M., Kono, K., Jiricny, J., Takeda, S., and Hirota, K. (2011). Involvement of SLX4 in interstrand cross-link repair is regulated by the Fanconi anemia pathway. Proc Natl Acad Sci U S A *108*, 6492-6496.

Yan, Z., Delannoy, M., Ling, C., Daee, D., Osman, F., Muniandy, P.A., Shen, X., Oostra, A.B., Du, H., Steltenpool, J., *et al.* A histone-fold complex and FANCM form a conserved DNA-remodeling complex to maintain genome stability. Mol Cell *37*, 865-878.

Yan, Z., Guo, R., Paramasivam, M., Shen, W., Ling, C., Fox, D., 3rd, Wang, Y., Oostra, A.B., Kuehl, J., Lee, D.Y., *et al.* A Ubiquitin-Binding Protein, FAAP20, Links RNF8-Mediated Ubiquitination to the Fanconi Anemia DNA Repair Network. Mol Cell.

Yang, Y., Kuang, Y., Montes De Oca, R., Hays, T., Moreau, L., Lu, N., Seed, B., and D'Andrea, A.D. (2001). Targeted disruption of the murine Fanconi anemia gene, Fancg/Xrcc9. Blood *98*, 3435-3440.

Yuan, F., Qian, L., Zhao, X., Liu, J.Y., Song, L., D'Urso, G., Jain, C., and Zhang, Y. (2012). Fanconi anemia complementation group A (FANCA) protein has intrinsic affinity for nucleic acids with preference for single-stranded forms. J Biol Chem *287*, 4800-4807.

Zheng, H., Wang, X., Warren, A.J., Legerski, R.J., Nairn, R.S., Hamilton, J.W., and Li, L. (2003). Nucleotide excision repair- and polymerase eta-mediated error-prone removal of mitomycin C interstrand cross-links. Mol Cell Biol *23*, 754-761.

Zimmerman, E.S., Schulman, B.A., and Zheng, N. (2010). Structural assembly of cullin-RING ubiquitin ligase complexes. Current opinion in structural biology *20*, 714-721.

VITA

Yaling Huang was born in Zixing, Hunan Province, People’s Republic of China on February 3rd, 1985, the second child of Wenbiao Huang and Mengjuan Xie. After attending Chenzhou No.1 High School, she entered Nanjing University, P. R. China in September 2002. She studied in Medical School, and got her Bachelor of Medicine degree in June 2007 and finished the first year study of Master of Medicine program (specialty, Stomatology) in June 2008. She then came to the United States as a graduate student in the University Of Texas Graduate School Of Biomedical Sciences Houston in August 2008. She joined Dr. Lei Li’s laboratory in The University of Texas M. D. Anderson Cancer center in June 2009 for PhD studies.